


1990

In situ lateral earth pressure and its effect on vertical hydraulic conductivity in a glacial till deposit

Hung-yu Wang
Iowa State University

Follow this and additional works at: <https://lib.dr.iastate.edu/rtd>

 Part of the [Civil Engineering Commons](#), and the [Environmental Sciences Commons](#)

Recommended Citation

Wang, Hung-yu, "In situ lateral earth pressure and its effect on vertical hydraulic conductivity in a glacial till deposit " (1990).
Retrospective Theses and Dissertations. 9906.
<https://lib.dr.iastate.edu/rtd/9906>

This Dissertation is brought to you for free and open access by the Iowa State University Capstones, Theses and Dissertations at Iowa State University Digital Repository. It has been accepted for inclusion in Retrospective Theses and Dissertations by an authorized administrator of Iowa State University Digital Repository. For more information, please contact digirep@iastate.edu.

RECORDED 1991

RECORDED 1991

UNI

6

7

8

0

1

1

0

INFORMATION TO USERS

The most advanced technology has been used to photograph and reproduce this manuscript from the microfilm master. UMI films the text directly from the original or copy submitted. Thus, some thesis and dissertation copies are in typewriter face, while others may be from any type of computer printer.

The quality of this reproduction is dependent upon the quality of the copy submitted. Broken or indistinct print, colored or poor quality illustrations and photographs, print bleedthrough, substandard margins, and improper alignment can adversely affect reproduction.

In the unlikely event that the author did not send UMI a complete manuscript and there are missing pages, these will be noted. Also, if unauthorized copyright material had to be removed, a note will indicate the deletion.

Oversize materials (e.g., maps, drawings, charts) are reproduced by sectioning the original, beginning at the upper left-hand corner and continuing from left to right in equal sections with small overlaps. Each original is also photographed in one exposure and is included in reduced form at the back of the book.

Photographs included in the original manuscript have been reproduced xerographically in this copy. Higher quality 6" x 9" black and white photographic prints are available for any photographs or illustrations appearing in this copy for an additional charge. Contact UMI directly to order.

U·M·I

University Microfilms International
A Bell & Howell Information Company
300 North Zeeb Road, Ann Arbor, MI 48106-1346 USA
313/761-4700 800/521-0600



Order Number 9110579

***In situ* lateral earth pressure and its effect on vertical hydraulic
conductivity in a glacial till deposit**

Wang, Hung-yu, Ph.D.

Iowa State University, 1990

U·M·I
300 N. Zeeb Rd.
Ann Arbor, MI 48106



**In situ lateral earth pressure and its effect
on vertical hydraulic conductivity
in a glacial till deposit**

by

Hung-yu Wang

**A Dissertation Submitted to the
Graduate Faculty in Partial Fulfillment of the
Requirements for the Degree of
DOCTOR OF PHILOSOPHY**

**Department: Civil and Construction Engineering
Major: Geotechnical Engineering
Civil Engineering Materials**

Approved:

Signature was redacted for privacy.

Signature was redacted for privacy.

In Charge of Major Work

Signature was redacted for privacy.

For the Major Department

Signature was redacted for privacy.

For the Graduate College

**Iowa State University
Ames, Iowa
1990**

TABLE OF CONTENTS

	Page
INTRODUCTION AND OBJECTIVES	1
LITERATURE REVIEW	3
Fractures in Glacial Deposits	3
Mechanics of fracture formation	5
Shear-stress related fractures	8
Tensile-stress related fractures	10
Laboratory Hydraulic Conductivity Tests	13
Darcy's law	13
Methods of permeability testing in the laboratory	14
Test apparatus	19
Factors affecting the measurement of permeability in laboratory	20
Mechanical factors controlling permeability	22
Fluid flow through a single fracture	24
Stresses Acting on Soil Samples	27
Lateral earth pressure measurement	30
Lateral earth pressure measurement by K ₀ Stepped Blade	35
Soil behavior and data interpretation	37
Previous SBT measurement	40
FIELD TESTS	43
Glacial Geology of North Central Iowa	43
Alden Member of Dows Formation	49
Investigation	50
Site description	50
Soil classification	53
K ₀ Stepped Blade test	55
Triaxial permeability test	57

	Page
RESULTS AND DISCUSSION	61
Soil Classification	61
Results	61
Discussion	67
Stepped Blade Test (SBT)	68
Results	68
Discussion	79
Triaxial Permeability Test	82
Results from intact samples	82
Results from split samples	86
Discussion	89
CONCLUSION	95
RECOMMENDATION FOR FURTHER RESEARCH	97
BIBLIOGRAPHY	98
ACKNOWLEDGMENTS	103
APPENDIX A	104
Original SBT Data	104
APPENDIX B	118
Interpreted Lateral Stresses and K_o's	118
APPENDIX C	124
Results of One-dimensional Consolidation Tests	124
APPENDIX D	129
Results of Triaxial Confining Permeability tests	129

LIST OF FIGURES

	Page
Figure 1. Acquisition, transportation and deposition of tills by a glacier	4
Figure 2. Orientation of slip lines for Rankine state (a) active state (b) passive state	7
Figure 3. Hypothetical direction of major and minor principal stresses of fractures with low dipping angles	9
Figure 4. Permeability tests (a) constant head method and (b) falling head method	15
Figure 5. Applied stress-coefficient of consolidation relationship for samples with a dispersing agent added	18
Figure 6. Effect of confining pressure on the hydraulic conductivity	28
Figure 7. Variation of the coefficient of permeability with applied effective stress for specimens from North Hanover St. Glasgow	29
Figure 8. Geological history and compressibility of an overconsolidated clay	34
Figure 9. K_0 Stepped Blade and its method of interpreting data	36
Figure 10. Theoretical and observed pressure-volume responses for soils, OA is consistent with linear e-logp relationship	36
Figure 11. Representative data plots of blade pressure on a vertical logarithmic scale versus blade thickness	38
Figure 12. Hypothetical Cary flow lines	44
Figure 13. Summary of textural data for the supra-glacial deposits and basal till of the Des Moines Lobe	47

	Page
Figure 14. Summary of bulk density data for materials in superglacial till and basal till	48
Figure 15. Location of test site	51
Figure 16. Topography of test site	52
Figure 17. Locations of SBT and soil sampling	54
Figure 18. Schematic diagram of triaxial permeability apparatus	59
Figure 19. Textural data for the test site	66
Figure 20. Lateral stresses at H1-1 (NW) vs. H1-2 (NE)	70
Figure 21. Lateral stresses at H3-1A (N) vs. H3-2A (E)	71
Figure 22. Lateral stresses at H5 (N) vs. H5-1 (E)	72
Figure 23. Lateral stresses at H8 (NW) vs. H8-1 (NE)	73
Figure 24. Lateral stresses at H1 (NW)	74
Figure 25. Lateral stresses at H6 (NW)	75
Figure 26. Lateral stresses at H7 (NW)	76
Figure 27. Lateral stresses at H1-2, H8-1, and H3-2A	78
Figure 28. Fractures in sample H5-5	81
Figure 29. Fractures in sample H5-10	81
Figure 30. Hydraulic conductivity of intact sample H5-15 at different confining stresses	83
Figure 31. Hydraulic conductivity of intact sample H5-20 at different confining stresses	83
Figure 32. Hydraulic conductivity of intact sample H6-10 at different confining stresses	84
Figure 33. Hydraulic conductivity of intact sample H8-15 at different confining stresses	84

	Page
Figure 34. Normalized permeability vs. normalized confining stresses	85
Figure 35. Hydraulic conductivity of split sample H5-15 at different confining stresses	87
Figure 36. Hydraulic conductivity of split sample H6-10 at different confining stresses	87
Figure 37. Hydraulic conductivity of split sample H8-15 at different confining stresses	88

LIST OF TABLES

	Page
Table 1a. Summary of soil classification tests	63
Table 1b. Summary of soil classification tests	64
Table 2. In situ lateral stresses and Horizontal preconsolidation stresses	92

INTRODUCTION AND OBJECTIVES

It is not uncommon to find fractures in glacial till deposits that are abundant in Northern America. Such fractures may result from shear or tensile stresses associated with glacial ice flow, consolidation, stress release due to deglaciation, desiccation, or weathering. Certain characters of a glacial deposit, such as preferential orientation of soil particles and fractures, were reported to be related to glacial ice flow. Recently, the problem of permeability and preferential direction of groundwater flow in fractured glacial till has increasingly attracted the attention of researchers, particularly with regard to the possible contribution of fractures to contamination of groundwater.

Past researches on permeability of fine-grained soils indicate that hydraulic conductivity is controlled by the pore size distribution of the soil, and the results of laboratory permeability tests were highly affected by effective stresses applied on soil samples. Due to limited techniques and theories of measurement of in situ stresses in the past, laboratory hydraulic conductivity tests used an arbitrary level of confining stresses or "theoretical" in situ stresses calculated by use of empirical equations. These have been found to be questionable as several in situ measuring devices have come into use recently.

The research consists of a field and a laboratory phase. In the field test Stepped Blade tests (SBT) were conducted at several depths and boring locations in a glacial till deposit containing vertical and sub-vertical fractures. The SBT's were used to measure directional lateral stresses in situ to determine if there was any directional anisotropic nature of lateral stresses attributable to glacial flow and geography, and the formation of the fractures, and to provide data on lateral stresses for triaxial permeability tests conducted in the laboratory. The purpose of these tests was to study the effect of lateral stresses on hydraulic conductivity of both intact and fractured soil samples.

LITERATURE REVIEW

Fractures in Glacial Deposits

Glacial landscapes abundant in Northern America involve a complex mixture of sediment types that often have different geotechnical properties such as particle size distribution, density, OCR (over-consolidation ratio), and hydraulic conductivity. The character of a glacial deposit is a function of three major parameters: the geochemical properties of the sediment source, the nature and distance of sediment transport, and the mode of sediment deposition (Stephenson et al., 1988).

Most glacial till deposits can be classified into two fundamental categories as shown in Figure 1: supraglacial till and subglacial till (or basal till) based on the depositional process (Kemmis et al., 1981). Subglacial till can be deposited by three different processes; lodgment, regelation melt-out, and basal melt-out. Oftentimes the subglacial till is formed by a combination of these processes instead of a single one. Supraglacial sedimentation also consist of three basic types; supraglacial melt-out till, resedimented deposits, and supraglacial melt-water deposits. Sedimentation in the glacial till environment may be extremely complex. Extensive discussion of glacial deposits

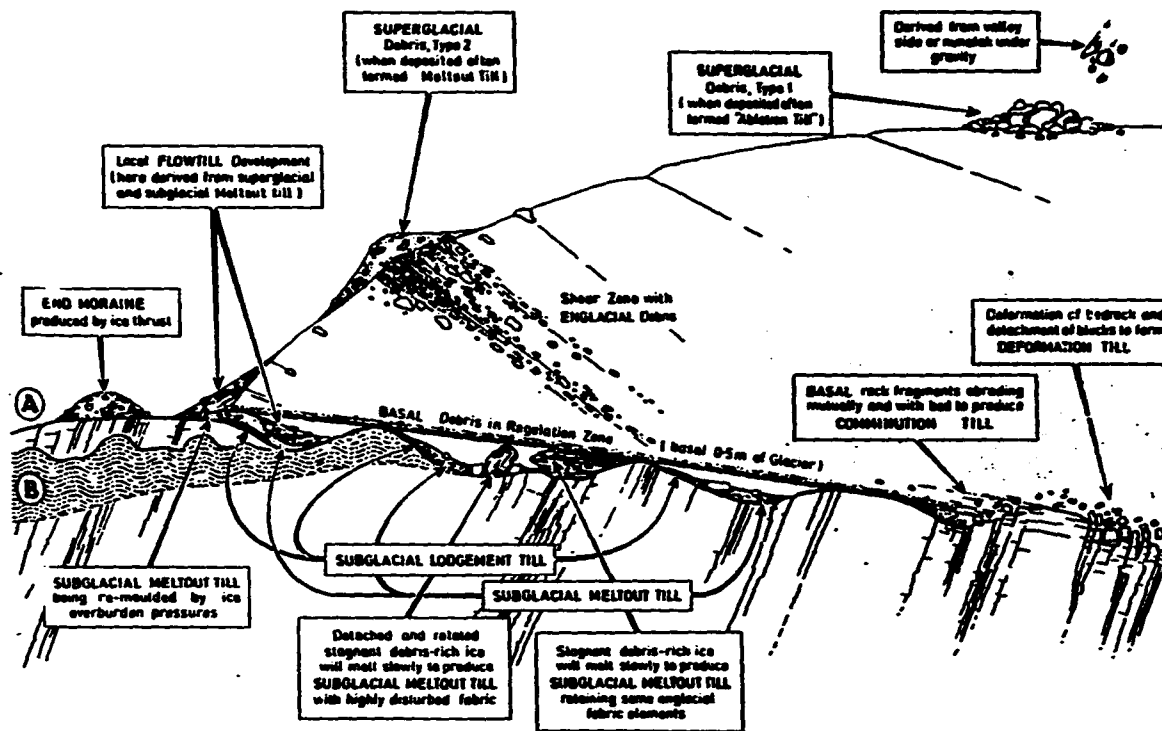


Figure 1. Acquisition, transportation and deposition of tills by a glacier (McGown and Derbyshire, 1977)

can be found in Kemmis et al., 1981, Boulton and Paul, 1976, and McGown and Derbyshire, 1977.

Basal till (subglacial till) deposits usually regarded as an impermeable aquatard have been reported to contain fractures that could affect the geotechnical and hydraulic properties of the deposit, particularly in regard to ground-water contamination.

Past investigations concluded that fracturing of a glacial till may result from a variety of causal factors such as shear stresses associated with glacial action, stress relief, desiccation, syneresis, and chemical action. Establishing the genesis of fractures in a till deposit may be difficult because different processes could work alone or in combination through time, and sometimes similar structures might be formed by several different processes. This section discusses the genesis of fractures in fine-grained till deposits. The term "fracture" is used in this paper to designate any discontinuities in the fine-grained sediments, described by researchers with different terms, such as joint, fissure, and joint plane, etc.

Mechanics of fracture formation

Past researches indicate that fractures in glacial till or fine-grained soil deposits may be considered in two general categories; fractures related to shear stresses and

those related to tensile stresses.

Mohr's failure theory has been found to be a suitable model to explain the failure behavior of a soil mass. According to this theory, shear failure will take place along planes having angles of $45^\circ + \phi/2$ to the major principal plane on which the major principal stress acts, where ϕ is the angle of internal friction. Principal stresses are normal stresses acting on three orthogonal planes of a stressed point on which there are no shear stresses. The largest of these three stresses is named the major principal stress, σ_1 , the smallest is called minor principal stress, σ_3 , and the third is called intermediate principal stress, σ_2 .

When the horizontal stress is the maximum principal stress of a soil mass, shear failure will take place along planes dipping at angles of $45^\circ - \phi/2$ to horizontal, and is defined as the passive state. The converse is the active state, wherein shear failure is caused by the vertical stress being the maximum principal stress, and shear planes have angles of $45^\circ + \phi/2$ to horizontal plane. These two orientations are shown in Figure 2 (Lambe and Whitman, 1979).

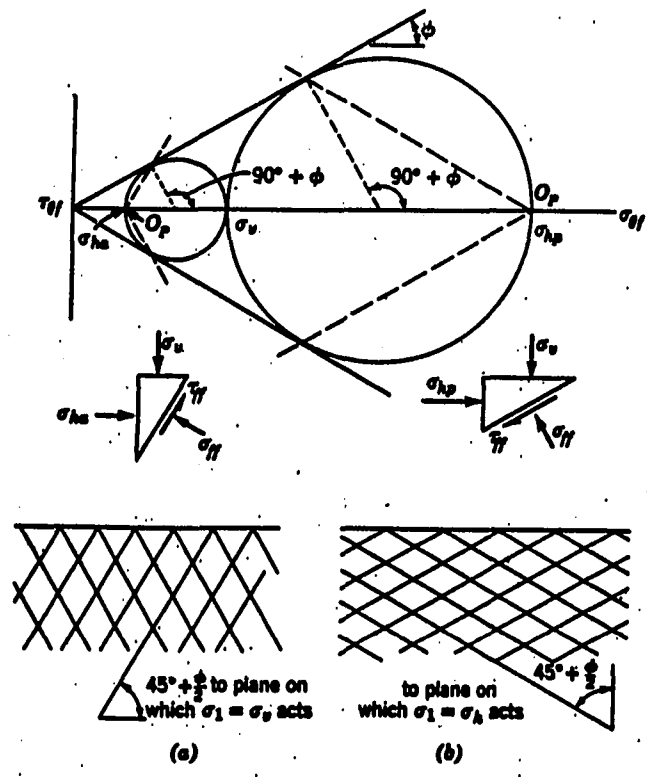


Figure 2. Orientation of slip lines for Rankine state
 (a) active state (b) passive state (Lambe and Whitman, 1979)

Shear-stress related fractures

Several researchers have reported "sub-horizontal" fractured observed in subglacial deposits. These fractures might be interpreted as being caused by passive thrust force, or dragging force induced by glacier during glaciation. Boulton and Paul (1970, 1976) found that lodgment till underneath Norden Siodbreen showed sub-horizontal fracture surfaces which carried heavy slickensides in the direction ice movement, confirming shear along these surfaces. Johnson (1983) also found sub-horizontal shear planes in the direction of ice-flow but dipping 14°, in the Hanson Creek Members of the Miller Creek Formation, in Wisconsin along the bluffs of Lake Superior. Such a low dipping angle implies that the major principal stress is not parallel to the ground surface but in a direction with a certain dipping angle to the ground surface, as shown in Figure 3. Johnson stated that the fractures might represent shearing shortly after deposition of the Hanson Creek Member or during a later advance.

Other passive shear fractures could occur from unloading or glacier retreat causing a decrease in vertical stress, as shown in Figure 2(b). Chandler (1973) indicated that such fractures often occur in weathered, overconsolidated clays and near the ground surface, which could be a consequence of in situ lateral stresses near the ground

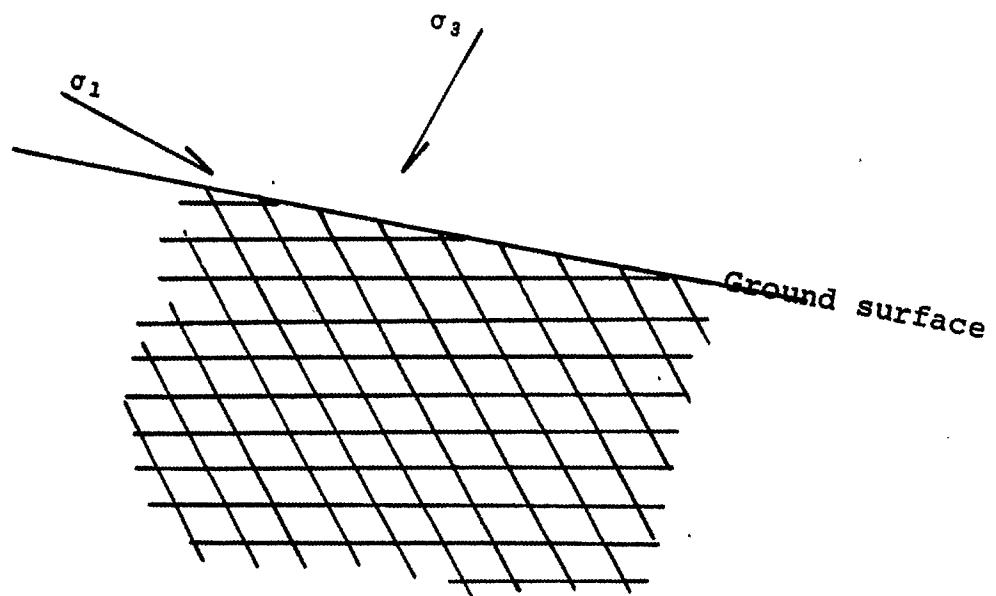


Figure 3. Hypothetical direction of major and minor principal stresses of fractures with low dipping angles

surface exceeding the available resistance.

Though lateral soil stresses commonly are considered to be isotropic, some cases suggest that directional anisotropic lateral earth pressure may exist. The differential horizontal stresses could be caused by geometry of land form, tectonic stress (Haimson, 1973) and the moving direction of the glacier. All factors listed above could cause vertical and sub-vertical fractures in soil. McGown et al. (1974) reported that the well-patterned vertical and sub-vertical fractures in till deposit at Hurlford, Ayrshire were caused by directional lateral stresses of which the principal stress trended roughly coinciding with the drumlin orientation. Skempton et al. (1969) observed vertical and subvertical fractures which were systematic in two directions in an overconsolidated Eocene clay and suggested that the fractures were related to directional horizontal soil stresses.

Tensile-stress related fractures

Tensile fractures are believed to be formed from weathering which leads to a decrease of the soil volume. The factors causing "tensile" fractures can be summarized as desiccation, syneresis, stress relief, and freezing of soil.

Desiccation was defined as a process of losing moisture in soil, and can lead to tensile failures in a fine-grained soil deposit (Kleppe, 1981). Desiccation fracturing is controlled by the clay content and mineralogy, and tends to be vertical or subvertical with a polygonal surface pattern (Boulton and Paul, 1976, Kleppe, 1981). The fracture width and depth are increased by repeated of wetting-drying cycles. The spacing between fractures increases with depth because moisture near the surface can more easily evaporate. Varying depths of desiccation fractures have been observed.

Syneresis, a spontaneous loss of water from a gel after aging (Kazi and Knill, 1973; Mitchell, 1976), can cause fractures in normally consolidated clays at moisture content well above the shrinkage limit (Skempton and Northey, 1952).

Stress relief caused by erosion of overburden or removal of lateral material can lead to the formation of fractures oriented perpendicular to the direction of unloading. Fookes and Dennes (1969) found fractures parallel to bedding and parallel to a slope surface, and suggested that the fractures were formed during unloading or stress release perpendicular to the bedding and the slope surface.

Freezing of the moisture contained in the pores of soil can cause the growth of ice lenses in till, which causes sub-horizontal fracture (Boulton and Paul, 1976). Because of the formation of ice in pores, the soil skeleton can

actually shrink due to desiccation of expansive clay minerals. Thus freezing could cause soil to expand in the vertical direction while contracting in the horizontal direction (Spangler and Handy, 1982) and enlarging existing fractures or creating new fractures.

Chemical weathering could also affect fracture formation with a decrease of soil volume by leaching or cation exchange. For instance, the release of potassium may result in fractures (Mitchell, 1976), and removal of carbonates may be responsible for fractures found in the leached pre-illinoian till at eastern Iowa (Connel, 1984). Loss of volume in sodium montmorillonite can occur when exposed to a more dilute water solution, or the sodium on the interlayer is replaced by calcium (Mitchell, 1976).

Fractures formed by weathering usually are found in a near-surface zone and show random orientation. Fractures in a weathered zone usually show oxidation along their surfaces, or organic materials brought in by vertical water movement that facilitates observation of fractures.

Laboratory Hydraulic Conductivity Tests**Darcy's law**

Darcy's law has been used to examine the flow rate of a fluid through saturated porous media since the law was published in 1856. The equation is:

$$Q = KiA \quad (1)$$

in which

Q : flow rate (L^3/T)

K : coefficient of permeability or hydraulic
conductivity (L/T)

i : head loss per unit length of a soil sample

A : cross sectional area (L^2)

Bear (1979) showed that the Darcy's law was only valid when the Reynolds number of the fluid flowing a soil sample does not exceed 10. The Reynolds number is defined as $Re = qd/v$, where d is some representative length of the porous matrix, and v is the kinematic viscosity of the fluid, and q is specific discharge which equals to Ki. Bear also suggested using D_{10} or D_{50} , they are grain sizes which 10% and 50% respectively of the soil particles are smaller than, of a soil sample in calculating the Reynolds number.

Methods of permeability testing in the laboratory

The methods most commonly used in laboratory measuring permeability of soils are constant head method, falling head method, and Terzaghi's one-dimensional consolidation theory. They are discussed as following:

1. Constant head method

In constant head permeability test, the head loss of permeant flowing through a soil sample is kept constant and the quantity of flow (Q) during a certain time interval (t) is recorded. Permeability of a soil sample is calculated as:

$$K = \frac{QL}{thA} \quad (2)$$

where

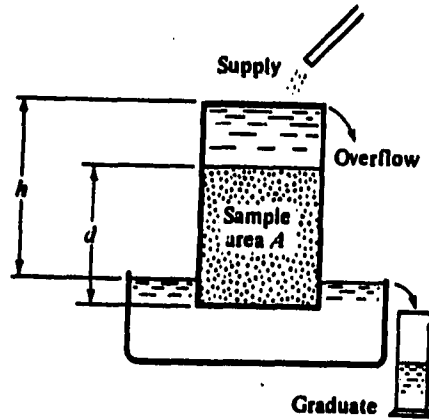
h : the total head loss

L : the length of soil sample

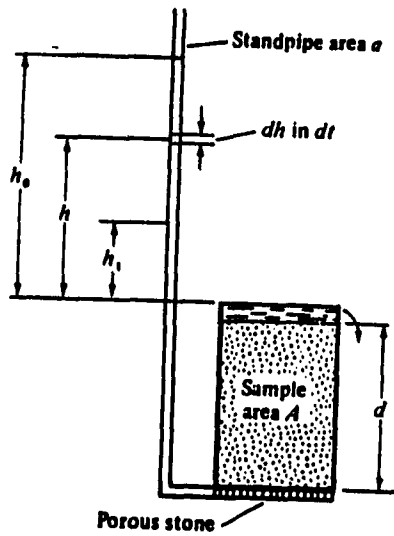
The method is usually suggested to be used in measuring the permeability of coarse-grained soil. The setup of the constant head method is schematically shown in Figure 4a.

2. Falling head method

The method is most used to measure the permeability of fine-grained soil. The setup of falling head method is schematically shown in Figure 4b. In the test, the head loss of permeant flowing through a soil sample, from h_1 to



(a)



(b)

Figure 4. Permeability tests (a) constant head method and (b) falling head method (Spangler and Handy, 1982)

h_2 , during time t are recorded. The coefficient of permeability is calculated as:

$$K = \frac{aL}{At} \left(\ln \frac{h_1}{h_2} \right) \quad (3)$$

where a is cross sectional area of the standpipe.

3. Terzaghi's one dimensional consolidation theory

Terzaghi's consolidation theory is also a common method used to measure the permeability of fine-grained soil.

The assumptions made by Terzaghi are (i) strains are small and one dimensional, (ii) the soil is saturated, (iii) the soil grains and the pore fluid are incompressible, (iv) the soil compressibility and permeability are constant during the consolidation process, (v) flow is one dimensional and according to Darcy's law, and (vi) linear relationship exist between effective stress and strain (Taylor, 1958, Tavenas et al., 1983a).

The closed-form solution of Terzaghi's consolidation theory is:

$$\frac{\partial u}{\partial t} = C_v \frac{\partial^2 u}{\partial z^2} \quad (4)$$

where C_v is coefficient of consolidation and is the parameter used to calculate the permeability of soil samples, the equation is:

$$K = \gamma_w C_v m \quad (5)$$

where m is modulus of deformability defined as $-e/\sigma_v(1+e_0)$, e_0 being the initial void ratio of soil.

Taylor (1958) reported that the permeability measured by using this theory usually is underestimated. Though Terzaghi reported that the theoretical results were close to measured permeability and Mesri and Olson (1971) also stated that the calculated permeability of normally consolidated clay were only 5 to 20 percent lower than the measured permeability, Tavenas et al. (1983a) measuring the permeability of natural clay reported that the use of Terzaghi's consolidation theory to interpret the result in terms of C_v and K appeared questionable. The problem could be due to an unrealistic assumption in the theory, that K , m , and C_v are constant. Actually, clays exhibit significant variation of K , m , and C_v as the void ratio reduces during consolidation (Taylor, 1958).

Carpenter (1982) performed consolidation tests on carefully controlled and homogeneous soil samples and reported that the parameter m eventually was kept a constant, while C_v reduced dramatically as the compressive stress exceeded preconsolidation stress, as shown in Figure 5.

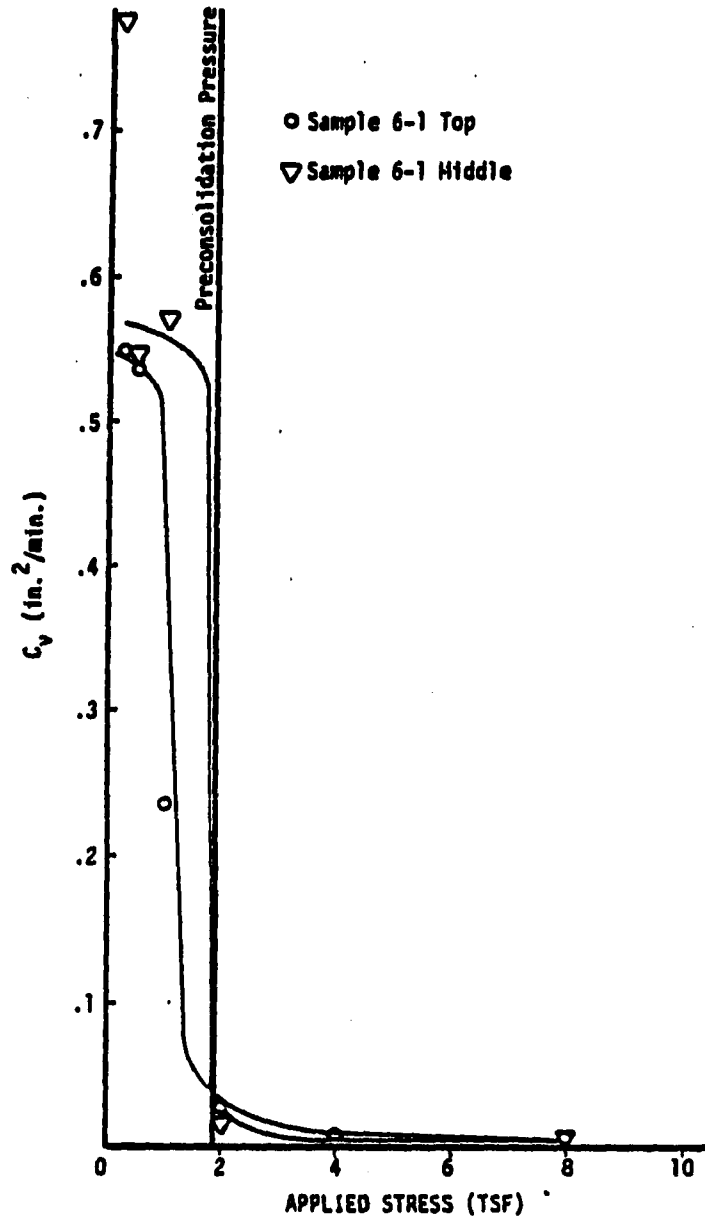


Figure 5. Applied stress-coefficient of consolidation relationship for samples with a dispersing agent added (Carpenter, 1982)

Test apparatus

Two major types of permeameter are commonly used in laboratory tests, a fixed-wall permeameter and a triaxial cell permeameter.

In a fixed-wall permeameter, soil samples are either trimmed into a metal ring or compacted into a cylinder and then tested in a permeameter setup or oedometer cell (Olson and Daniel, 1981).

The problems associated with using a fixed-wall permeameter are (i) the stress field acting on soil in situ can't be reproduced, and (ii) leakage tends to occur along the interface between soil samples and the wall of permeameter. As expected, the fixed-wall permeameter usually gives a higher hydraulic conductivity than does a triaxial permeameter (Boynton, 1983).

In a triaxial permeameter, a rubber membrane replaces the rigid ring or cylinder and is kept tightly compressed against the sample with a confining pressure applied to the fluid in the triaxial chamber. The main advantages of this apparatus are (i) the leakage through the interface between soil sample and rubber membrane can be minimized or eliminated and (ii) the in-situ stresses can be simulated in the triaxial chamber.

It should be noted that the "triaxial cell permeameter" used by some researchers is not a true triaxial apparatus if only isotropic confining pressure can be applied to the soil samples, i.e., vertical stress always equals to horizontal stress, a situation that is well known to be uncommon in the field.

Factors affecting the measurement of permeability in laboratory

Several factors can affect results of laboratory permeability testing, they are:

1. Sample preparation: Disturbance commonly occurs when trimming the soil samples, such as cracks forming around the edges of samples, fractures opening as the result of stress release, or a smear zone that can form across the surface of sample and block the path of permeant (Carpenter, 1982, Moore and Ali, 1982). These problems can be only minimized by careful handling and the use of proper technique, but are not eliminated.
2. Effective stress applied to soil sample: Stress-related problems include unrealistic stresses applied to the soil, and an unrealistically high gradient of permeant flowing through a soil sample. Unrealistic stresses may be due to the limitations of the permeameter, as in a fixed-wall permeameter, or may reflect a lack of measurement of the

applied in-situ stresses. Research shows that the effective stresses applied to a soil sample directly affect the void ratio, which should change the results of permeability (Carpenter, 1982, Daniel, 1984).

A decrease of hydraulic conductivity as a result of high hydraulic gradient used in tests was reported by researchers (Moore and Ali, 1982). This may be due to the migration and accumulation of fine particles blocking the path of permeant, or an excessive effective stress reducing the void space at the outflow end (Carpenter, 1982).

3. Properties of permeant: Mesri and Olson (1971) reported that the measured permeability was larger for a nonpolar fluid than for a polar fluid, and that a reduction in electrolyte concentration in the permeant tended to reduce the permeability. Other factors, such as viscosity, density, and temperature of permeant can also affect the measurement of permeability (Bear, 1979; Williams and Garvolden, 1967).

4. Sample size: Several researches have shown that, in laboratory tests, small soil samples always reveal lower hydraulic conductivity than large samples, and permeability measured in laboratory was always smaller than in situ permeability. That could be due to small specimens not containing the same structures, such as fractures or micro cracks, and the compaction effects occurring in sampling which cause soil samples to be denser than the in situ soil.

Mechanical factors controlling permeability

Mesri and Olson (1971) after testing hydraulic conductivity of different kinds of clays with different permeant, concluded that the distribution of void sizes and their tortuosity play a main roll controlling the hydraulic conductivity. Other researchers have published several empirical equations relating void ratio and permeability.

Hazen suggested an empirical equation to estimate the permeability of filter sand, which can be expressed as (Taylor, 1958):

$$K = C D_{10}^2 \quad (6)$$

where C is a constant, if cgs units system was used, C is 100. Taylor (1958) recommended that this equation could be only accepted as an expression for average conditions for the range represented in Hazen's data, and might not give satisfactory results for soils of other types.

Another well-known theoretical equation to express the relationship between permeability and void ratio is the Kozeny-Carman equation:

$$K = \frac{1}{CS^2} \frac{\gamma}{\mu} \frac{e^3}{(1+e)} \quad (7)$$

in which

C : factor depending on pore shape and ratio of length of actual flow path to soil bed

thickness

S : specific surface area

γ : unit weight of permeant

μ : viscosity of permeant

e : void ratio

Taylor (1958) also published an empirical equation based on Poiseuille equation to reflect the influence of the permeant and soil characteristics on permeability:

$$K = D_s^2 \frac{\gamma}{\mu} \frac{e^3}{(1+e)} C \quad (8)$$

where C is a shape factor and D_s is an effective particle diameter. Taylor's equation can be considered as a simplification of the Kozeny-Carman equation. Taylor also showed that the equations are valid only for sand and can not be applied for clay.

Several researchers published empirical equations to correlate void ratio and permeability of normally consolidated cohesive soil samples.

Mesri and Olson (1971) suggested a linear relationship between $\log K$ and $\log e$:

$$\log K = A \log e + B \quad (9)$$

Samarasingie et al. (1982) suggested a slightly modified equation:

$$\log K(1+e) = n \log e + C \quad (10)$$

where A, B, C, and n are constants depending on the type of clay.

In addition to the void ratio, fractures in fine-grained soil can be a dominant factor controlling the ground water flow. Williams and Garvolden (1967) using piezometers to measure the ground water in glacial till, suggested that joints in glacial till control the characteristics of ground water movement. Several researchers have found that fractures can dramatically increase the conductivity of the landfill liners. Contributing factors include the opening, length, and orientation of cracks, as discussed in the next section.

Fluid flow through a single fracture

The cubic law is commonly used to analyze the hydraulic properties of a fractured rock (Snow 1968; Iwai, 1976; Witherspoon et al. 1980). In this theory, flow is assumed to be steady, isothermal, and incompressible in a single fracture. The basis is an idealized concept of flow in a fracture with parallel planar surfaces. The result may be given in a simplified form:

$$\frac{Q}{\Delta h} = cb^3 \quad (11)$$

Where Q is the flow rate, Δh is the loss of hydraulic head along the flow path, c is a constant that depends on fracture geometry and the properties of the fluid, and b is the aperture of the fracture. Iwai, 1976, performed permeability tests on different rocks containing artificial fractures and subjected to different axial stresses oriented perpendicular to the fractures, and concluded that the flow rate is a function not only of the magnitude of stress applied, but also the stress history acting on rocks.

Perhaps due to the difficulties in monitoring the behavior of fractured soil samples under stresses, no references stating a relationship between the aperture of a fracture and the flow rate in a soil sample has been found. Williams and Garvolden (1967) observed groundwater flows by installing piezometers in a glacial till, and reported that some piezometers experienced a large, rapid increase in potential after precipitation which implies that some path of high permeability must exist in the glacial till. Grisak (1975) used piezometers and computer program simulation to analyze the permeability of a systematically fractured glacial till, and found that the equation presented by Snow (1968) for the porosity of a systematically fractured material can be used to calculate the fracture porosity, that in

turn is related to the fracture spacing and intrinsic permeability of a glacial till.

$$n = 5.45 \left(\frac{k}{\Delta^2} \right)^{1/2} \quad (12)$$

where n : fracture porosity

k : intrinsic permeability (L^2)

Δ : spacing between fractures of each set

The results of a series of permeability tests by Bosscher et al. (1988) on a spherical sample with a single fracture under constant confining pressure indicated that the permeability in the direction parallel to the joint was significantly higher than the permeability perpendicular to the joint. Bosscher et al. further indicated that as the orientation of the fracture came closer to the direction of fluid flow, the flow rate increased dramatically, the critical angle appearing to lie between 20 to 30 degrees. Relative to fractures in clay liners, a computer simulation by Moore and Ali (1982) indicated that if the penetration ratio is more than 75 percent of the thickness of the liner, a crack will cause a significant increase in vertical permeability.

Stresses Acting on Soil Samples

As mentioned in foregoing discussion, the stresses applied to soil samples play a important roll in the measurement of permeability. Typical results of measuring permeabilities under different confining stresses are shown in Figure 6. It can be seen that the permeability of soil samples dropped to a lower and more stable value after the confining stress reached a "certain level". McGown and Radwan (1975) conducted one-dimensional consolidation on fissured soil and reported that in-situ overburden stress was the main factor controlling the changing of hydraulic conductivity (Figure 7). However, the data reported by Carpenter (1982) suggested that the preconsolidation stress rather than the in situ overburden stress is the controlling factor, as shown in Figure 4. These conclusions were based on results of one-dimensional consolidation tests in which the lateral stress could not be reproduced. Also the theory used to calculate permeability from time-consolidation data, as indicated by several researchers, may be in question.

To produce a more reliable result in laboratory permeability tests, the similitude to in situ stresses acting on the soil could be important.

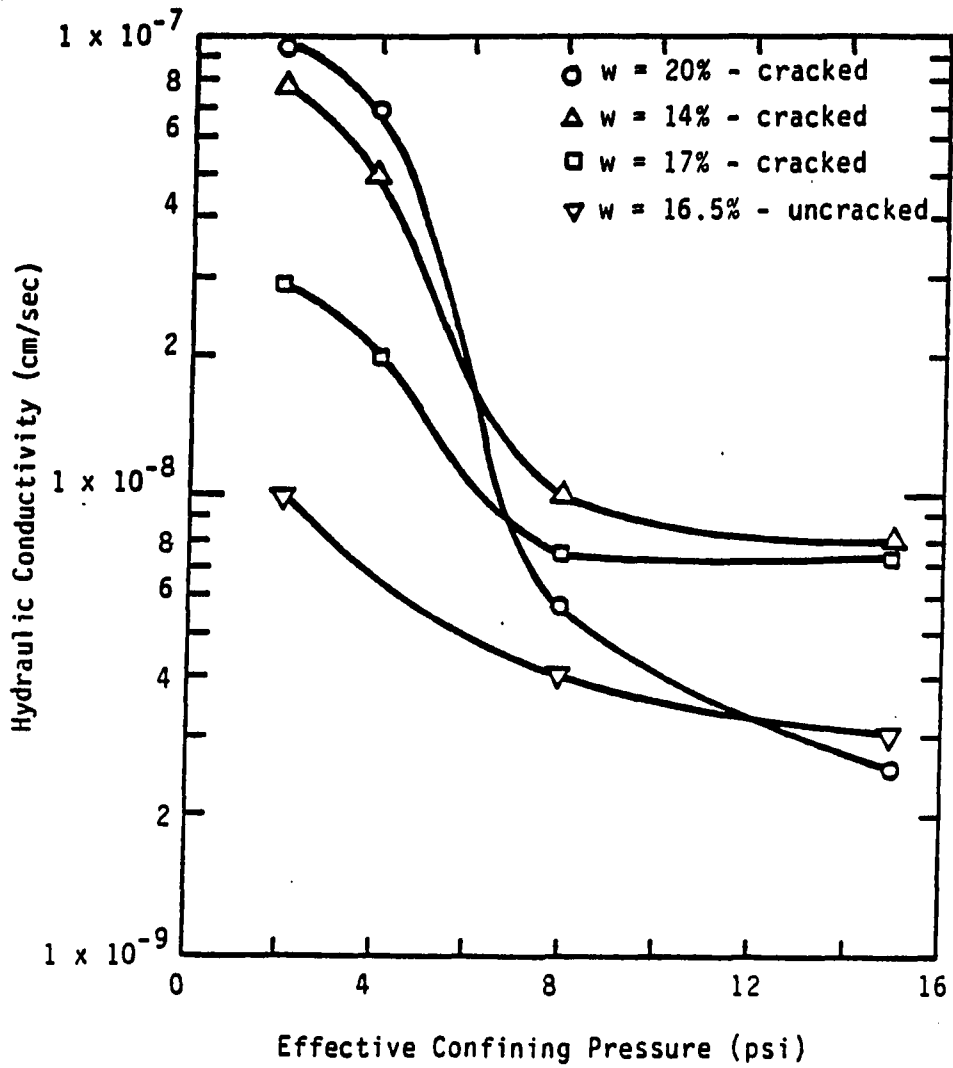


Figure 6. Effect of confining pressure on the hydraulic conductivity (Boynton, 1983)

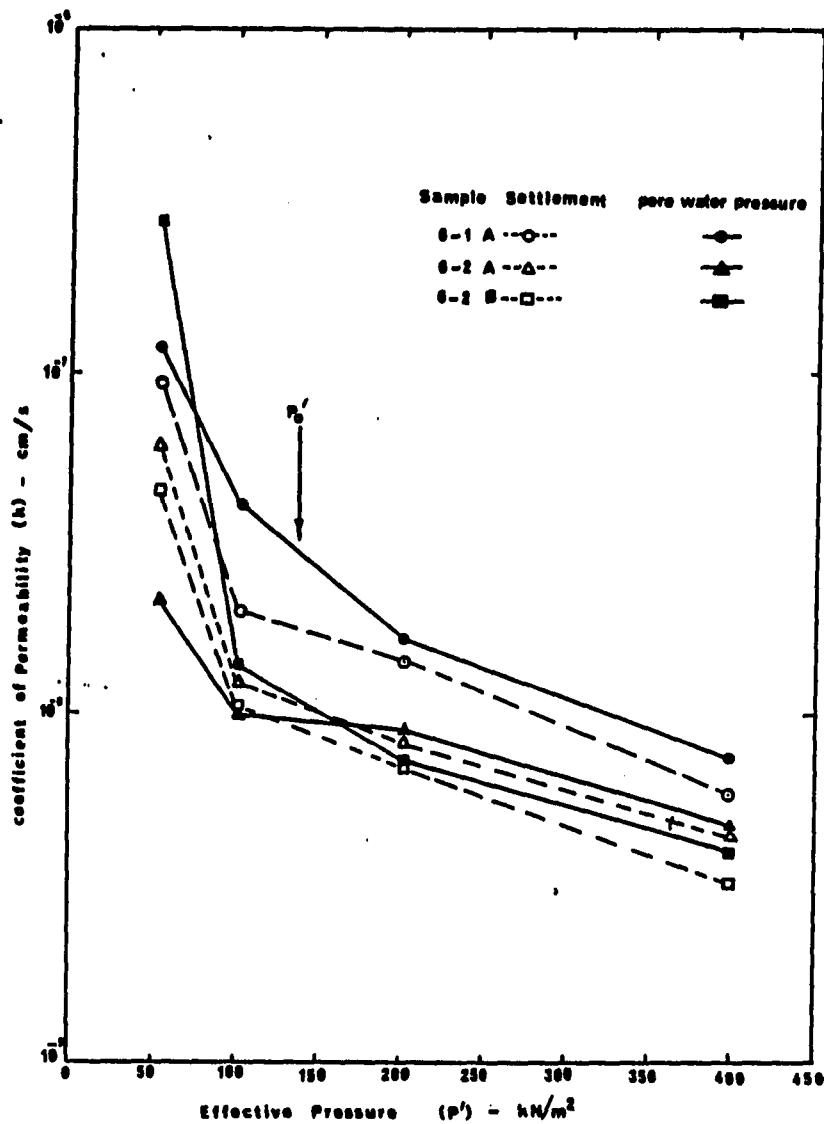


Figure 7. Variation of the coefficient of permeability with applied effective stress for specimens from North Hanover St. Glasgow (McGown and Radwan, 1975)

Lateral earth pressure measurement

As indicated by Schmertmann (1985), the in situ lateral earth stress has been shown to play a major role in geotechnical engineering problems, such as pile foundation design, retaining walls, and slope stability. Lateral earth stress also can relate to the formation of fractures in glacial deposits and bedrock, as discussed in foregoing section.

Conventionally, lateral soil stress is indicated by ratio K_0 that is the ratio of effective horizontal stress to effective vertical stress. Effective vertical stress can be calculated by the equation $h\gamma - u$ with relatively small error, where γ is unit weight of the soil, h is the depth, and u is the pore pressure at depth h . Lateral earth stress is less predictable.

In the past, researchers have attempted to express K_0 by simple equations. The well-known Jaky equation (cited from Spangler and Handy, 1982) relates K_0 to the effective internal friction angle (ϕ) of soil;

$$K_0 = 1 - \sin \phi \quad (13)$$

The equation has been proven to be accurate for normally consolidated sand (Brooker and Ireland, 1965). Brooker and Ireland (1965) also proposed equations of K_0 for normally consolidated cohesive soil;

$$K_0 = 0.95 - \sin \phi \quad (14)$$

or $K_o = 0.44 + 0.42(PI)$

in which PI is the plastic index. For over-consolidated soil, K_o has been related to the effective friction angle and the over-consolidation ratio (OCR):

$$K_o = (1 - \sin \phi) OCR^n \quad (15)$$

where a value of $n=0.4-0.5$ is frequently used, but $n=0.7$ was reported by Sheriff and Ishibashi (1981) for dry sand. Mayne and Kulhawy (1982) modified the equation to account for OCR effects on K_o after one cycle of unloading and partial reloading, by reviewing 170 different published data and suggested that n equals to $\sin \phi$.

Recent research indicates that the in situ lateral earth stress may vary widely and generally is not predicted by above equations. Schmertmann (1985) referenced a range in K_o from 0.2 to 6.4 in the literature. The variability of K_o was attributed to the pattern of soil formation, past loading history, aging, man-induced effects, and shrink-swell properties of soil, etc. Due to this complication, it is difficult for engineers to make reasonable estimate of lateral soil pressure without some in situ measurement.

The factors listed above are discussed as following:

1. Loading history: Loading factors that influence lateral in-situ stress include natural erosion and removal of over-

burden, landslides, man-induced compaction, and excavation. For instance, after a landslide occurs, stress is relieved on soil in the slide zone, and dilatant shear can convert from overconsolidated soil into normally a consolidated soil. Actual measurements of lateral stresses in compacted embankments in Iowa (Yang, 1987) indicated that the lateral stresses in a slide, a potential slide, and a nonsliding part of slope showed the results of lateral stress relief at different stages of sliding. K_0 could also increase after compaction or driving of displacement piles (Schmertmann, 1985).

2. Soil swelling effects: Some active clay minerals have a strong tendency to expand or contract when water equilibrium conditions change. A number of examples of high K_0 condition documented by Schmertmann (1985) are believed due to the swelling of clay minerals. K_0 as high as 3.5 was measured by Tse (1988) using an electric K_0 Stepped Blade in an alluvial floodplain test site with a high shrink-swell potential. On the other hand, the contraction of a soil mass due to desiccation will decrease K_0 and apparent OCR especially in a fractured zone. The results of hydraulic fracture test performed by Al-Shaikh-Ali et al., 1981, showed that the K_0 in the weathered zone of a lodgement till was as low as 0.72.

3. **Weathering effect:** Bjerrum and Huder (1967) illustrated several examples of high K_0 caused by the weathering of overconsolidated plastic clay and clay shale. Bjerrum explained that the weathering process broke the diagenetic bonds generated as a result of overburden pressure, time, and physical and chemical properties of clay, thus releasing the strain energy in the bonding of the clay particles. The release of this stored energy then creates high lateral stresses as lateral movement is restrained. The high lateral stress is regarded as one of the factors causing progressive slope failure.

4. **Time effect:** The secondary compression which involves a time-dependent adjustment of soil structure also can cause an increase in preconsolidation stress (Bjerrum, 1972). Theoretically, an increase in over-consolidation ratio will increase the K_0 , as shown for example by equation 15. Figure 8 shows the effect of age of a soil: a "young" clay left under a constant effective stress P_0 for hundreds or thousands of years will continue to settle into a more stable structure, after which the soil can carry a load that is in addition to the effective overburden pressure without significant volume change. If this "aged" normally consolidated clay is subjected to a consolidation test, the resulting e - $\log P$ curve will look like the curve marked "aged" with a preconsolidation stress P_c .

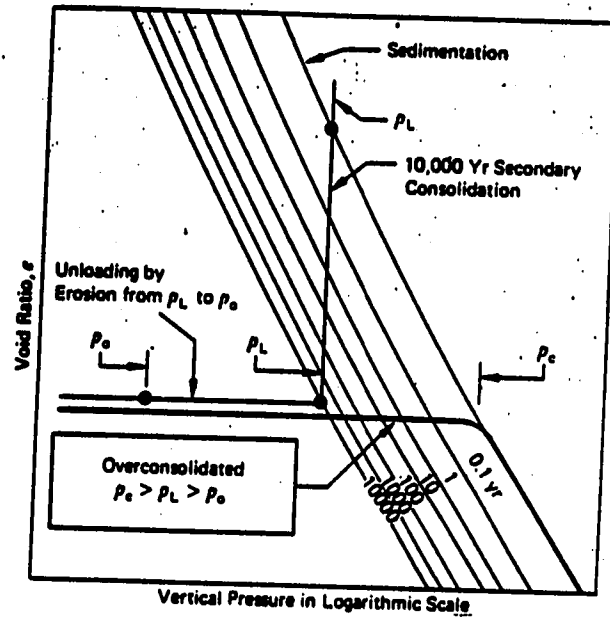


Figure 8. Geological history and compressibility of an overconsolidated clay (Bjerrum, 1972)

Assume the original consolidation and aging is under effective overburden pressure P_L , as shown in Figure 8. The overburden pressure is reduced to P_o . Under the effect of aging the apparent over-consolidation ratio will equal to P_c/P_o instead of P_L/P_o .

Lateral earth pressure measurement by K_o Stepped Blade

The K_o Stepped Blade was initially introduced by Handy et al. (1982) as a device to measure the lateral earth pressure in situ. The original principle of the measurement of lateral stresses by K_o Stepped Blade was to introduce known amounts of displacement of soil by pushing a flat-plate penetrometer into the soil and measuring stresses acting on steps with different thickness, then extrapolating the data to determine a stress at zero thickness (Figure 9).

The observed exponential relationship corresponds to a strain hardening behavior implying densification (Figure 10). Based on a series of controlled laboratory tests using compacted soil, Handy et al. (1982) suggested that the initial stress condition could be expressed as:

$$P_o = a P_1 e^{bt} \quad (16)$$

in which P_o = in situ lateral stress

P_1 = pressure measured on a blade with thickness t

a = coefficient, assumed to equal to 1

b = coefficient, slope of the extrapolating line

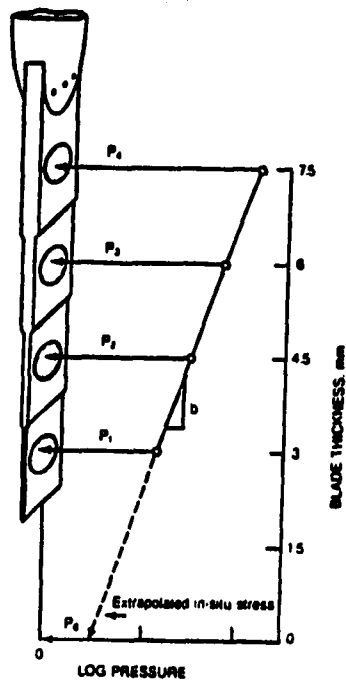


Figure 9. Schematic K_0 Stepped Blade and its method of interpreting data (Handy et al., 1987)

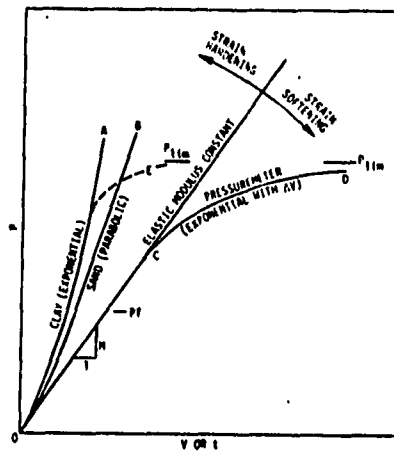


Figure 10. Theoretical and observed pressure-volume responses for soils, OA is consistent with linear e - $\log p$ relationship (Handy et al., 1982)

The coefficient b was originally regarded as an indication of drained soil compressibility equal to $m/2h$ (Handy et al., 1982), where m is a constant related to compressive tangent modulus of normally consolidating clay and h is the effective thickness of consolidating soil induced representing a summation through the gradually dissipating pressure bulb by the insertion of the blade. Lutenecker and Timian, 1986, found that b generally varied in a wide range and suggested that b is an indication of the generalization of pore pressure in the soil instead of drained soil compressibility.

Soil behavior and data interpretation

Often, due to the complication of natural soil structure, the data of in situ SBT do not show the behavior as shown in Figure 9. Data published by Handy et al. (1987) showed that in one third to one fourth of the tests, the first point was a high "outliner" reading (Figures 11b, c), and in most tests the thickest step generally gave pressure reading lower than the previous one. Such soil reactions were explained by (1) elastic soil behavior, (2) consolidation, and (3) plastic failure (Handy et al., 1987), discussed as following:

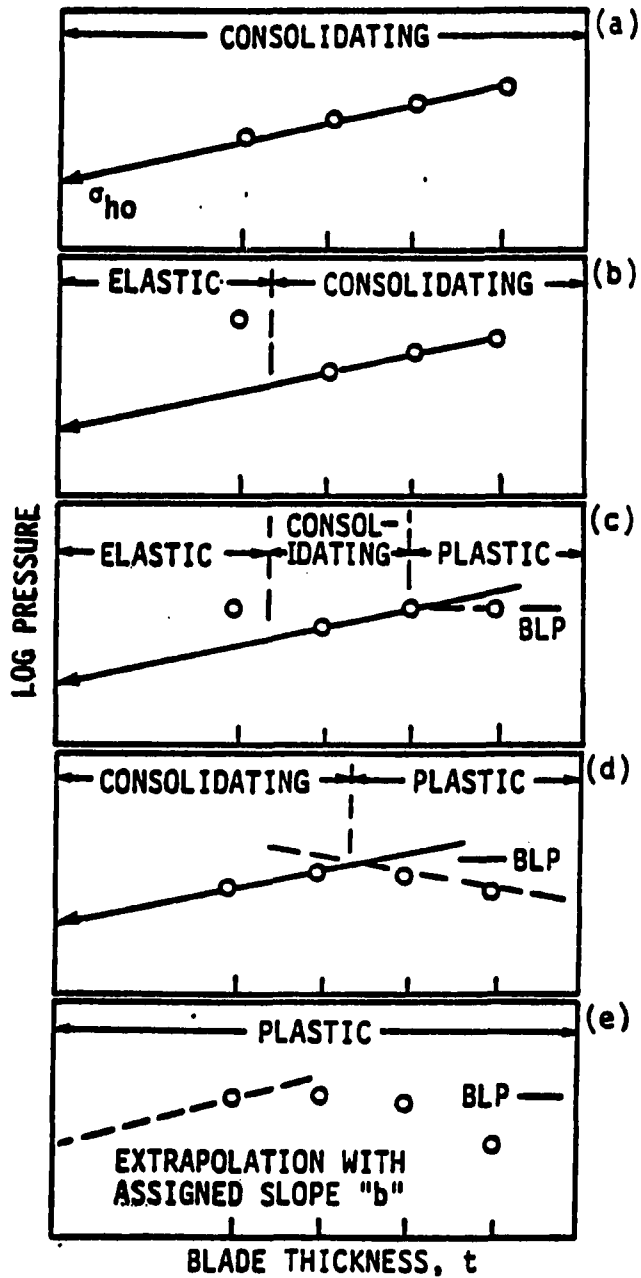


Figure 11. Representative data plots of blade pressure on a vertical logarithmic scale versus blade thickness (Handy et al., 1987)

1. **Elastic soil behavior:** Elastic behavior is indicated by a pressure reading that is higher than the reading given by the extrapolating line (Figures 11b, c). This "high pressure reading", only occurs from the thinnest step, and was hypothesized to be an essentially elastic response prior to breaking down the soil structure. Such a pressure reading on first step may relate to the horizontal preconsolidation stress in saturated soils, or to a false preconsolidation pressure attributed to cementation or apparent cohesion in unsaturated soils.
2. **Consolidation:** Consolidation behavior of soil after the insertion of blade results in a linear relationship between blade thickness and the logarithm of measured pressure (Figures 11a, b, c, d). This relationship is consistent with a linear "e-logP" graph in conventional consolidation testing (Handy et al., 1987). Only those pressures associated with an observed consolidation behavior are used for extrapolation to a "zero thickness" horizontal stress. As mentioned by Handy et al. (1987), blade pressures should be determined at uniform times after blade insertion because that the degree of consolidation is time-dependent.
3. **Plastic failure:** In this behavior, the measured stresses stay constant or decrease regardless of increased blade thickness. This suggests that the rate of generation of pore pressure during the breakdown of soil structures is

about the same as the rate of pore pressure dissipation, coupled with loss of strength through remolding. Plastic failure was found to be predominate in blade steps where the ratio of blade width (w) to thickness (t) is less than 7. It may also occur at thinner steps when used in weak soils, if the soils are close to a failure condition due to high lateral in situ stress from containing expansive clays. Handy et al. (1987) defined the lateral stress experienced at the point of failure as the K_0 blade limit pressure.

Previous SBT measurement

The main disadvantage of current pneumatic stepped blade is the lack of a pore pressure measuring device. The hydrostatic pore pressure ($u = \gamma_w * h$) is used to calculate the effective lateral stress, e.g., effective lateral stress equals to measured lateral stress minus hydrostatic pore pressure. However, if the test is conducted in clays, the stress acting on the face of the blade is a total stress and consists of several component (Lutenegger and Timian, 1986):

$$\sigma_b = \sigma_h' + U_o + \sigma_{oh}' + U_e \quad (17)$$

where σ_b = stress measured on the blade

σ_h' = in situ horizontal effective stress

U_o = initial in situ pore pressure

σ_{oh}' = effective horizontal overstress from inserting

the blade

U_e = excess pore pressure generated from inserting the blade

In a normally or lightly consolidated soil, the contribution from σ_{oh}' is probably small and the majority of measured stress is probably excessive pore water pressure. For sequential steps of the blade, the measured stress would increase from a further increase in excess pore pressure (Lutenegger and Timian, 1986). The results of SBT at an alluvial floodplain, which was located at the north of the Spangler Geotechnical Laboratory at the Iowa State University, showed that K_0 could be as high as 12. Due to the lack of measuring pore pressure, Mings (1987) concluded that the coefficient a in equation 16 should equal to 0.5 instead of 1.0 to obtain reasonable K_0 values. Tse (1988) used an electric K_0 Stepped Blade to measure the lateral stresses at the same test site. The electric blade was constructed of a high strength stainless steel with the same shape as the first two steps of the pneumatic Stepped Blade, in which the total stress transducer and pore pressure transducers were used to measure the total lateral stress and pore water pressure, respectively. The results of electric SBT confirmed that in this soil, the pneumatic Stepped Blade (with $a=1$) could overestimate the lateral stresses by a factor 1.5

to 2.5.

In an overconsolidated soil that does not generate positive pore pressure after insertion of the blade, the increase in b for successive blades is primarily from oh which may be offset by negative pore pressure from the tendency to dilation (Lutenegger and Timian, 1986). However, no relevant tests have been performed to verify the above statement.

FIELD TESTS

Glacial Geology of North Central Iowa

Glaciation is an integral part of the pleistocene history of Iowa. According to classic concepts four periods of continental glaciation covered all or part of the state: the Nebraskan, Kansan, Illinoian and, Wisconsin glaciers. Wisconsin glaciation, the most recent and less extensive than the Nebraskan and Kansan, is characterized in Iowa by two stages. Ice during the Tazewell stage (20,000 years before the present) terminated about 100 miles south of the Iowa-Minnesota border. Tazewell drift has been obscured, in part, by the second stage, Cary drift. The Cary drift glacier (14,000 years b.p.) extended 135 miles into Iowa to its terminus at Des Moines, creating a deposit known as the Des Moines Lobe (Ruhe, 1969).

The thickness of Cary Ice is estimated approximately to be 2,700 feet (840 m) in the vicinity of Ames, Iowa, which is 34 km from the limiting margin of ice (Foster, 1969). Foster also estimated that the rate of Cary advance was approximately 1,000 ft/year. The hypothetical glacial flow lines of the Cary Glacier at the time of the maximum extension are shown in Figure 12.

Hypothetical Cary Flow Lines

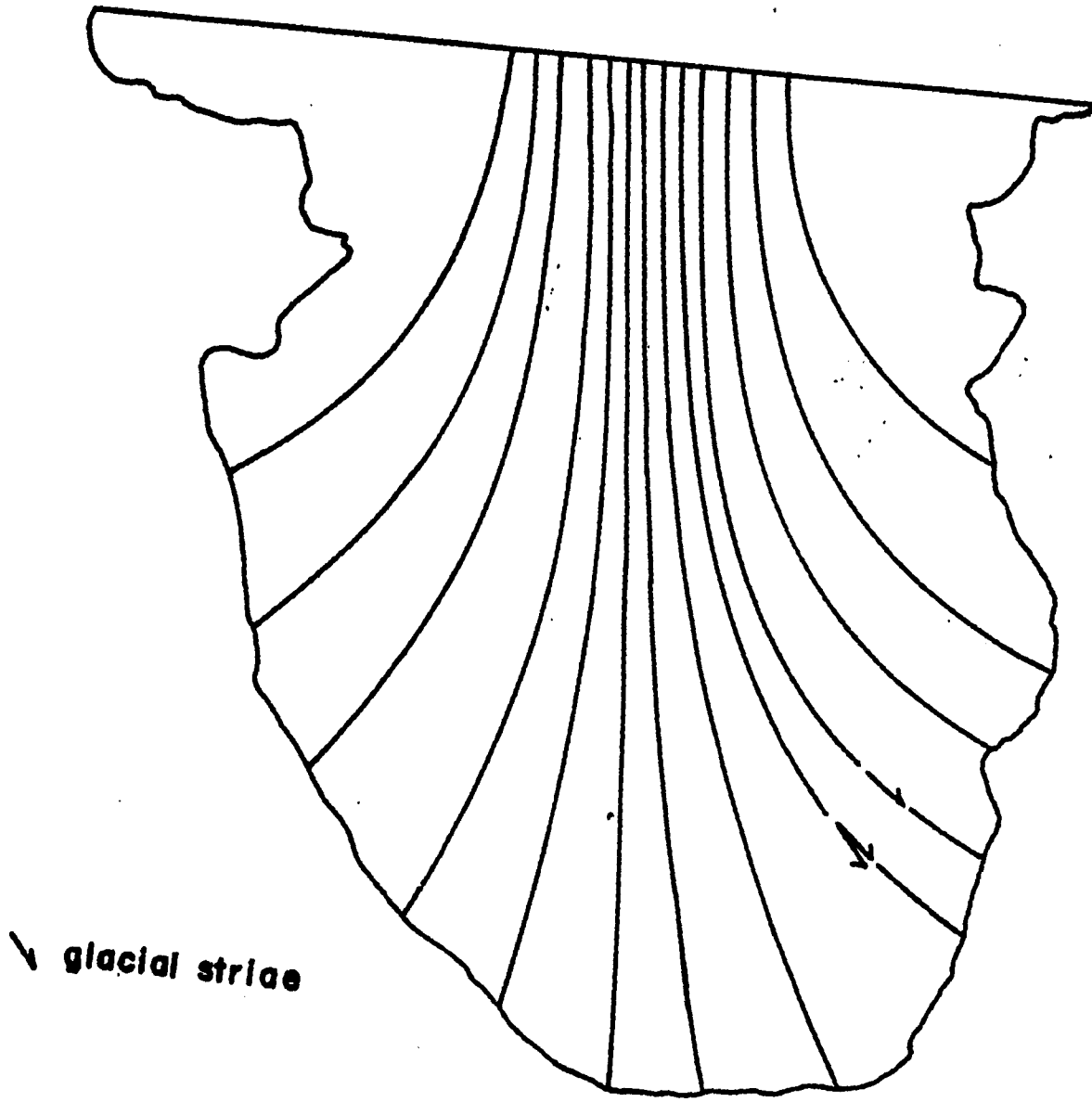


Figure 12. Hypothetical Cary flow lines (Foster, 1969)

Generally, till deposits consist of different size of particles carried and then dumped by melting glacial ice. The mixture of different-sized particles is deposited without sorting or stratification (Anderson, 1983). Cary till and till-related deposits in Iowa are presently differentiated by the Iowa Geological Survey into two fundamental categories: basal till and supraglacial sediment (Kemmis et al., 1981). The basal till and supraglacial sediments are differentiated through the combined use of several types of data: (1) texture, (2) the nature of stratification and sorting, (3) stratigraphic position with the sequence of sediments and the nature of contacts between unit, and 4) geotechnical properties.

There are marked differences in the ranges of matrix texture (less than 2 mm fraction) between the basal till and the supraglacial sediments. Over the Des Moines area the basal till is loam-textured and quite uniform with small standard deviations and a relatively small total range of texture, except for a instances occur in the lowest portion of the basal till. The basal till is often remarkably uniform, varying only a few percent in any particle-size category.

In contrast to the texture of basal till, the supraglacial sediments have great variability of texture and material, due to their different processes of deposition. The

differences of texture between basal till and supraglacial sediments are shown in Figure 13. Other than the texture, the supraglacial sediments also differ from basal till in density, particle sorting, greater lateral and vertical variability in deposits, and location of the deposits. For further details one may refer to the Iowa Geological Survey Guide Book, Series No. 6 (Kemmis et al., 1981).

In terms of geotechnical properties, the basal till generally reveals a higher bulk density and over-consolidation ratio than supraglacial sediments. The result from Kemmis et al. shows that the supraglacial deposits range in dry bulk density from 1.44 to 1.85 g/cc (89.7 to 115 pcf) with a mean value 1.62 g/cc (103 pcf), and basal till ranges from 1.69 to 2.09 g/cc (105 to 130 pcf) with a mean value 1.89 g/cc (117.7 pcf) (Figure 14).

It also was reported by several researchers that most basal till tends to be heavily overconsolidated except where deposited in a poor subglacial drainage condition. Some OCR values have been found to be as high as 25 (Boulton and Paul, 1976).

Drift deposits of the Des Moines Lobe in Iowa are tentatively classified rock-stratigraphically as the Dows Formation. The Dows consists of the surfacial glacial deposits in north-central Iowa and the youngest Wisconsin (Cary) glacial deposits in the state. In the Iowa

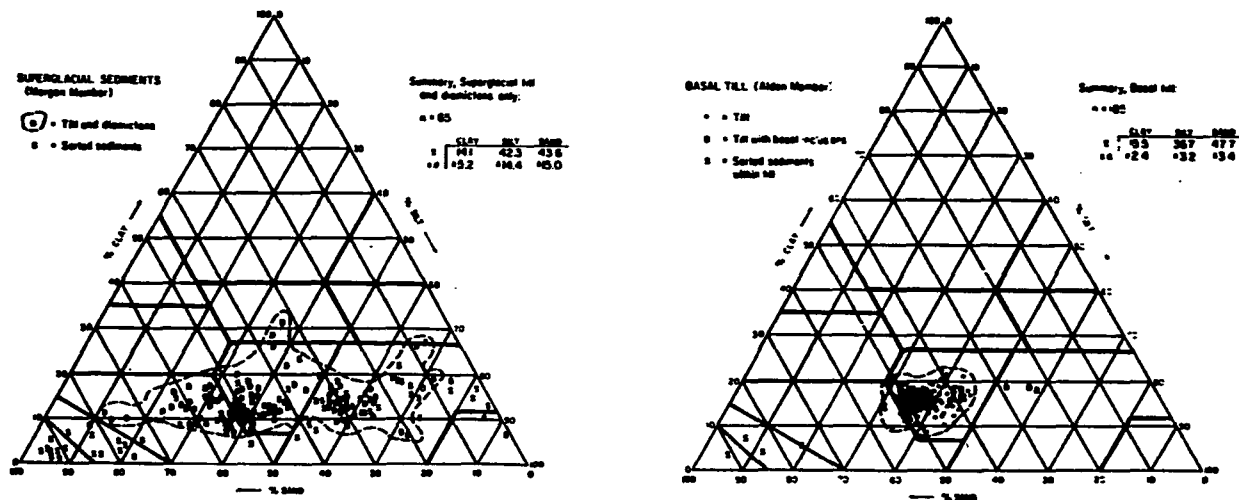


Figure 13. Summary of textural data for the supra-glacial deposits and basal till of the Des Moines Lobe (Kemmis et al., 1981)

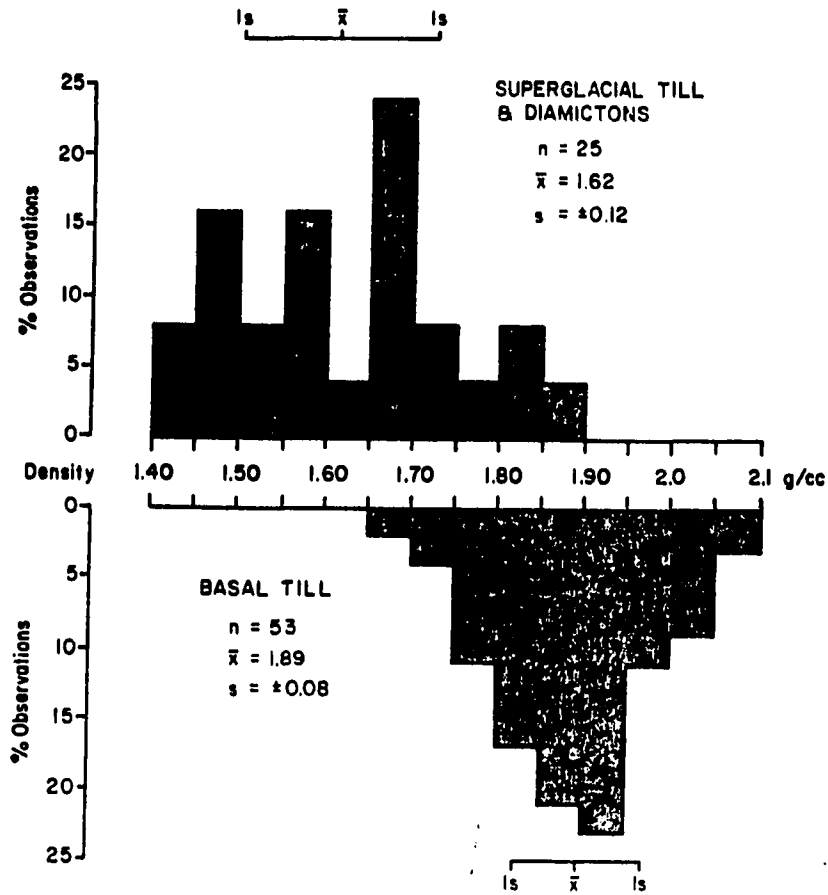


Figure 14. Summary of bulk density data for materials in superglacial till and basal till (Kemmis et al. 1981)

Geological survey guidebook, the Dows is subdivided into four members: the Alden Member (basal till), Morgan Member (supraglacially-deposited till, diamictons and associated melt water deposits), Lake Mills Member (dominantly fine-grained glaciolacustrine sediments), and Pilot Knob Member (upland sand and gravel deposits, dominantly ice-contact glaciofluvial deposits). Since the basal till is related to this research, only the Alden Member is discussed in the following section, details of other Members can be referred to the survey guidebook.

Alden Member of Dows Formation

The Alden Member is comprised predominantly of basal till. Properties of the member deposits are summarized in Figures 12 and 13, the basal till being quite uniform in texture and mineralogy. The till generally exhibits a texture averaging about 15% clay, 37% silt, and 48% sand in the matrix and has a mean dry bulk density of 1.89 g/cc (117.7 pcf).

Till of the Alden Member is believed to have been deposited by a number of subglacial processes; classic lodgement, regelation melt-out, and basal melt-out. These processes may have taken place either successively or concurrently. The till of the Alden Member is variable in thickness, which ranges from approximately 30-55 feet in

areas other than the ice-marginal area.

Investigation

Site description

The area under investigation is located 7.5 miles west of Ames and 0.5 mile south of highway I-30, at SE 1/4 of NW 1/4 of section 8, T. 83N, R. 25W (Iowa Soil Survey Report, Boone County). A U.S.G.S. topographic map (Boone East, Iowa) of the test area is given in Figure 15. Figure 16 shows the detailed topography of the area. According to the soil survey report, the soil mainly consists of the Clarion series surrounded by smaller areas of Canisteo series at the southwest corner and Nicollet series, at southern and northern boundaries of the test area.

The Clarion Series consists of well drained, moderately permeable soils on upland and formed in loamy glacial till. Down to 5 feet deep, the soil has a low shrink-swell potential. The Canisteo and Nicollet Serieses consist of poorly drained, moderately permeable soils on upland and also formed in loamy glacial till. These soils contain low to moderate shrink-swell potential.

The overall site slopes gently (about 2.5%) from the northeast to the southwest corner.

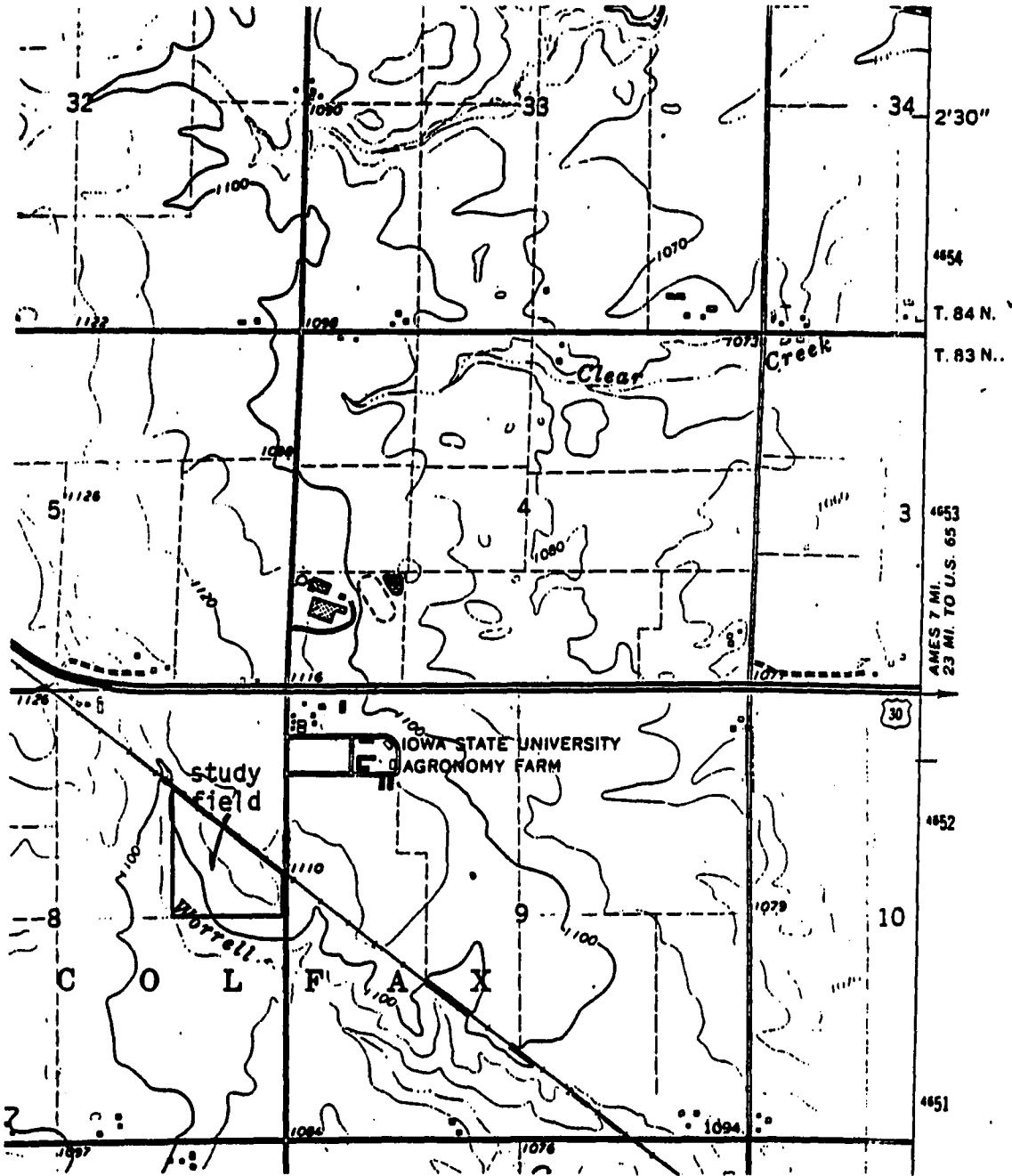
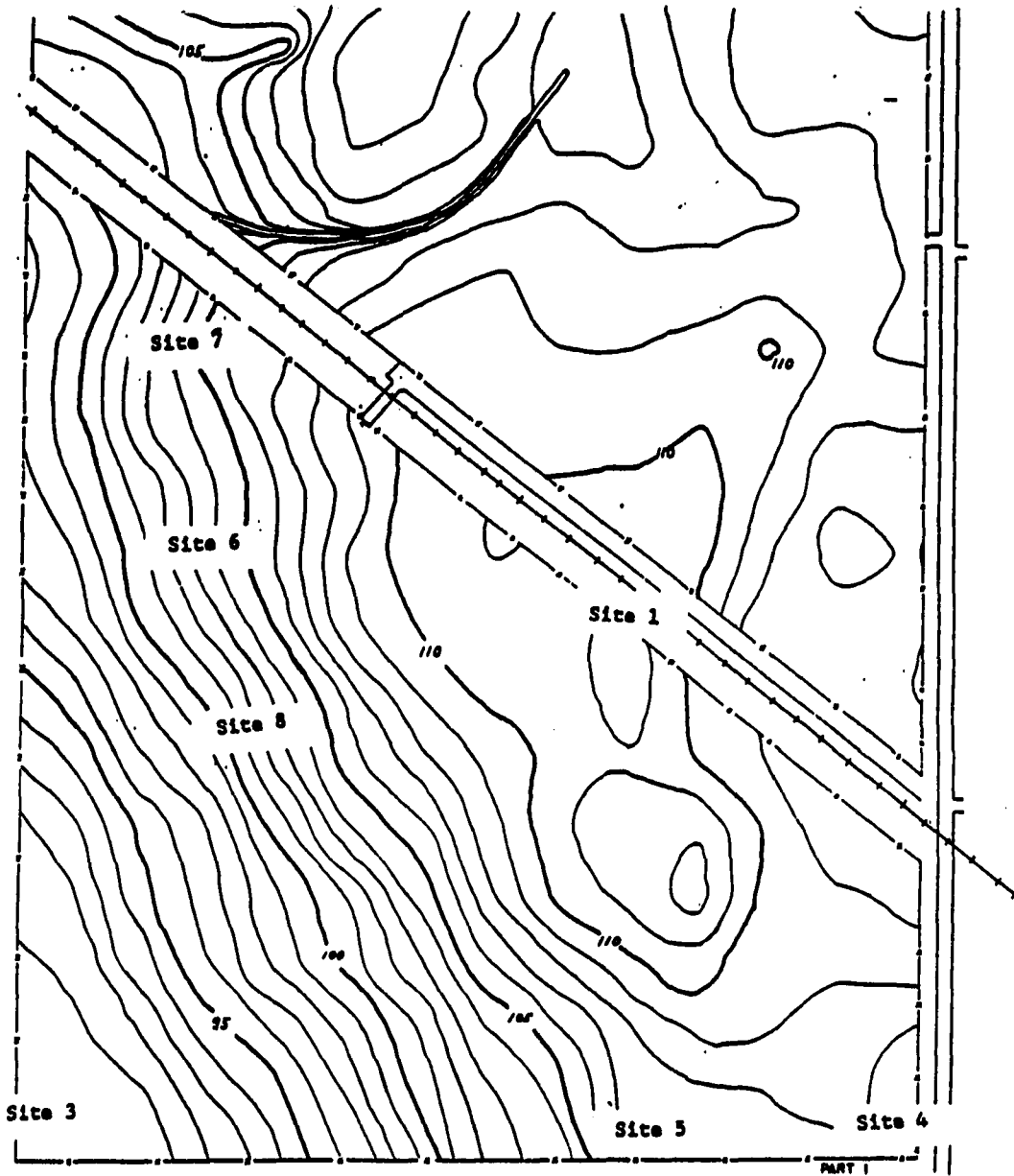


Figure 15. Location of test site



AGRICULTURAL ENGINEERING - AGRONOMY FARM

BOONE COUNTY, IOWA

TEAM R2SW IN SECTIONS 10 & 10
SOIL SURVEY AGRONOMY DEPT. 1960
TOPOGRAPHIC SURVEY A.E. DEPT. 1960



SCALE

CONTOUR INTERVAL - 1 FOOT



Figure 16. Topography of test site

This research mainly involved three investigations; soil classification tests, Ko Stepped Blade tests (SBT), and triaxial confined permeability tests. These respectively were used to verify the character of the till deposit at the test site, measure and investigate possible directional anisotropic lateral earth pressure, and determine the effect of lateral earth pressure on vertical hydraulic conductivity of the soil, respectively.

Soil classification

Soil samples were obtained by use of 3 in. diameter thin-wall Shelby tubes, at locations immediately above each SBT. The locations of SBTs are shown in Figure 17. Samples were numbered by the combination of hole number and depth from which the sample was obtained; for instance, sample H5-15 meant that the sample was obtained from H5 at 15 feet below ground surface.

In the field, the Shelby tube and soil were sealed with aluminum foil and cohesive tapes after sampling. Soil samples then were extruded in the laboratory, trimmed off at both ends to about 6 inches in length, wrapped in plastic wrap and aluminum foil, and stored in a humidity room until the triaxial confined permeability tests were conducted.

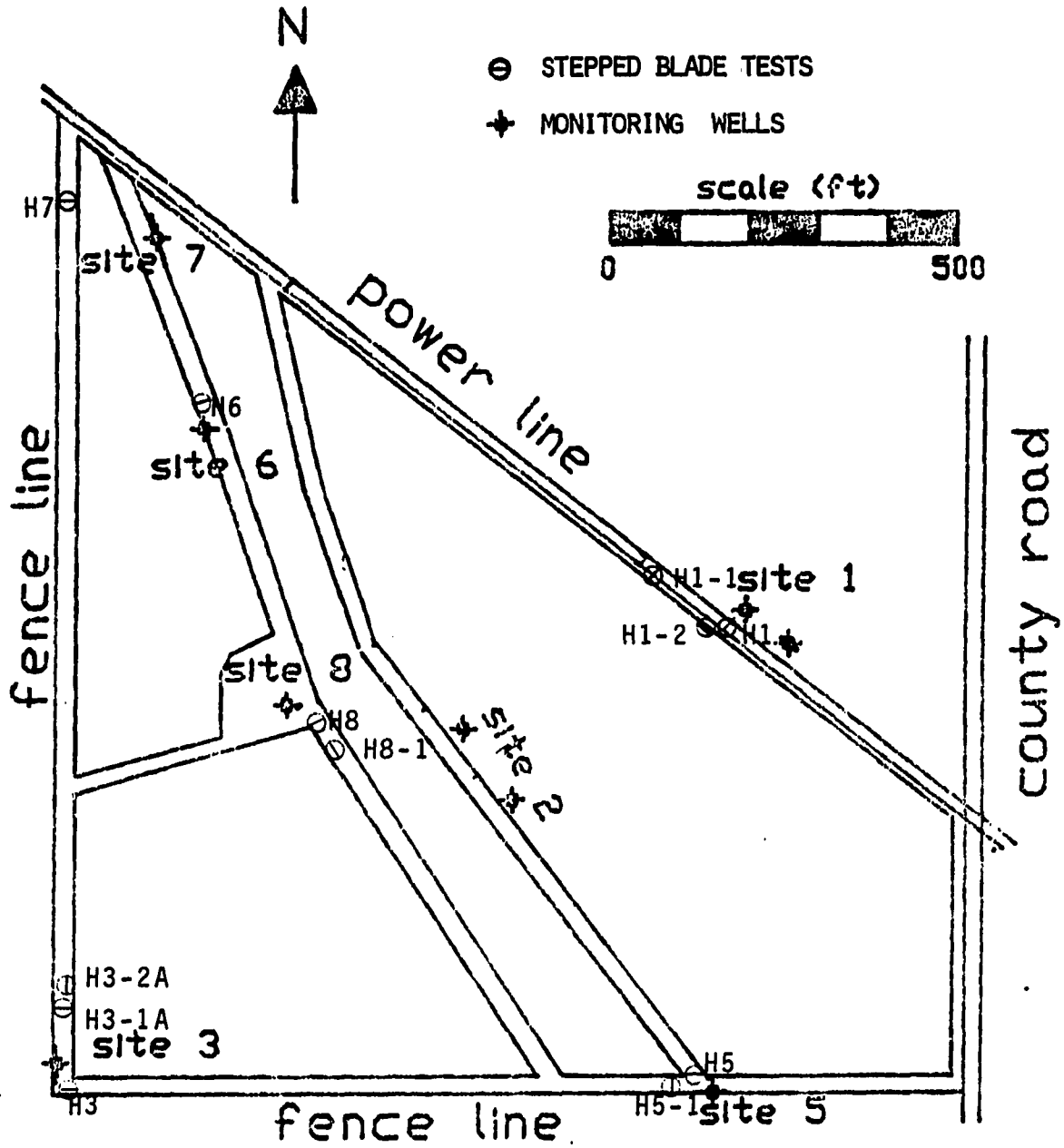


Figure 17. Locations of SBT and soil sampling

The disturbed soil cut off from the Shelby tube samples was used for soil classification tests that included Atterburg Limit tests, moisture content, and particle size analysis. Wet bulk densities were measured by weighing undisturbed samples right after being trimmed.

One-dimensional consolidation tests were conducted to measure the preconsolidation stresses. The tests generally followed the procedures described by ASTM D2453-80, in a fixed-ring consolidometer with distilled water as the saturating fluid. A standard load duration of 24 hours at each load increment was used.

Atterburg limit tests were conducted following ASTM D4318-84. A one-point liquid limit method was used due to the limited quantities of soil sample.

Particle size distribution analysis were performed on oven-dried pulverized soil samples by sieve analysis and hydrometer tests, by procedures described in ASTM D423. The reported clay and silt contents (<0.002 mm and $0.002-0.05$ mm) were obtained by linear interpolation between bracketing particle sizes calculated from hydrometer analysis data.

K_o Stepped Blade test

As discussed in the forgoing chapter, directionally anisotropic lateral earth stresses are not uncommon. The directional nature of lateral earth stress could be related

to the direction of glacier flow, tectonic movement, or topographic location, and may relate to the formation of fractures in glacial tills.

SBTs were proposed to detect the effect of glacier flow and topography on in situ lateral earth pressure, and the formation of fractures in the till deposit. A four-step pneumatic Stepped Blade was used in measuring lateral earth stress. The SBTs were conducted evenly over the test site, and oriented to measure stresses in different directions. In the investigation, the blade was faced to the north to measure north-south stress at H3, H3-1A, H5, and H7; to the east at H3-2A and H5-1; to the northeast at H1-2 and H8-1; and to the northwest at H1, H1-1, H6 and H8. SBTs were conducted in each boring hole at 5-foot depth increments to maximum 35 feet in depth.

The test procedures were:

1. Drill to the first test depth by using 4 in. solid stem augers.
2. Sample soil in the bottom of the hole using 3 in. thin-wall Shelby tubes, for later laboratory tests.
3. Orient and insert the stepped blade 5 in. into the bottom of the sampled hole.
4. Measure the lateral pressure acting on each pressure (first) pressure cell, push an additional 5 in. and repeat, and so on until all four pressure cells have been inserted

and read.

5. Plot the measured pressure versus blade step thickness on logarithmic scale.
6. Extrapolate the data to obtain a total lateral pressure at zero blade thickness.
7. Obtain the effective lateral stress by subtracting hydrostatic pore water pressure from the total lateral earth pressure.

Triaxial permeability test

Though the procedure of laboratory permeability testing has been standardized in ASTM (ASTM, 1988) the accuracy of the test results is still in controversy. A common conclusion is that laboratory permeability often is not the same as the in-place permeability due to the specimen size, disturbance, and soil structure effects. However, laboratory permeability tests remain the best way to study the hydraulic behavior of a porous material while subjected to different controlled conditions. It has been known that the hydraulic conductivity is a function of the void ratio of a particular soil sample, that in turn is related to the confining stress acting on that sample. Recent studies show that the hydraulic conductivity of soil decreases down to a stable value when the applied stresses reach a "certain level". From the reported data, the "certain stress" could

be (1) preconsolidation stress (Carpenter, 1982) or (2) in-situ overburden pressure (McGown and Radwan, 1975).

A triaxial permeability test is perhaps the best method to study the hydraulic conductivity under different stress fields, because of the capability for their being controllable in a triaxial chamber.

The triaxial test apparatus was modified in order to simulate measured in-situ stress conditions in which horizontal stresses are always higher than vertical overburden stresses, i.e., $K_0 > 1$. One end of the piston rod was internally threaded to be connected to a threaded top platen by a T-connector with the upper end sealed. The other end of the rod was attached to a proving ring by a steel rod frame (Figure 18). With such an arrangement, an upward load could be applied to counteract the cell pressure on the top platen, allowing the in situ K_0 value to be reproduced.

The main purposes of laboratory permeability test in this research were to show the relationship of vertical hydraulic conductivity of intact and single-fractured samples of glacial till to stresses acting on the soil.

Prior to testing, each sample was carefully trimmed at both ends to fit into the triaxial cell. Samples are in average 4.5 inches long by 2.85 inches in diameter. The use of a long sample minimized platen frictional resistance that

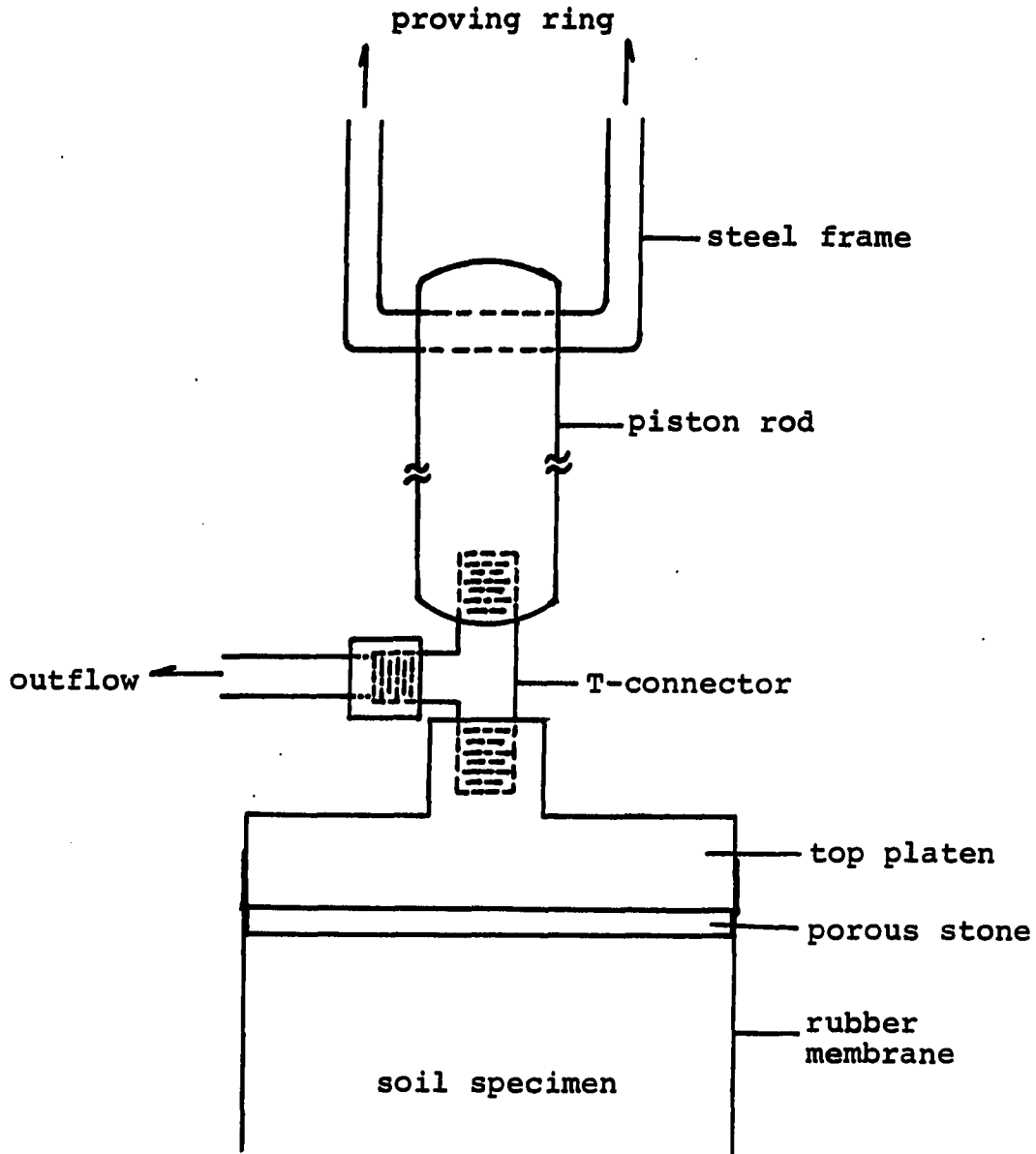


Figure 18. Schematic diagram of triaxial permeability apparatus

could restrict the lateral movement of soil particles near both ends of a sample.

A falling-head method was used in the test. Because the pore pressure affects the distribution of effective stresses within a soil sample, the pressure head at the inflow end was kept low, about 2.0 psi above atmospheric pressure, and the outflow end was exposed to the atmosphere. It can be expected that permeability tests will be very slow with a long sample of glacial till.

Test procedures are:

1. Trim a soil sample to be 4.5-5.0 in. in length.
2. Fix the sample in a triaxial cell.
3. Use a back-pressure method, to assure that the soil sample is saturated with water: A pressurized inflow with a pressure lower than or equal to the confining pressure is applied to force the air out of soil sample.
4. Connect the inflow to a standpipe for measuring the hydraulic gradient, and adjust the stresses acting on the soil to the desired condition.
5. Record the loss of hydraulic head and time elapsed after the consolidation of soil is completed at each increment of lateral stress, indicated by equality of the quantities of inflow and outflow.

RESULTS AND DISCUSSION

Soil Classification

Results

Soil classification tests mainly were performed on samples from boring H8 and H5, where the SBTs and sampling were conducted earliest in this research, to verify the character of the till deposit of the test site. Additional classification tests were conducted on samples from H1, H6, H7 to check for possible variations of soil properties in the till deposit of the test site.

Based on observation of disturbed soil carried out by the auger when drilling, the dark-colored A horizon topsoil was about 1 foot thick, underlain by a layer of soil oxidized to brown or yellow-brown color down to around 10 to 13 feet in depth. Below the oxidized layer is the unoxidized material, indicated by a gray color, that extended down to the full depth of drilling at a depth of 35 feet.

A soft sand layer occurred approximately at a depth range of 7 to 10 feet in boring H3. Squeeze and collapse of the soft sand in the hole made it impossible to obtain Shelby tube samples or perform SBT's in deeper layer at the first drilling. Six-inch stovepipe assembled to a length of 10 feet then was used as a temporary casing, to allow test-

ing in the deeper zone. However, the larger diameter of the cased hole allowed the 4 in. to rotate along the wall of the stovepipe, which caused disturbance and falling of material in the wall in the lower depth. While this did not preclude SBT's, it did prevent proper Shelby tube sampling, so no undisturbed soil samples were obtained in H3. Similar soft deposits were also found in test holes H3-1A and H3-2A, drilled about 100 feet north of H3. Observation of the disturbed soil and results of the SBT in H3, H3-1A, H3-2A, indicated that soils under the soft sand deposits were dense, and unoxidized till. Coupled with results of SBTs, it was reasonable to assume the materials were similar to soils at other test holes. Without further investigation, the horizontal extent of this sand deposit has remained unknown.

The results of the laboratory tests are shown in Tables 1a and 1b, and indicate that the oxidized till has a slightly lower density and higher moisture content than the underlying unoxidized till. The average wet bulk density of the oxidized material is 133.1 pcf (standard deviation, S.D.=±3.8 pcf, n=9) and of the unoxidized layer is 137.2 pcf (S.D.=±3.2 pcf, n=18). The average moisture content of the oxidized material is 16.27% (S.D.=±1.23%, n=9) and unoxidized zone 14.3% (S.D.=±0.70%, n=17). The above data give an average dry bulk density 114.4 pcf (1.83 gm/cc) for the oxidized layer and 120.0 pcf (1.92 gm/cc) for the unoxidized

Table 1a. Summary of soil classification tests

Hole	Depth (ft.)	wet γ_t (pcf.)	W %	P.L. %	L.L. %	P.I. %	L.I.	Unif. sand ^a Classif.	silt ^b %	clay ^c %	Saturtn. ^d S %	
H5	5	129.0	17.7	15.9	24.9	9.0	0.20	CL	54.52	28.93	14.03	89.6
	10	136.3	15.5	16.4	24.7	8.3	-0.11	CL	55.58	30.91	14.14	98.7
	15	139.6	13.6	14.8	21.8	7.0	-0.17	ML-CL	52.56	32.28	15.16	100.0
UW. ^e zone	20	138.7	14.2	15.0	22.7	7.7	-0.10	CL	50.75	33.94	15.31	100.0
	25	138.8	14.0	13.9	23.5	9.6	0.01	CL	51.31	32.21	16.48	99.5
	30	140.2	13.2	13.9	21.4	7.5	-0.09	CL	52.89	28.96	18.15	98.7
	35	135.5							50.53	31.57	18.30	99.9
H8	5	134.6	15.6	15.6	23.5	7.9	0.00	CL	54.21	31.07	14.72	95.0
	10	(unsuccessful sampling)										
UW. zone	15	135.9	15.3	15.2	23.4	8.2	0.01	CL	54.50	30.29	15.21	97.0
	20	137.4	14.2	12.9	22.6	9.7	0.13	CL				96.7
	25	136.9	14.1	13.8	22.4	8.6	0.03	CL	51.20	34.06	14.72	95.1
	30	138.6	14.2	13.8	23.9	10.1	0.04	CL				99.7
	35	134.0	16.2	14.4	24.5	10.1	0.18	CL				95.7

^aSand, 2.00 - 0.05 mm.

^bSilt, 0.05 - 0.002 mm.

^cClay, < 0.002 mm.

^dCalculation of percentage of saturation is based on specific gravity of soil, G = 2.69.

^eUnweathered zone.

Table 1b. Summary of soil classification tests

Hole	Dep (ft)	wet γ_t (pcf.)	W %	P.L. %	L.L. %	P.I. %	L.I.	Unif. Classif.	Saturtn. S %
H1	8	129.5	17.3	13.6	23.5	9.9	0.38	CL	88.0
	13	131.2	18.0	14.8	23.6	8.8	0.36	CL	95.0
UW. zone	23	135.9	14.7	13.0	23.4	10.5	0.16	CL	94.9
	28	138.8	13.9	13.0	22.4	9.5	0.10	CL	99.1
H6	5	127.8	16.0	14.6	24.8	10.2	0.14	CL	82.2
	10	135.8	14.8	13.6	23.1	9.5	0.13	CL	95.0
	15	126.0	14.3	13.0	22.4	9.4	0.14	CL	73.6
UW. zone	20	139.5	13.6	13.1	22.5	9.4	0.05	CL	99.7
	25	143.0	14.6	13.3	22.2	8.9	0.15	CL	99.7
	30	138.6	13.8	12.9	21.1	8.2	0.11	CL	98.2
H7	5	134.7	17.0	14.5	21.5	7.1	0.35	ML-CL	99.8
	10	138.9	14.6	13.8	20.6	6.8	0.12	CL	99.7
UW. zone	17	138.7	14.2	14.0	22.7	8.7	0.02	CL	99.5
	20	137.6	14.8	13.8	23.1	9.3	0.11	CL	99.4

layer. Both of these values are consistent with the densities given in the earlier investigation of Alden Member of Des Moines Lobe deposit (Figure 14).

The textural analyses of samples from H5 and H8 are shown in Table 1 and by points in Figure 19. Also shown in Figure 19 is the approximate boundary of textural distribution of basal till given by Kemmis et al., 1981. The soils are very uniform and have a small standard deviation of each particle size category through the depth of sampling. The soils are classified as sandy loam to loam. The average percentages from 10 soil samples at different depth and location of particle size are: clay (<0.002 mm diameter) 15.70% (S.D.=±1.46%), silt (0.002-0.05mm) 31.59% (S.D.=±1.59%), and sand (0.05-2.00mm) 52.31% (S.D.=±1.82%).

Atterburg tests show that the composition and characteristics of the test site soil with the exception of the sand layer that occurred in boring H3 are very uniform. Almost all the soils classified as CL soil, inorganic clay of low to medium plasticity in the Unified Classification system. Using the moisture content and plasticity data of the soils, the liquidity Index (LI) is defined as:

$$LI = \frac{(W-PL)}{PI}$$

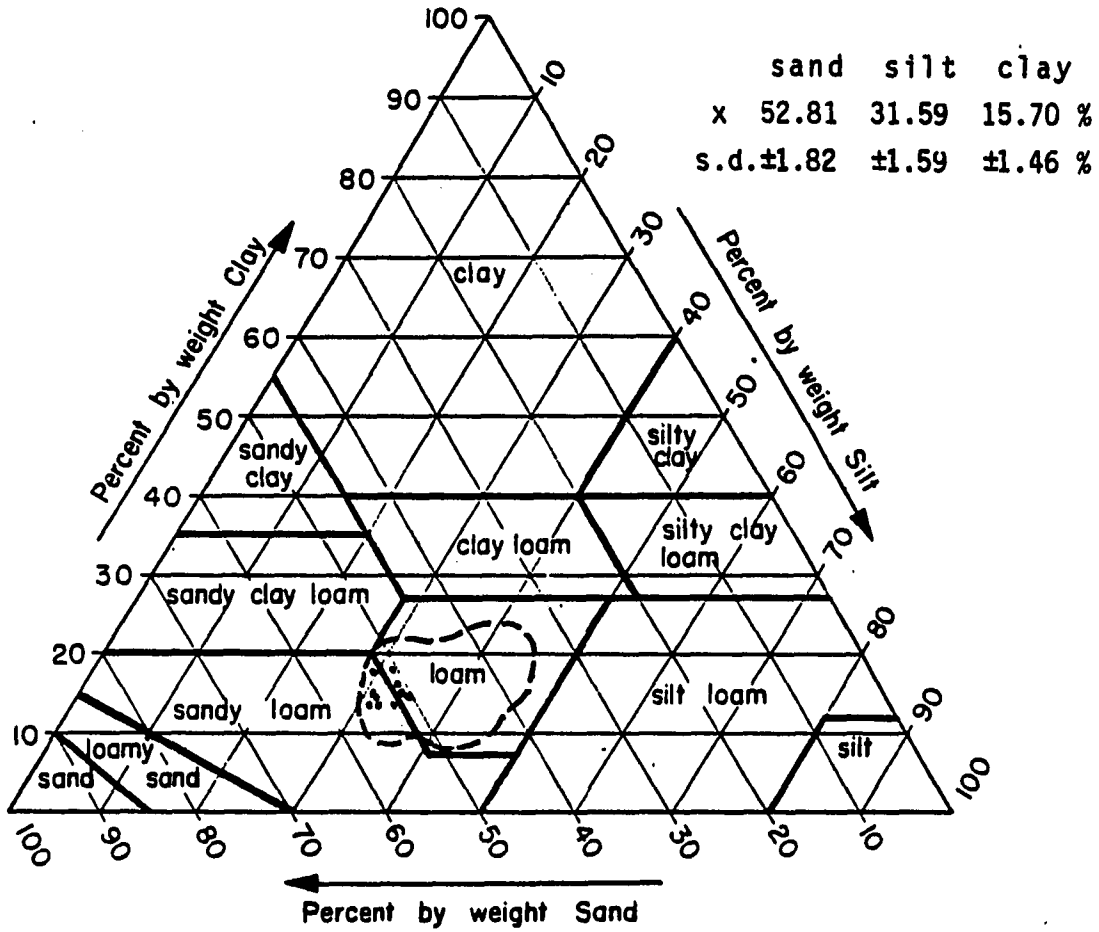


Figure 19. Textural data for the test site

where W is the natural moisture content, PL is the plastic limit, and PI is the plastic index which equals the liquid limit minus the plastic limit. In most of the samples, the moisture content was close to the plastic limit, and the average $LI=0.09$ ($S.D.=\pm 0.14$). This indicates that the soils are very stiff and are in a high state of density, which is consistent with results from bulk densities measurements.

Two one-dimensional consolidation tests were conducted, on samples H5-15 and H5-20, to investigate the stress history of the soil. The consolidation curves and the interpretation of preconsolidation stress are given in Appendix C. The OCR of sample H5-15 is about 7, and of H5-20 is about 2.8, based on in situ effective vertical stresses given in Appendix B.

Discussion

The lower density of the oxidized material than of the unoxidized material may be caused by the effects of the weathering processes, that decreases the bonding forces between soil particles and induces a less dense structure of soils.

The results of above tests indicate that the till sampled at the test site is very uniform in texture, and is dense and overconsolidated through the whole depth of sampling, except for the sand zone found in H3, H3-1A and H3-

2A. Though analyses such as clay mineralogy and matrix carbonates content reported in the geological report by Kemmis et al., 1981, were not conducted, the geotechnical properties of the soils of the test site match well with those of the Alden Member of the Dows Formation. Therefore, it can be concluded that the till deposit in the test site consists of subglacial till. As discussed in the previous chapter, the formation and orientation of fractures which were found in the oxidized (weathered) zone and directional anisotropic lateral earth stress in this area may be related to the flow direction of Cary glacier.

Stepped Blade Test (SBT)

Results

The results of SBTs are given in the Appendix A and the interpreted lateral stresses in Appendix B. The lateral stresses were obtained graphically without calculating the coefficients a and b in equation 16 and correlation coefficient r as in previous researches on K_0 Stepped Blade, since most of the lateral stresses were obtained by extrapolating the stresses sensed on the first two or 2nd and 3rd steps. As in the previous researches, the stresses measured by the Stepped Blade turned out to be widely scattered. The previous researchers have indicated that the Stepped Blade is

very sensitive to changes of stress-condition in soil. Another factor contributing to data scatter is the gravel-rich nature of the basal till deposit, the average content of gravels in about 5% by weight of the disturbed soil samples. Some of the gravels encountered in the test site was up to 1 inch in diameter.

The effective lateral stress profiles at each test hole are shown in Figures 20 to 26, in which trend bands of stresses bracketed by minimum and maximum measured lateral stresses instead of average values are used to express the relationship of lateral stress to depth. The effective lateral stresses were obtained by subtracting hydrostatic pressures of groundwater from the total pressure sensed by the Stepped Blade, based on groundwater levels measured over 24 hours after drilling. SBTs were originally proposed to be conducted at each test hole at every 5-foot depth increment to maximum 35 feet in depth. Due to the hard nature of the soil which caused bending of one of the AX drill rods used to push the blade, most SBTs were conducted within 30 feet of the ground surface.

Also shown on the graphs are calculated stresses for several values of coefficients of lateral earth stress, K_0 , which is defined as the ratio of vertical effective stress to horizontal stress. Generally, the lateral stresses in

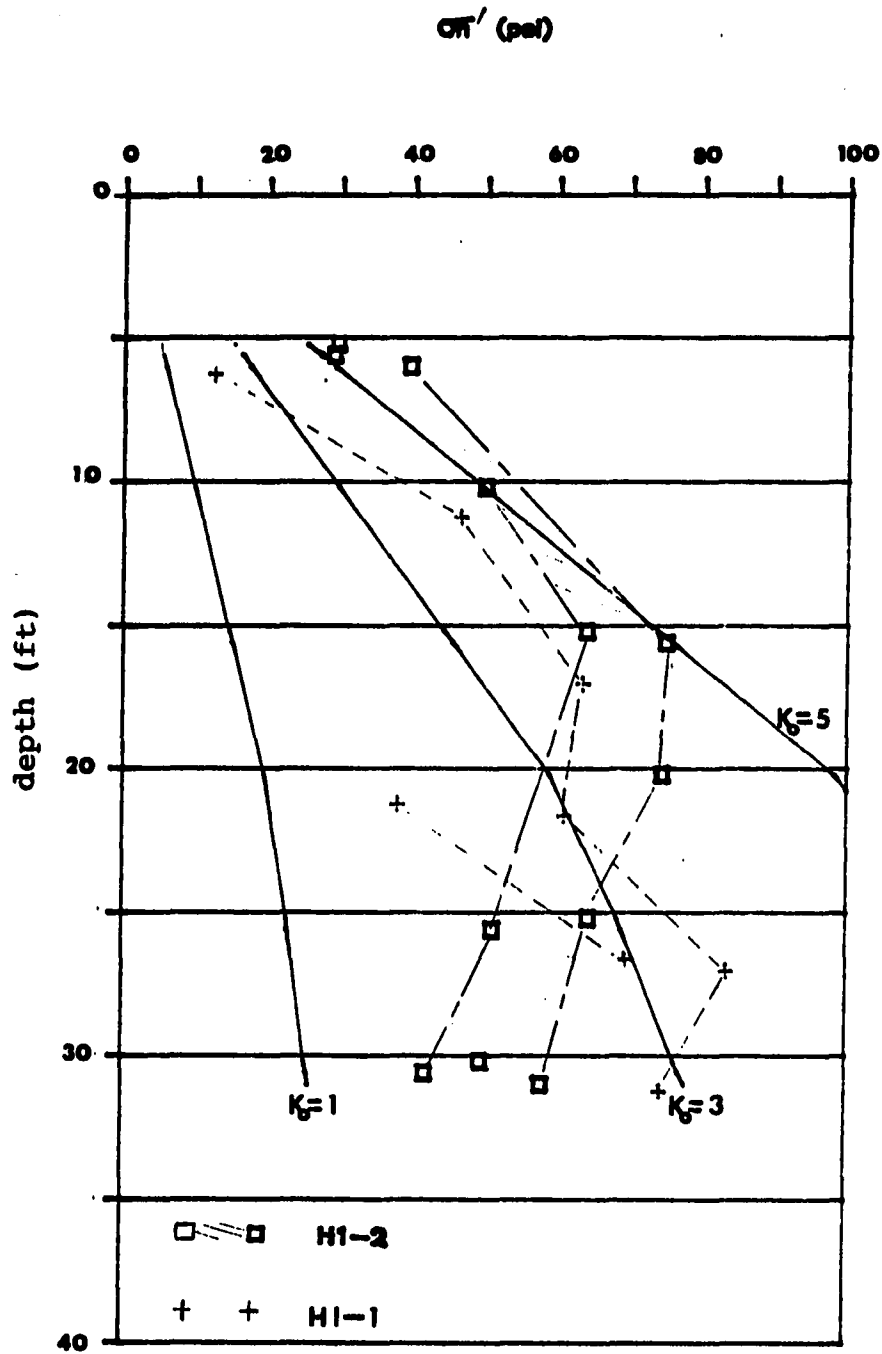


Figure 20. Lateral stresses at H1-1 (NW) vs. H1-2 (NE)

σ_H' (psf)

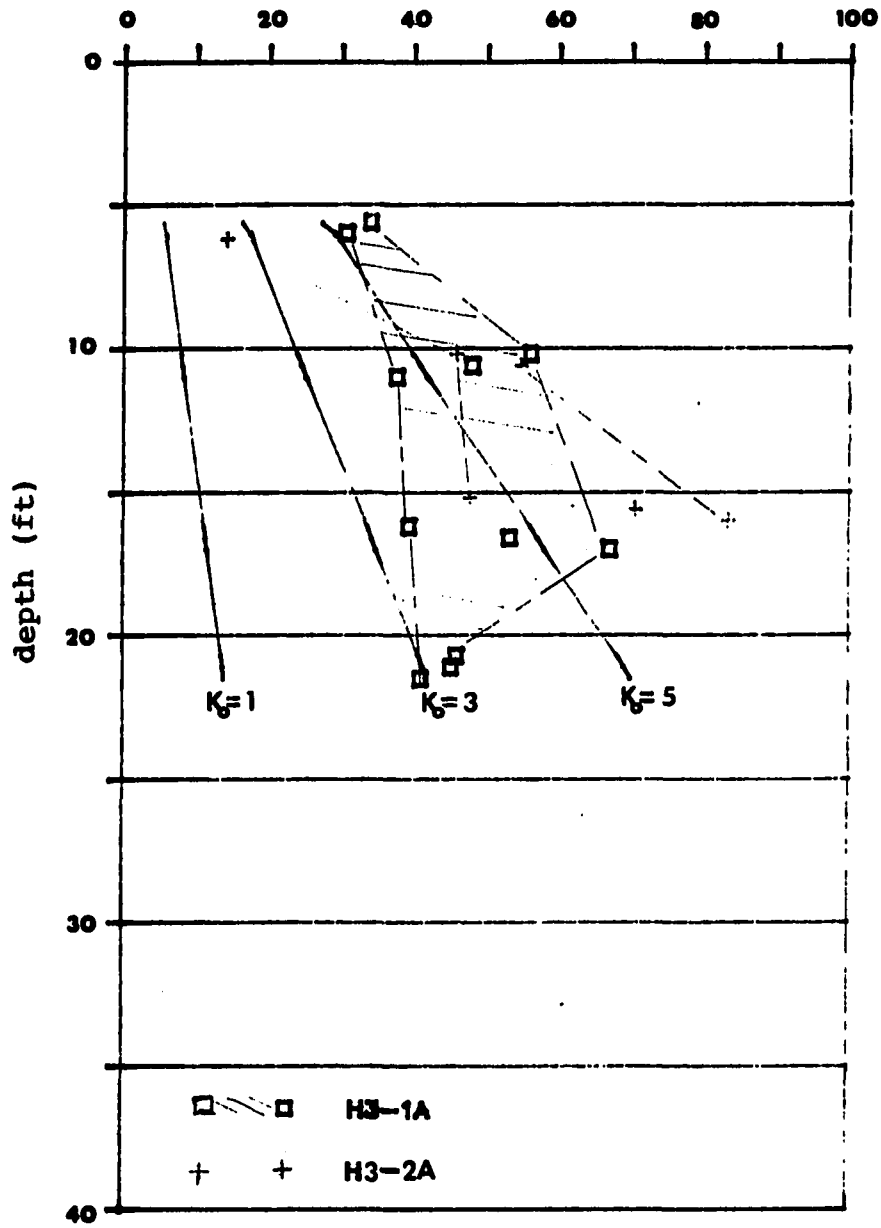


Figure 21. Lateral stresses at H3-1A (N) vs. H3-2A (E)

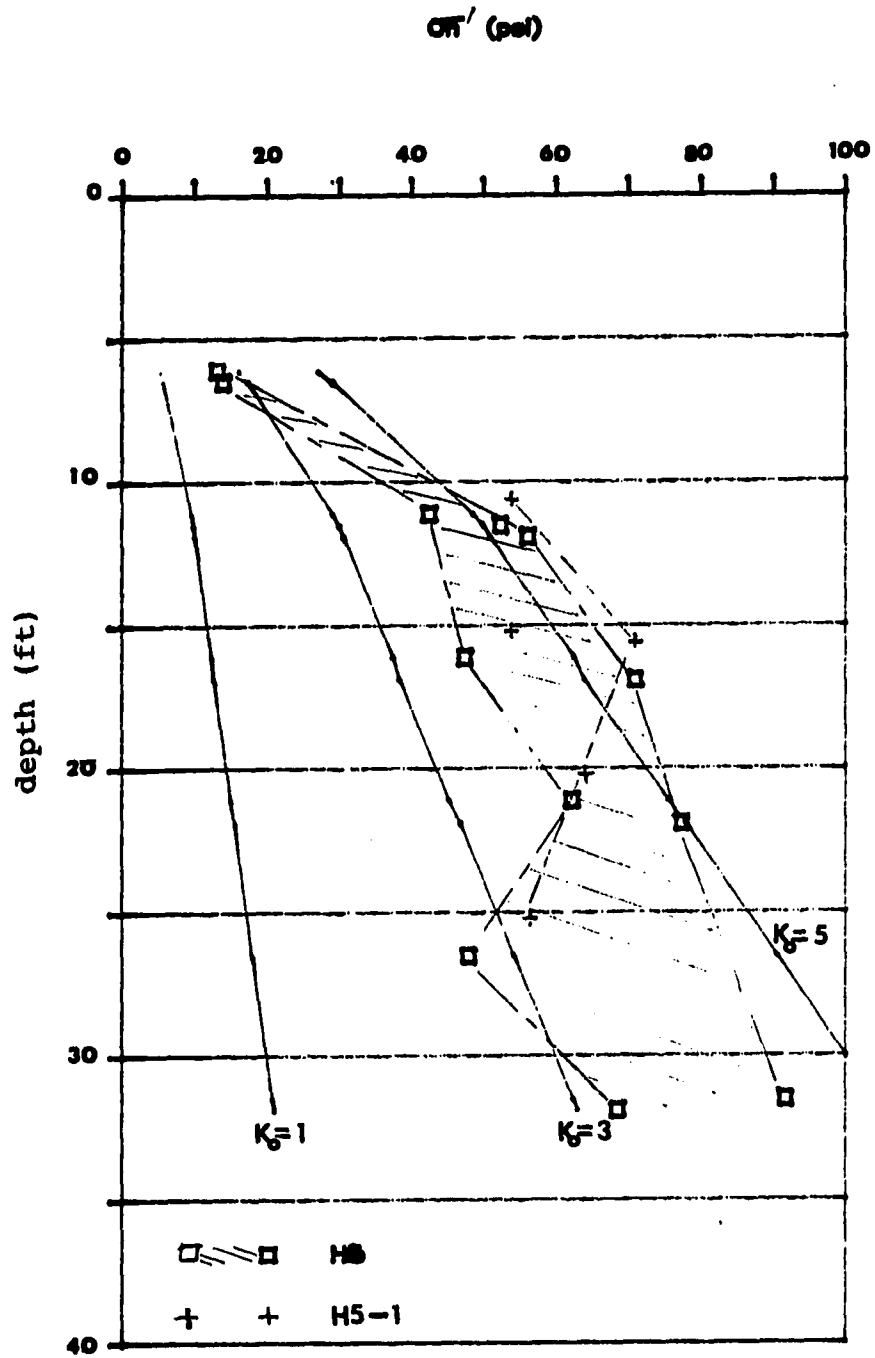


Figure 22. Lateral stresses at H5 (N) vs. H5-1 (E)

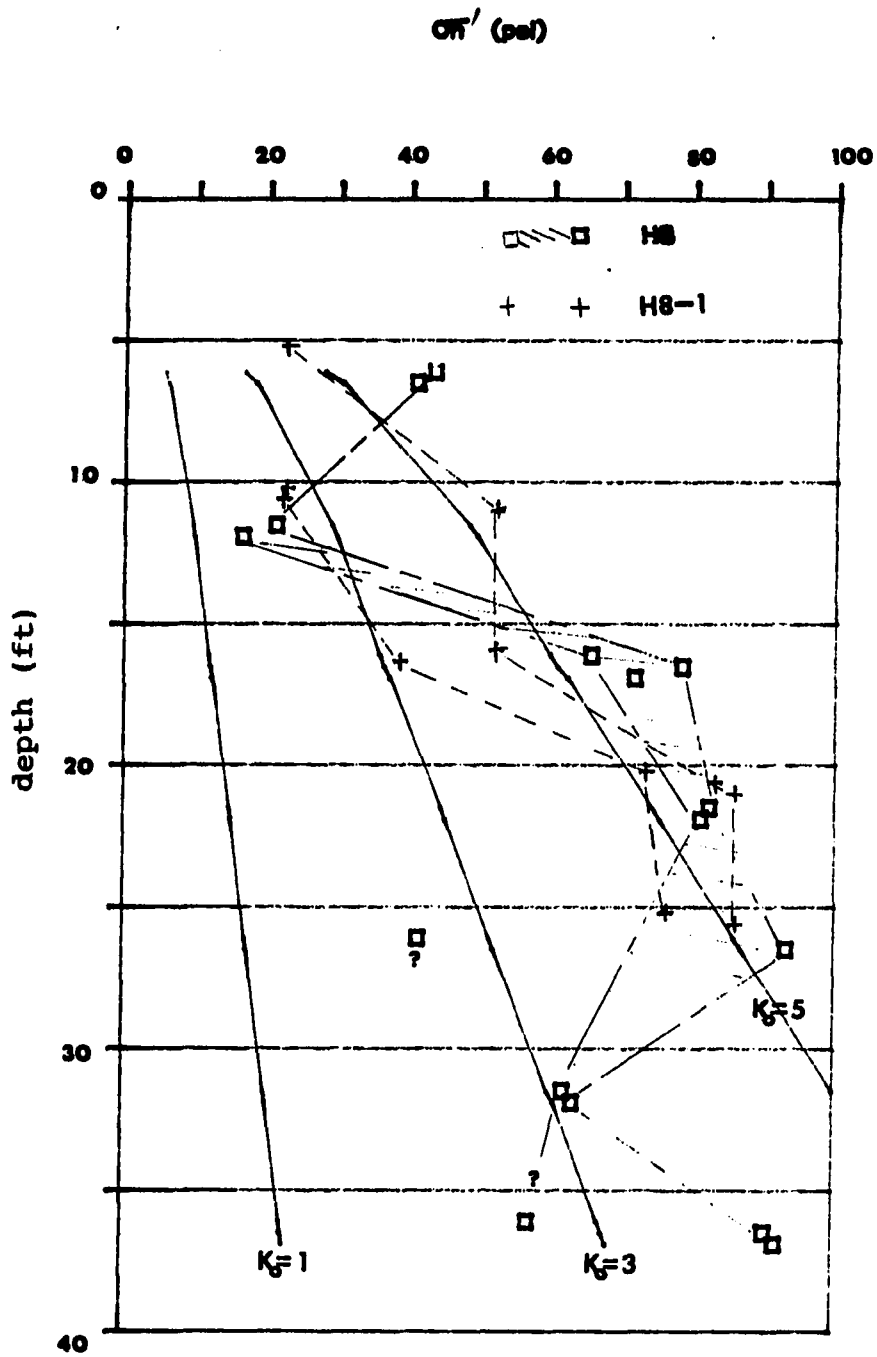


Figure 23. Lateral stresses at H8 (NW) vs. H8-1 (NE)

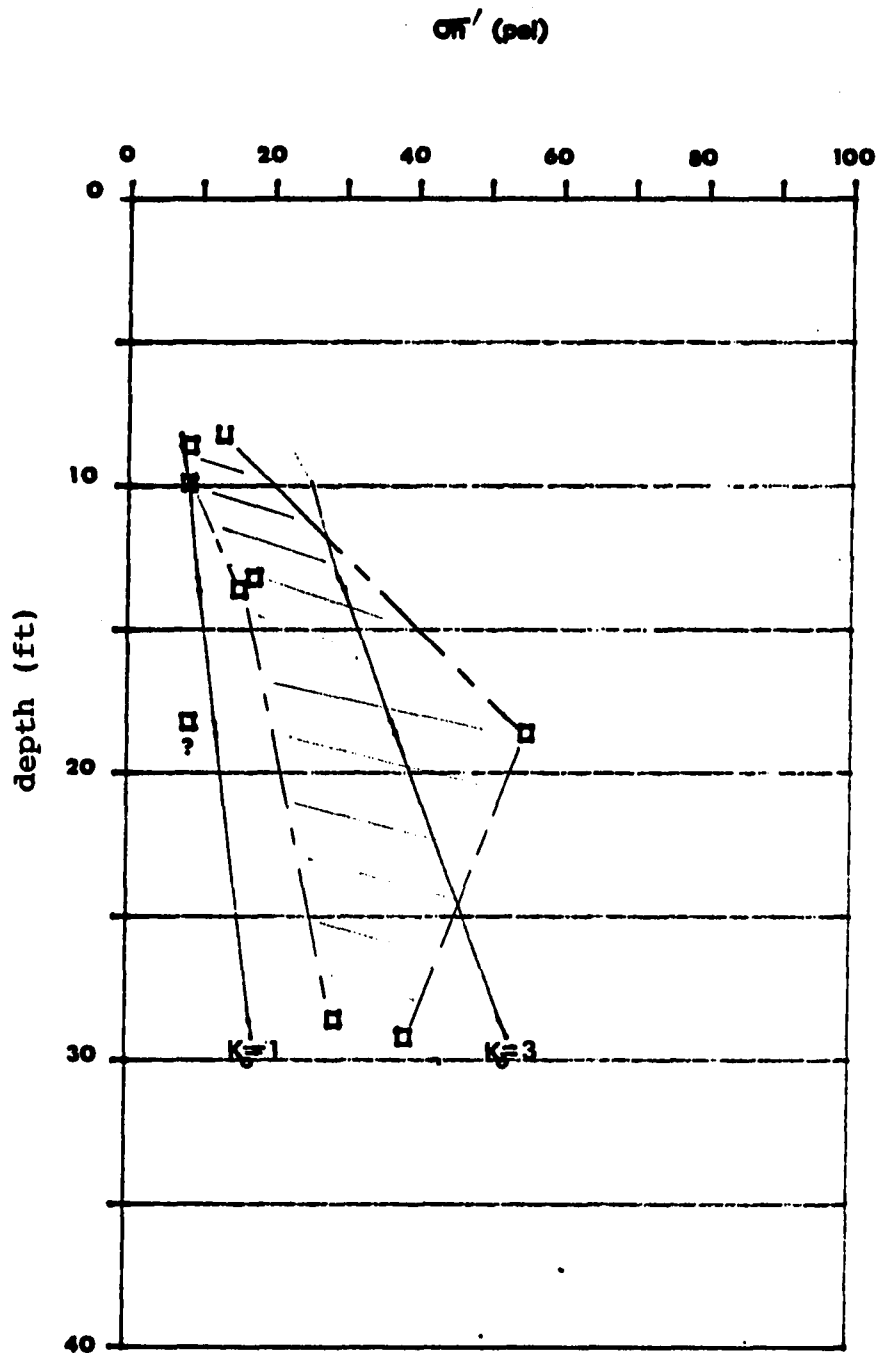


Figure 24. Lateral stresses at H1 (NW)

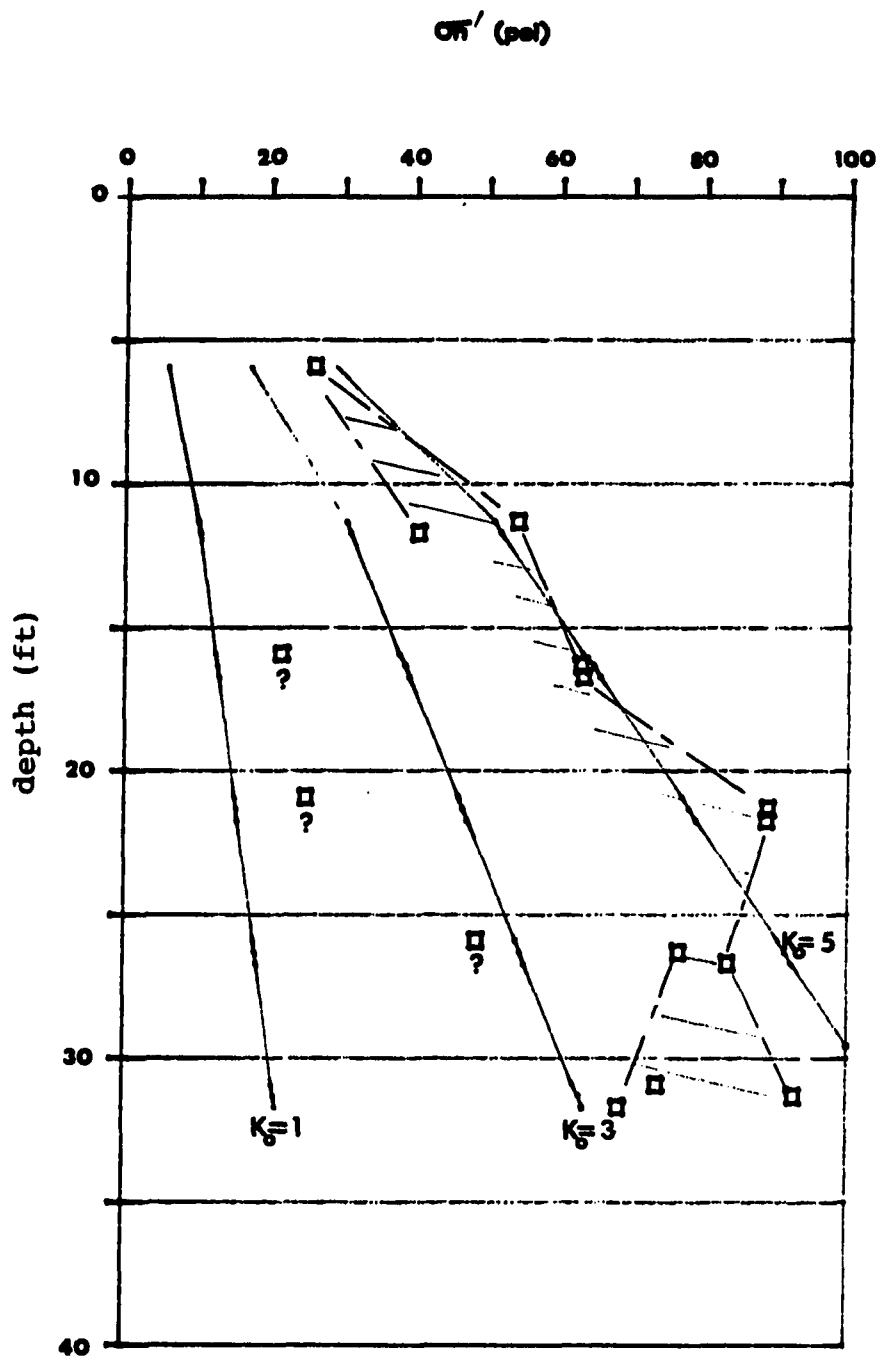


Figure 25. Lateral stresses at H6 (NW)

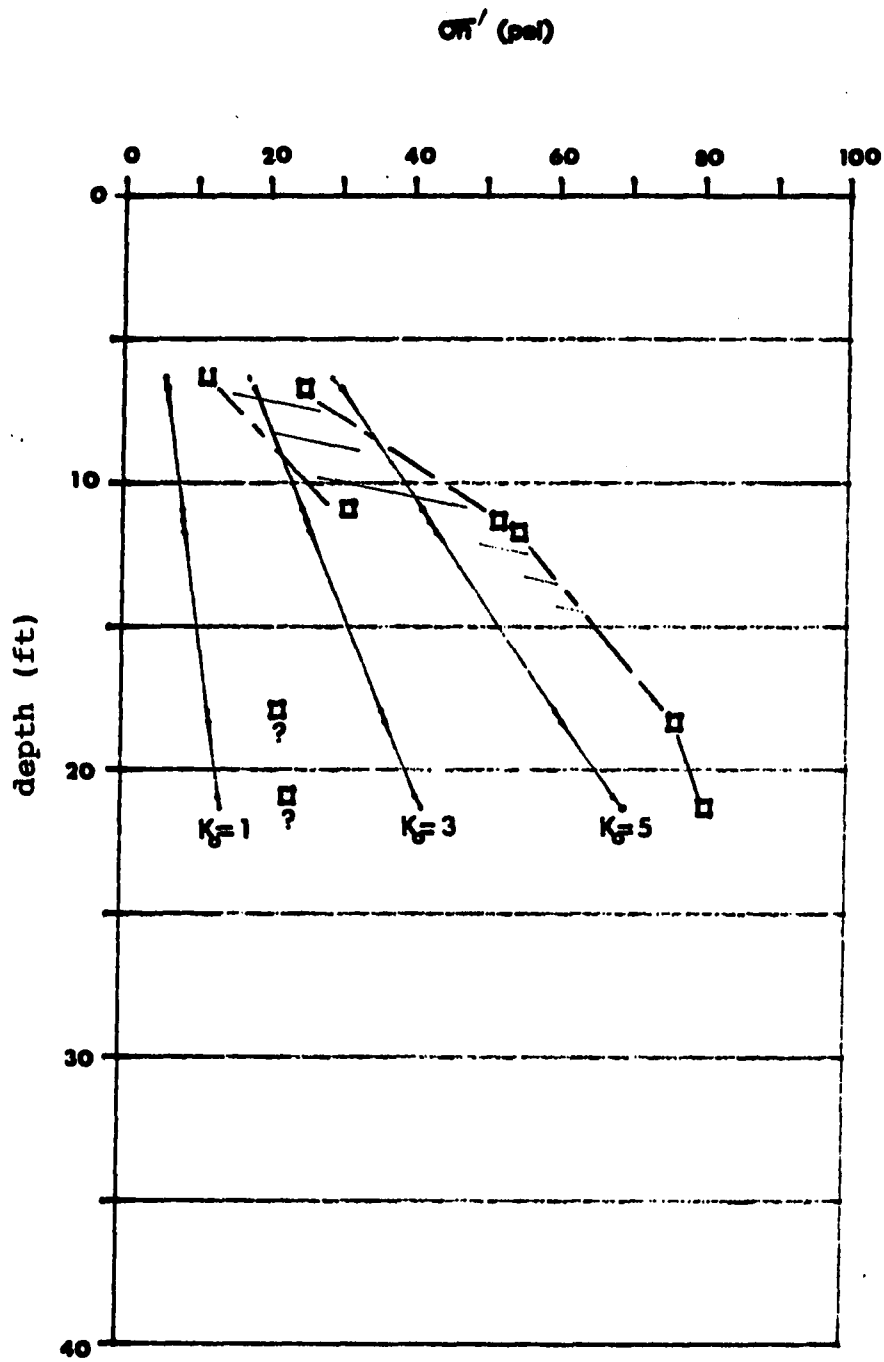


Figure 26. Lateral stresses at H7 (N)

this particular site are very high, giving K_0 's in the range from 3 to 6, indicating that the soil is highly overconsolidated.

Figures 20 and 23 to 25 show the lateral stresses measured with the Stepped Blade faced to the northwest which is regarded as the direction from which the Cary glacier advanced and might be the direction of the major principal stress. Figures 20 and 23 compare lateral stresses in the northwest and northeast directions, and Figures 21 and 22 compare those to the north and the east. The results indicate that there is no significant difference in lateral stresses with respect to direction nor to locations.

Figure 27 shows the lateral stresses of test holes, H1-2, H3-2A, and H8-1, at different location on the slope. Boring H3-2A is located at the toe of the slope, boring H1-2 is at the top and boring H8-1 is in the middle of the two boring holes. The faces of the Stepped Blade were rotated about parallel to the elevation contour lines to determine any influence of topography on lateral stresses. There appears to be no significant difference of the lateral stresses between the three locations, H1-2, H8-1, and H3-2A, which may be because the slope of the test site is gentle (2.5%) and test depth may be below any influence from soil creep. Therefore, in this particular site, the lateral earth pressure can be considered to be isotropic.

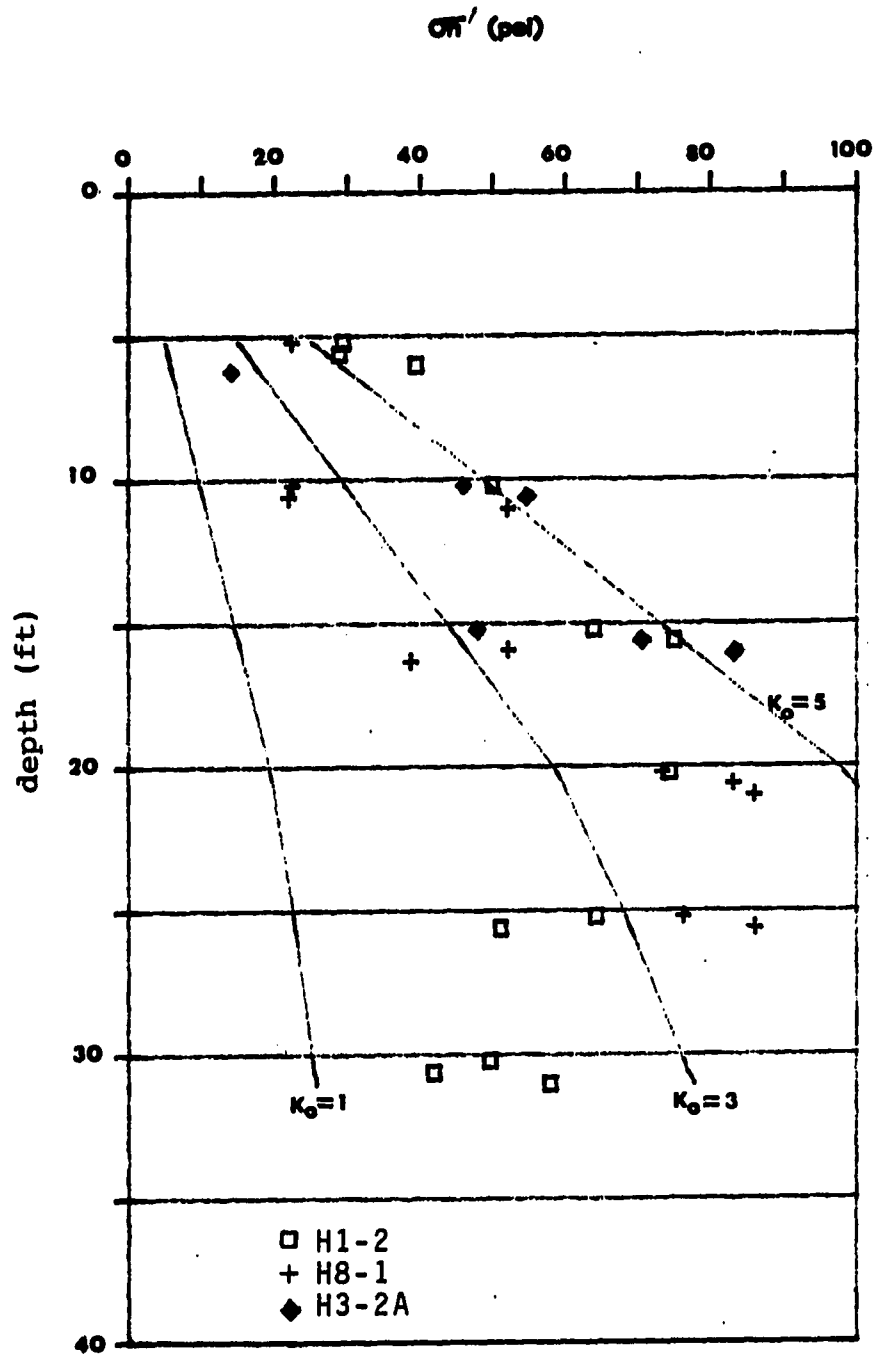


Figure 27. Lateral stresses at H1-2, H8-1, and H3-2A

Discussion

One Bore Hole shear test was conducted in boring H5-1 at the 20 feet depth. Results indicated that the till deposit has a friction angle 21.3 degrees and a cohesion of 1.49 psi ($r=0.995$) in normal pressure range 6.9 to 17.2. For a cohesive soil, the passive lateral earth pressure coefficient K_p , i.e., the ratio of the largest horizontal stress which a soil matrix can tolerate to vertical stress is:

$$K_p = \tan^2(45^\circ + \phi/2) + \frac{2C}{\gamma h} \tan(45^\circ + \phi/2) \quad (18)$$

With the friction angle 21.3 degrees and cohesion 1.49 psi K_p equals to $2.14 + 4.36/\gamma h$ where h is depth and γ is the effective density of soil. At a depth of 5 feet, K_p is about 3.1 and the K_p 's at greater depths deeper should be less, approaching a minimum value of 2.1. The above calculation indicates that the K_0 and lateral earth stresses measured by the stepped blade may be overestimated. However, as previous discussion indicated, aging of the deposit and some other factors may have predominant effects in increasing the K_0 , also the triaxial permeability test which will be discussed later shows that the measurement of the stress is reliable.

One purpose of this research was to investigate the source of the fracture formation. Due to lack of opportunity for direct observation of the fractures in the test site, such as in a trench or open cut, visual observations were made of Shelby tube samples after splitting lengthwise.

Fractures were concentrated in the samples taken from the weathered zone. The fractures were usually denoted by iron oxides on the surfaces or by concentrations of dark colored organic material, perhaps brought down from the ground surface by infiltration. The fractures were commonly non-planar, oriented vertically to sub-vertically, as shown in Figures 28 and 29. Some low-angled irregular fractures were also found in the samples. Few fractures were observed in the samples from 13 feet and 15 feet depths. None of the apparent fractures revealed any systematic pattern or preferential orientation. Samples from deeper layers appeared to be very intact and no fractures were found.

The irregular pattern of fractures coupled by the isotropic condition of lateral earth pressure indicated that the fractures in the weathered zone were mainly caused by desiccation or some other weathering processes discussed in the Chapter II.

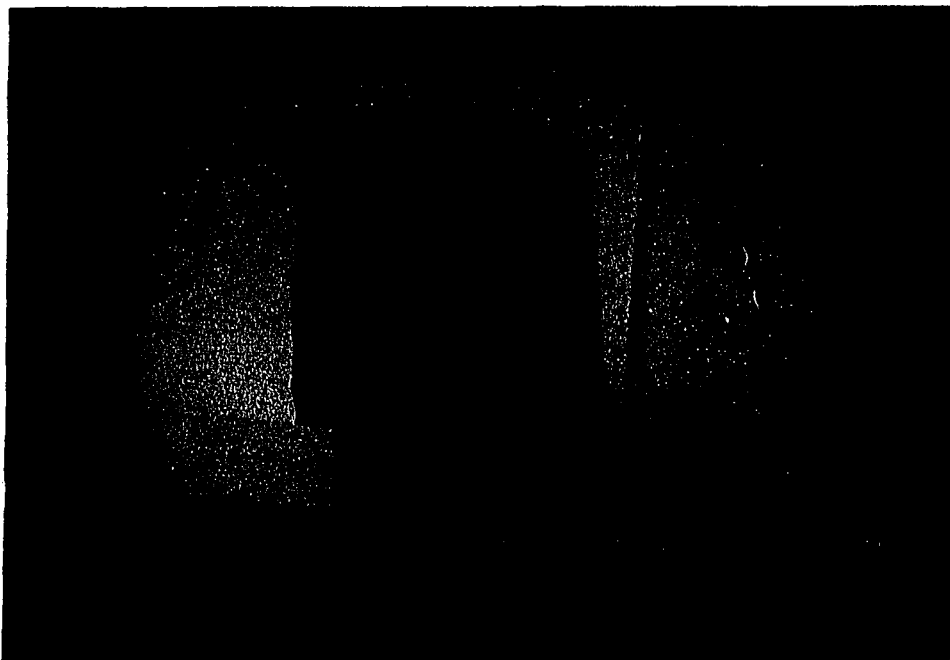


Figure 28. Fractures in sample H5-5

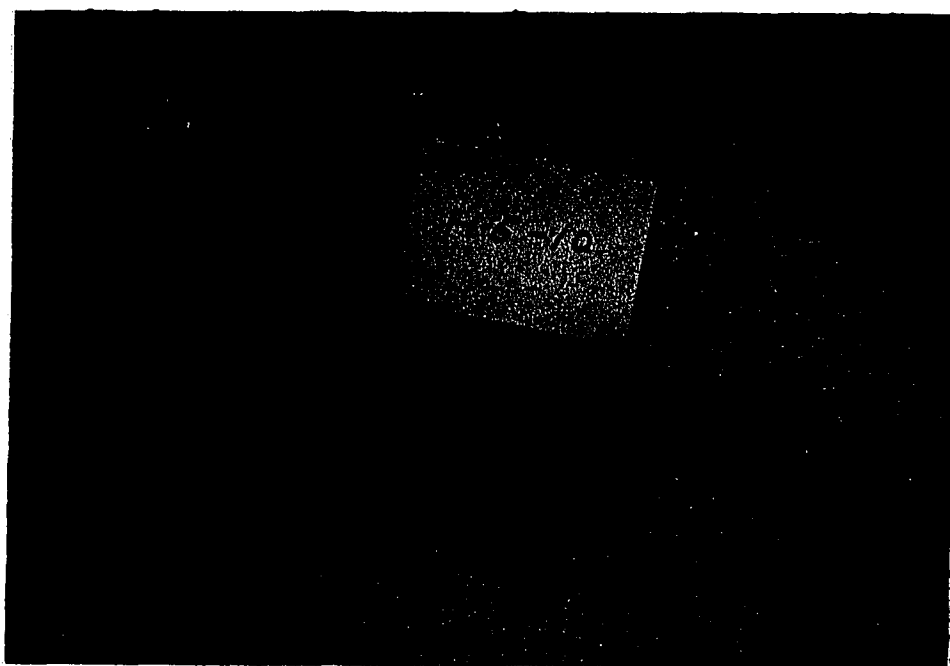


Figure 29. Fractures in sample H5-10

Triaxial Permeability Test

Results from intact samples

Four intact samples, H5-15, H8-15, H5-20, and H6-10, were used in measuring the hydraulic conductivity. In the tests, samples H5-15, H5-20, H8-15 were tested under the reproduced in situ stress, $K_0 > 1$, and H6-10 was under an isotropic confining stress, $K_0 = 1$, to investigate the influence of confining stress on hydraulic conductivity.

The results show that the samples from the unweathered layer gave hydraulic conductivities ranging from 1.66×10^{-7} to 1.99×10^{-8} cm/sec, and the sample from the weathered zone has values ranging from 6.30×10^{-7} to 2.17×10^{-7} cm/sec, depending on the confining stresses applied on the soil samples, given in Appendix D.

Surprisingly, results shown in Figures 30 to 33 from all four intact samples show a common trend, that when the applied lateral stress or confining stress increases to a value close to the minimum situ lateral stress measured by the Stepped Blade -- 47 psi for sample H5-15, 62 psi for H5-20, 65 psi for H8-15 and 40 psi for H6-10 -- the hydraulic conductivity of soil sample becomes nearly constant with further increases in pressure. This trend is shown more clearly in Figure 34, wherein the normalized permeability, based on maximum measured permeability, is plotted versus

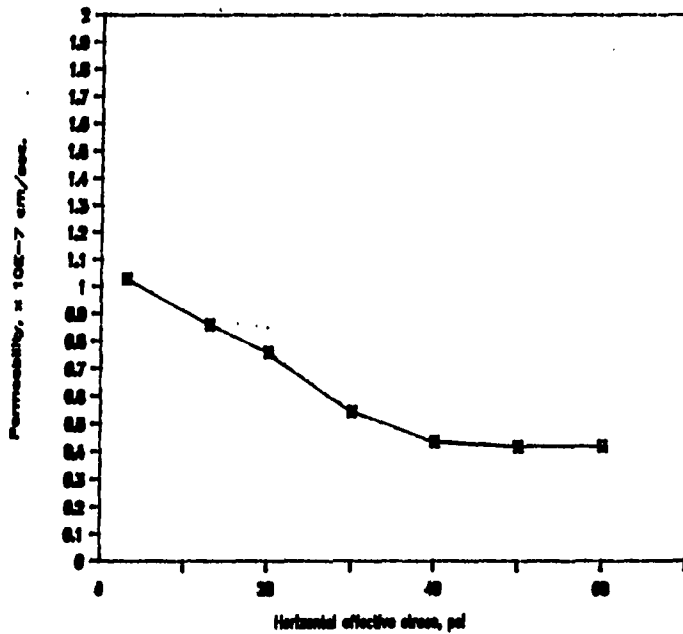


Figure 30. Hydraulic conductivity of intact sample H5-15 at different confining stresses

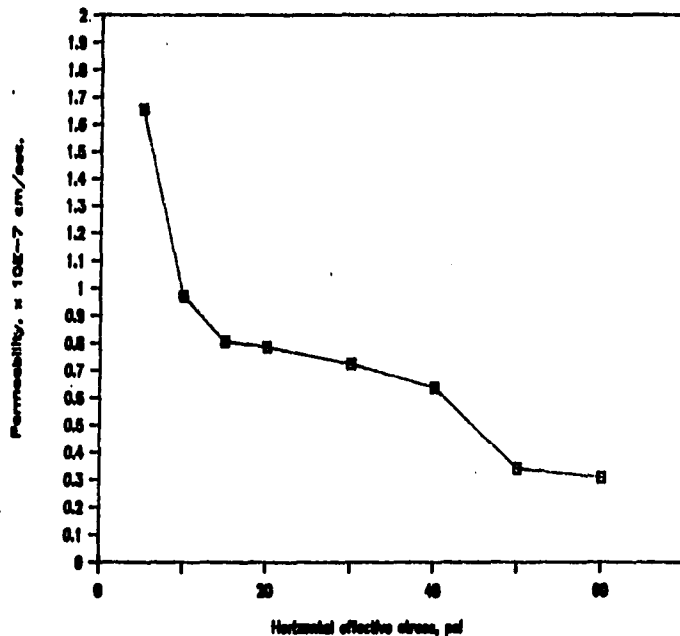


Figure 31. Hydraulic conductivity of intact sample H5-20 at different confining stresses

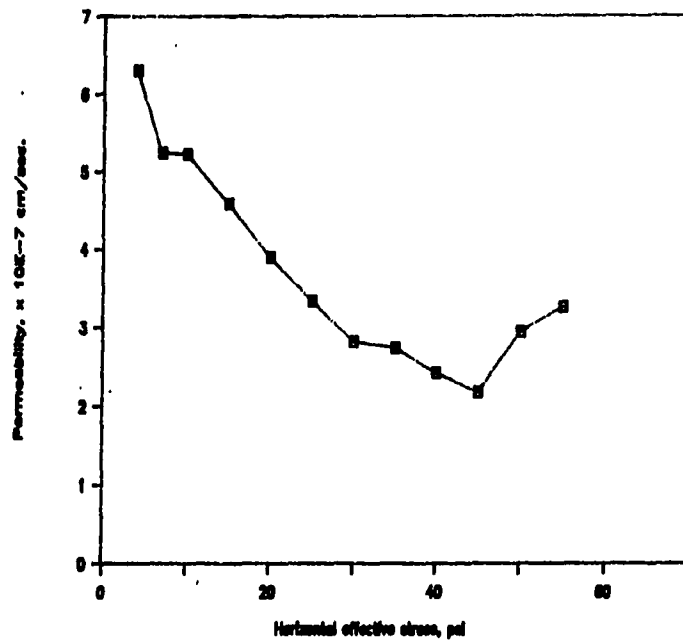


Figure 32. Hydraulic conductivity of intact sample H6-10 at different confining stresses

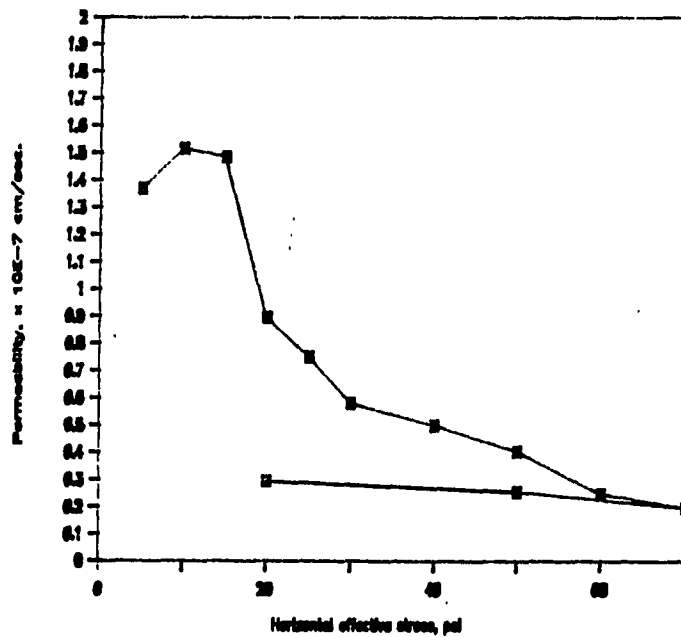


Figure 33. Hydraulic conductivity of intact sample H8-15 at different confining stresses

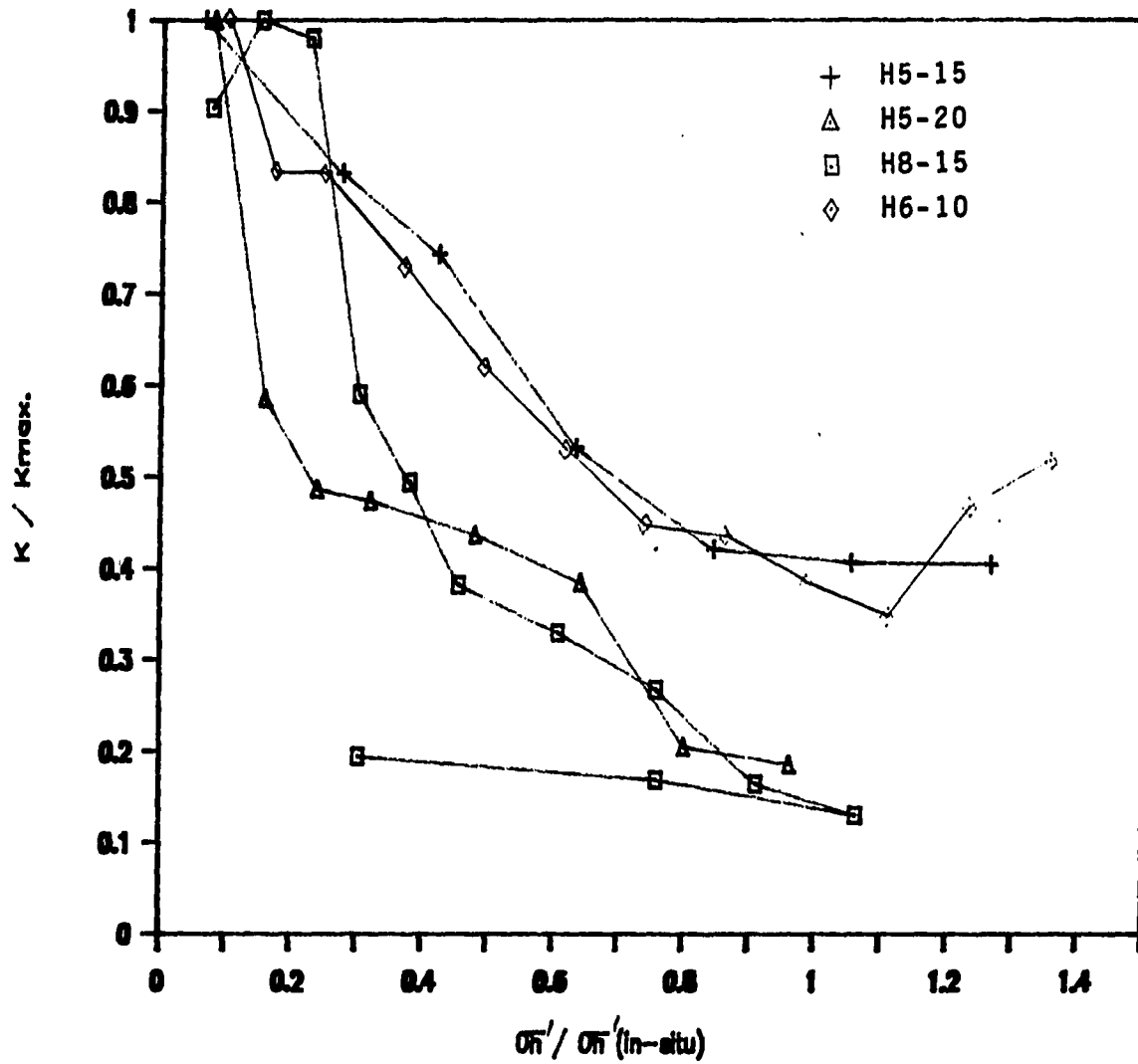


Figure 34. Normalized permeability vs. normalized confining stresses

the normalized confining stress, based on the minimum in situ stress acting on the sample. This indicates that as a practical matter, in a hydraulic conductivity test the reproducing in situ stresses is important and the confining stress is not critical when it equals or exceeds the in situ lateral earth pressure. The change of hydraulic conductivity of sample H6-10, tested in an isotropic stress field, generally follows the same trend as the other samples but the permeability seems to reach the "stable" level, about at 70% of lateral stress measured by the Stepped Blade, while the permeabilities of other samples "stabilize" at about 85% of the in situ lateral stresses. This is expected, since the sample H6-10 was subjected to a higher stress than the in situ stress in vertical direction, which might cause additional compression.

Results from split samples

After measuring permeabilities of intact samples, an artificial crack was then made by split-tensile method through samples, H5-15, H8-15, and H6-10. The hydraulic conductivity of the fractured samples then was measured with the samples confined under various lateral confining stresses. These results are shown in Figures 35 and 37 and Appendix D. The permeability of split sample H5-15 ranges from 1.56×10^{-7} to 5.64×10^{-8} cm/sec, of split sample H6-10

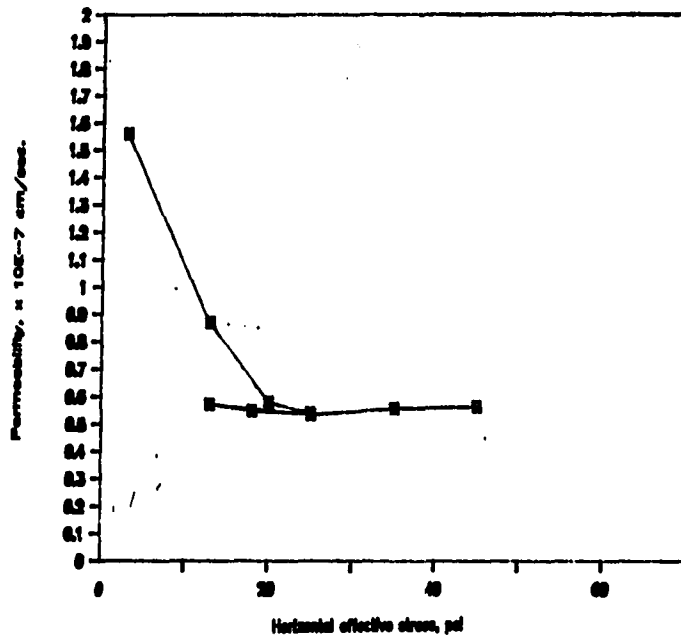


Figure 35. Hydraulic conductivity of split sample H5-15 at different confining stresses

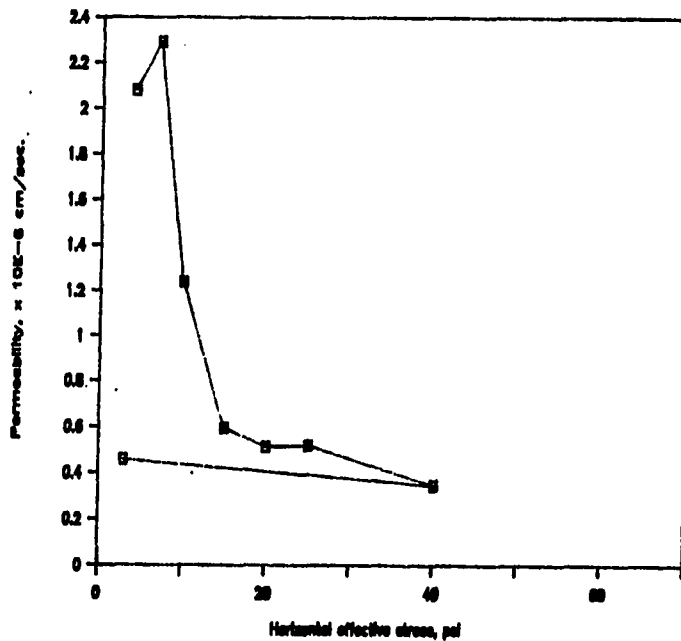


Figure 36. Hydraulic conductivity of split sample H6-10 at different confining stresses

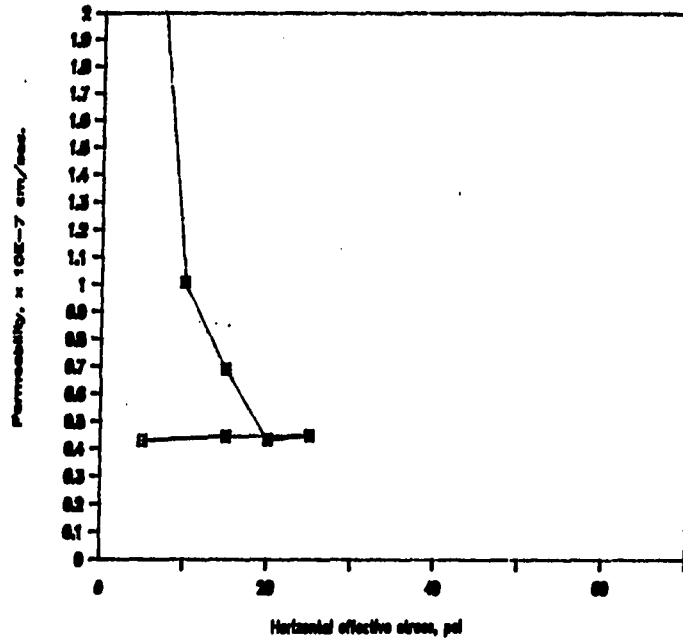


Figure 37. Hydraulic conductivity of split sample H8-15 at different confining stresses

ranges from 4.58×10^{-7} to 2.08×10^{-6} cm/sec, and of split sample H8-15 ranges from 4.3×10^{-8} to 9.66×10^{-7} cm/sec, varying by a factor of 2.8, 4.5, and 22.5 respectively. The decrease of permeability due to increase of confining stresses follows the same trend as the data from intact samples.

The results show that all the permeability of split samples are stabilized at about 20 psi, independent of the measured lateral stresses. The "stabilized" permeabilities of split samples are not higher than 1.5 times of those of intact samples.

These permeability data from fractured samples also imply that under a certain confining stress the crack in soil sample becomes closed. These tests illustrate the importance of measuring in situ stresses in the field and simulating them when evaluating soil hydraulic conductivity in the laboratory.

Discussion

The triaxial confining permeability showed that hydraulic conductivity is highly stress-dependent varying by a factor of 10 under different confining stresses. However, the tests also indicated that the permeability of a soil sample becomes nearly a constant above a lateral confining stress that is 85% of the minimum lateral stresses measured

in situ by the Stepped Blade was applied.

These results may suggest that, under a confining stress equal to the minimum in situ lateral stress measured by the Stepped Blade, the soil samples resume their original internal structures and keep the structure nearly unchanged. Because of a limited capacity of the triaxial apparatus, the tests originally proposed to investigate the effect of the preconsolidation stress on hydraulic conductivity could not be conducted.

Though the in situ lateral stresses did show a significant effect on measuring hydraulic conductivity, the conclusion of the test, that the in situ lateral stress is a main factor controlling the permeability measurement in the laboratory, remains uncertain, since the pneumatic stepped blade was reported that it could overestimate the lateral stress up to a factor of 1.5 to 2.5 in a normally consolidated to lightly overconsolidated soil, due to the excess pore water pressure caused by insertion of the blade.

The data reported by Mings (1987) indicated that the lateral stresses measured by use of pneumatic stepped blade in an alluvial plain were higher than or close to the horizontal preconsolidation stress. Mings indicated that the tested soil was highly sensitive to the displacement induced by inserting the Stepped Blade and exceeded the limit pressure after the insertion of the Blade, therefore the interpreted

K_0 's were unreasonably high. If the overestimation remained in the measuring lateral stresses in the till deposit, the previous conclusion that the hydraulic conductivity became nearly constant when the confining stress was close to the in situ stress would be questionable.

Several one-dimensional consolidation tests were conducted on samples trimmed to be tested in a horizontal direction to investigate the horizontal preconsolidation stress. The purpose was to verify the difference between the lateral stresses measured by the blade and the horizontal preconsolidation stress in this till deposit.

The measured lateral stresses and horizontal preconsolidation stress are shown in Table 2. The consolidation curves and interpretation of horizontal preconsolidation stress are given in Appendix C.

The ratio of horizontal preconsolidation stresses to the measured in situ stresses has an average value of 1.22 for the unweathered samples and a value of 2.3 for the weathered sample, listed in Table 2. These results suggest that the in situ lateral stresses measured by the Stepped Blade, though scattered, are reasonable. Table 2 can be also regarded as a supporting evidence to the conclusion of the triaxial confining permeability test.

Table 2. In situ lateral stresses and horizontal preconsolidation stresses

Sample	lateral stress (a)		(b) H. preconsld. stress (psi)	stress ratio (b)/(a)	
	Min. (psi)	Max. (psi)		Max.	Min.
H5-20	62	77	90	1.44	1.16
H6-5		26 ¹	60		2.3
H6-20 ²		88	60		0.68
H7-17		76 ¹	85		1.12
H8-25		93 ¹	110		1.18

¹Only one stress was successfully obtained.

²The sample was severely disturbed when sampling.

The effect of stress relief on hydraulic conductivity was studied by tests on sample H8-15, where it was revealed that the stress-permeability relationship is not reversible that is, a reduction in lateral stress does not reinstate a higher conductivity. That might be because of two possibilities; (1) insufficient time for stress release in the soil samples, only 3 days being allowed for each stage of the stress decrease, compared to a period of time over 3 months of being stored in the humidity room, and (2) sampling disturbance being offset by the high confining stresses, that is analogous to the results of similar procedures on split samples H5-15 and H8-15, the irreversible stress-permeability relationship may be due to lack of circumstance reproducing tensile stress to reopen the fractures.

Among the four intact samples, sample H6-10 showed a lightly irregular change in hydraulic conductivity. When the confining stress was higher than measured in situ lateral stress, the hydraulic conductivity increased slightly, to about 1.5 times of the lowest permeability. The result could be due to the unknown changes of the internal structure originally containing fractures in the sample, and the type of confining stress being applied. The details of this irregularity require further research.

This research also shows that the artificial fractures can increase the hydraulic conductivity by a factor of 5 to 50, depending in part on the amount of opening of the crack. Unfortunately, measuring changes in crack with soil samples sealed in the triaxial chamber was not possible. Thus the details of changes of hydraulic conductivity contributed by fractures remain unsolved.

CONCLUSION

1. Soils investigated in 6 borings at the test site were relatively dense, uniform in texture, and over-consolidated, characteristic of a basal till deposit of the Alden member of the Dows Formation of Des Moines Lobe of Late Wisconsin glaciation.
2. The distribution of lateral stresses in soils at this site was determined from Stepped Blade tests to be isotropic and independent of the direction of glacial flow or topographic position.
3. Visual observation and the isotropic lateral stress condition suggest that vertical and sub-vertical fractures, occurring mainly within the upper 10 to 13 feet of till may be caused by desiccation and other weathering processes rather than shear stresses induced by glacial action.
4. Hydraulic conductivity of core samples in a vertical direction is highly stress-dependent, the lateral in situ stress having a significant influence on the measured hydraulic confining. The hydraulic conductivity of a soil sample becomes nearly a constant above a lateral confining stress that is approximately 85% of the minimum lateral stress measured in situ by the Stepped Blade.

5. The hydraulic conductivity tests on split samples indicated that artificial fractures could be healed under a confining stress equal to 20 psi, about 1/3 to 1/2 of the minimum lateral stress measured by the Stepped Blade. The results also suggest that controlling confining stresses in a laboratory permeability test is important.

RECOMMENDATION FOR FURTHER RESEARCH

1. SBT's should be performed in a well-defined shear-fractured area to verify the relationship between glacial flow, lateral stresses, and formation of fractures in a lodgment glacial till.
2. The conditions of soil in the deeper zone should be studied to find any possible changes of soil properties and stress conditions.
3. The extent of the sand layer occurring at boring H3 and its influence on groundwater flow should be further investigated.

BIBLIOGRAPHY

- Al-Shaikh-Ali, M. M. H., A. G. Davis, and M. J. Loyd. "In Situ Measurement of K_0 in a Stiff Fissured Glacial Till by Hydraulic Fracturing." *Ground Engineering*, 14, No. 1 (Jan. 1981): 19-25.
- American Society of Testing and Materials. 1988 Annual Book of ASTM Standards. Volume 04.08 Soil and Rock, Building Stones: Geotextiles. Section 4. American Society of Testing and Materials, Philadelphia, 1988.
- Anderson, W. I. "Cenozoic: Erosion Climaxed by the Great Ice Age." Pp. 215-237. In W. I. Anderson. *Geology of Iowa -- Over Two Billion Years of Change.* The Iowa State University Press, Ames, Iowa, 1983.
- Bear, J. Hydraulics of Groundwater. McGraw-Hill International Book Co., New York, 1979.
- Bjerrum, L. "Embandments on Soft Ground." *Proceedings of the ASCE Specialty Conference on Performance of Earth and Earth-Supported Structures, II (1972)*, 1-54.
- Bjerrum, L. and J. Huder. "Measurement of the Permeability of Compacted Clays." *Proceedings of the 4th International Conference of Soil Mechanics and foundation Engineering*, London, 1967.
- Bosscher, P. J., G. P. Bruxvoort, and T. E. Kelley. "Influence of Discontinuous Joints on Permeability." *Journal of Geotechnical Engineering, ASCE*, 114, No. 11 (Nov. 1988): 1318-1311.
- Boulton, G. S. "On the Deposition of Subglacial and Melt-Out Tillis at the Margins of Certain Svalbard Glaciers." *Journal of Glaciology*, 9, No. 56 (1970): 231-245.
- Boulton, G. S. and M. A. Paul. "The Influence of Genetic Processes on Some Geotechnical Properties of Glacial Tillis." *Quarterly Journal of Engineering Geology*, 9, No. 3 (1976): 159-194.
- Boynton, S. S. "An Investigation of Selected Factors Affecting the Hydraulic Conductivity of Compacted Clay." M.S. Thesis, University of Texas at Austin, 1983.

Brooker, E. W. and Ireland, H. O. "Earth Pressures at Rest Related to Stress History." Canadian Geotechnical Journal, 11, No. 1 (1965): 1-75.

Carpenter, G. W. "Assessment of the Triaxial Falling Head Permeability Testing Technique." Ph.D. Dissertation, University of Missouri, Rolla, 1982.

Chandler, R. J. "A Study of Structural discontinuities in Stiff Clays Using A Polarising Microscope." Proceedings, International Symposium on soil structure, Gothenburg, Aug. 1-2, 1973.

Connel, D. E. "Distribution, Characteristics, and Genesis of Joints in Fine-Grained Till and Locustrine Sediment, Eastern and Northwestern Wisconsin." M.S. Thesis, University of Wisconsin, Madison, Wisconsin, 1984.

Daniel, D. E. "Predicting Hydraulic Conductivity of Clay Liners." Journal of Geotechnical Engineering, ASCE, 111, No. 2 (Feb. 1984): 285-300.

Fookes, P. G. and Dennes, B. "Observational Studies on Fissure Patterns in Cretaceous Sediments of South-East England." Geotechnique, 19, No. 4 (1969): 453-477.

Foster, J. D. "Glacial Morphology of the Cary Age Deposits in a Portion of Central Iowa." M.S. Thesis, Iowa State University, Ames, Iowa, 1969.

Grisak, G. E. "The Fracture Porosity of Glacial Till." Canadian Journal of Earth Science, 12, No. 3 (March 1975): 513-515.

Haimson, B. C. "A Simple Method for Estimating In Situ Stresses at Great Depths." Field Testing and Instrumentation of Rock. ASTM, Special Technical Publication, No. 554 (1973): 156-182.

Handy, R. L., B. Remmes, S. Moldt, A. J. Lutenecker, and G. Trott. "In Situ Stress Determination by Iowa Stepped Blade." Journal of Geotechnical Engineering, ASCE, 108, No. GT11 (Nov. 1982): 1405-1422.

Handy, R. L., J. L. Briaud, K. C. Gan, C. L. Mings, D. W. Retz, and J.-F. J. Yang. "Use of The K_0 Stepped Blade in Foundation Design, Volume I." Final Report, No. FHWA/RD-87-102, Dec., 1987.

Iwai, K. "Fundamental Studies of Fluid flow Through a Single Fracture." Ph.D. Dissertation, University of California, Berkeley, 1976.

Johnson, M. D. "The Origin and Microfabric of Lake Superior Red Clay." *Journal of Sedimentary Petrology*, 53, No. 3 (Sept. 1983): 859-873.

Kazi, A. and J. L. Knill. "Fissuring in Glacial Lake Clays and Tills on the Norfolk Coast, United Kingdom." *Engineering Geology*, 7, No. 1 (June 1973): 35-48.

Kemmis, T. J., G. R. Hallbery, and A. J. Lutenecker. "Depositional Environments of Glacial Sediments and Landform on the Des Moines Lobe, Iowa." Iowa Geological Survey Guidebook Series No. 6, 1981.

Kleppe, J. H. "Desiccation Cracking of Compacted Soil." M. S. Thesis, University of Texas at Austin, 1981.

Lambe, T. W. and R. V. Whitman. Soil Mechanics, SI Version. John Wiley & Sons, Inc., New York, 1979.

Lutenecker, A. J. and A. Timian. "In Situ Tests with K_0 Stepped Blade." Use of In-Situ Test in Geotechnical Engineering, ASCE, Geotechnical Special Publication No. 6 (1986): 730-751.

Mayne, P. W. and F. H. Kulhawy. " K_0 -OCR Relationships in Soil." *Journal of Geotechnical Engineering, ASCE*, 108, No. GT6 (June 1982): 851-872.

McGown, A. and E. Derbyshire. "Genetic Influences on the Properties of tills." *Quarterly Journal of Engineering Geology*, 10, No. 4 (1977): 389-410.

McGown, A. and A. M. Radwan. "The Presence and Influence of Fissures in the Boulder Clays of West Central Scotland." *Canadian Geotechnical Journal*, 12, No. 1 (Feb., 1975): 84-97.

McGown, A., A. Saldivar-Sali, and A. M. Radwan. "Fissure Patterns and Slope Failures in Till at Hurlford, Ayrshire." *The Quarterly Journal of Engineering Geology*, 7, No. 1 (1974): 1-26.

Mesri, G. and R. E. Olson. "Mechanisms Controlling the Permeability of Clays." *Clay and Clay Minerals, Journal of Clay Minerals Society*, 19, No. 3 (1971): 151-158.

- Mings, C. L. "K_o Stepped Blade Tests in Alluvial Clay." M. S. Thesis, Iowa State University, Ames, Iowa, 1987.
- Mitchell, J. K. Fundamentals of Soil Behavior. John Wiley & Sons, Inc., New York, 1976.
- Moore, C. A. and E. M. Ali. "Permeability of Cracked Clay Liners." Proceedings, Eighth Annual Research Symposium on Land Disposal of Hazardous Waste, Cincinnati, Ohio, EPA-600/9-82-002, 1982.
- Olson, R. E. and D. E. Daniel. "Measurement of the Hydraulic Conductivity of Fine-Grained Soils." ASTM Special Technical Publication No. 746, 1981.
- Ruhe, R. V. Quaternary Landscapes in Iowa. The Iowa State University Press, Ames, Iowa, 1969.
- Samarasinghe, A. M., Y. H. Huang, and V. P. Drnevich. "Permeability and Consolidation of Normally Consolidated Soils." Journal of the Geotechnical Engineering, ASCE, 108, No. GT6 (June, 1982): 835-850.
- Schmertmann, J. H. "Measure and Use of the In Situ Lateral Stress." Pp. 189-213. The Practice of Foundation Engineering, Honoring Volume of Dr. J. Osterberg. Department of Civil Engineering, Northwestern University, Evanston, Ill., 1985.
- Sherif, M. A. and I. Ishibashi. "Overconsolidation Effects on Ko Values." Proceedings of the 10th International Conference on Soil Mechanics and Foundation Engineering, Stockholm, 1981.
- Skempton, A. W. and R. D. Northey. "The Sensitivity of Clays." Geotechnique, 3, No. 1 (March 1952): 30-53.
- Skempton, A. W., R. L. Shuster, and D. J. Pettey. "Joints and Fissures in the London Clay at Wraysbury and Edgware." Geotechnique, 19, No. 2 (June 1969): 205-217.
- Snow, T. "Rock Fracture Spacings, Openings, and Porosities." Journal of the Soil Mechanics and Foundation Division, Proceedings of ASCE, 94, No. SM1 (Jan. 1968): 73-91.
- Spangler, M. G. and R. H. Handy. Soil Engineering. Fourth Edition. Harper & Row, Publishers, New York, 1982.

Stephenson, D. A., A. H. Fleming, and D. M. Mickelson. "Glacial Deposits." Pp. 301-314. *The Geology of North America*. Vol. O-2. Hydrogeology. The Geological Society of America, Boulder, Colorado, 1988.

Tavenas, F., P. Leblond, and S. Leroueil. "The Permeability of Natural Soft Clays, Part I: Methods of Laboratory Measurement." *Canadian Geotechnical Journal*, 20, No. 4 (Nov. 1983a): 629-644.

Tavenas, F., P. Leblond, and S. Leroueil. "The Permeability of Natural Soft Clays, Part II: Permeability Characteristics." *Canadian Geotechnical Journal*, 20, No. 4 (Nov. 1983b): 645-660.

Taylor, D. W. Fundamentals of Soil Mechanics. John Wiley & Sons, Inc., New York, 1958.

Tse, E. W. "Application of Critical State Soil Mechanics to Electric K_0 Stepped Blade." Ph.D. Dissertation, Iowa State University, Ames, Iowa, 1988.

Williams, R. E. and R. N. Garvolden. "The Influence of Joints on the Movement of Ground Water Through Glacial Till." *Journal of Hydrology*, Amsterdam, 5, No. 2 (June 1967): 163-170.

Witherspoon, P. A., J. S. Y. Wang, D. Iwai, and J. E. Gale. "Validity of Cubic Law for Flow in a Deformable Rock Fracture." *Water Resources Research*, 16, No. 6 (Dec. 1980): 1016-1024.

Yang, J.-F. J. "Role of Lateral Stress in Slope Stability of Stiff Overconsolidated Clays and Clay Shales." Ph.D. Dissertation, Iowa State University, Ames, Iowa, 1987.

ACKNOWLEDGMENTS

This research is part of the Aquatard Hydrology Project sponsored by the Iowa Department of Natural Resources.

I wish to express my sincere appreciation to Dr. Richard L. Handy for his support, encouragement and guidance through every stage of my study. Special thanks to Dr. Dah-Yinn Lee and Dr. John M. Pitt for their assistance in my study in the U. S. Thanks to Dr. Frederick M. Graham and Dr. Robert Horton, Jr. for serving on my Program of Study Committee. A special thanks to Professor James M. Hoover for his assistance in the experiment. I also thank Mr. C. Detrik, Mr. G. Hunter and Mr. S. Lee for helping with the SBTs.

I am also indebted to my parents and my grandmother for fulfilling my life with love. Without their support, my goal would never have been accomplished.

A very special thanks to my beloved wife, Hui-Tsen, who patiently typed the rough draft and whose love and devotion were a major source of encouragement to complete this work.

APPENDIX A
Original SBT Data

 Ttest site: H1

Date: 9/30/89

Operators: Hung-yu Wang, Shis-hsiung Lee

Recorder: Hung-yu Wang

Ddpth (ft)	Measured Pressure, psi				Cells used
	Cell 1	Cell 2	Cell 3	Cell 4	
8.2	NG	36	50	42	2,3
8.6	40	40	65		2,3
9.0	36	70			1,2
9.4	38				
13.2	NG	46	60	80	1,2,3
13.6	NG	54	78		2,3
14.0	NG	60			---
14.4	NG				
18.2	NG	50	48	67	3,4
18.6	NG	88	100		2,3
19.0	NG	100			---
19.4	NG				
23.2	NG	NG	18	42	---
23.6	NG	19	44		---
24.0	NG	44			---
24.4	NG				
28.6	NG	82	94	118	3,4
29.0	NG	92	114		2,3
29.4	NG	110			---
29.8	NG				

Groundwater table after 24 hrs.:7.5 ft.

 Ttest site: H1-1

Date: 9/30/89

Operators: Hung-yu Wang, Shis-hsiung Lee

Recorder: Hung-yu Wang

Ddpth (ft)	Measured Pressure, psi				Cells used
	Cell 1	Cell 2	Cell 3	Cell 4	
6.2	28	42	54	NG	1,2
6.6	36	34	30		---
7.0	56	40			---
7.4	56				
11.2	72	90	88	NG	1,2
11.6	108	96	NG		---
12.0	140	118			---
12.4	106				
16.2	66	66	60	88	---
16.6	88	80	66		---
17.0	74	80			1,2
17.4	78				
21.2	56	60	70	60	2,3
21.6	96	86	96		2,3
22.0	100	96			---
22.4	98				
26.2	85	72	70	44	---
26.6	88	98	96		1,2
27.0	92	94			1,2
27.4	96				
31.2	96	106	110	90	1,2
31.6	118	114	106		---
32.0	110	106			---
32.4	110				

Groundwater table after 24 hrs.: 23 ft.

 Ttest site: H1-2
 Date: 11/4/89
 Operators: Hung-yu Wang, Glenn Hunter
 Recorder: Hung-yu Wang

Ddpth (ft)	Measured Pressure, psi				Cells used
	Cell 1	Cell 2	Cell 3	Cell 4	
5.2	42	50	46	30	1,2
5.6	58	70	56		1,2
6.0	48	623			1,2
6.4	50				
10.2	64	72	78	30	2,3
10.6	NG	58	46		---
11.0	78	46			---
11.4	62				
15.2	86	88	98	90	2,3
15.6	90	86	90		2,3
16.0	90	80			---
16.4	84				
20.2	86	92	100	24	1,2,3
20.6	108	106	84		---
21.0	82	76			---
21.4	60				
25.2	70	72	68	74	1,2
25.6	90	84	98		2,3
26.0	92	84			---
26.4	82				
30.2	80	76	86	96	2,3,4
30.6	80	76	90		2,3
31.0	76	84			1,2
31.4	72				

Groundwater table after 24 hrs.: 21.3 ft.

 Ttest site: H3

Date: 8/24/89

Operators: Hung-yu Wang, Shis-hsiung Lee

Recorder: Hung-yu wang

Ddpth (ft)	Measured Pressure, psi				Cells used
	Cell 1	Cell 2	Cell 3	Cell 4	
7.2	NG	16	26	26	2,3
7.6	NG	20	28		2,3
8.0	NG	26			---
8.4	NG				
13.2	28	36	42	40	1,2
13.6	42	42	48		2,3
14.0	46	46			1,2
14.4	46				---
17.7	36	42	38	50	1,2
18.1	58	48	52		2,3
18.5	60	50			---
18.9	56				
20.2	76	66	70	74	2,3,4
20.6	70	72	74		1,2,3
21.0	68	64			---
21.4	42				
25.2	70	68	72	74	2,3
25.6	94	94	80		1,2
26.0	114	98			---
26.4	94				
30.2	30	42	28		---
30.6	66	62			---
31.0	82				---

Groundwater table after 24 hrs.: 6.2 ft.

 Ttest site: H3-1A
 Date: 9/23/89
 Operators: Hung-yu Wang, Shis-hsiung Lee
 Recorder: Hung-yu wang

Ddpth (ft)	Measured Pressure, psi				Cells used
	Cell 1	Cell 2	Cell 3	Cell 4	
5.2	NG	24	20	20	---
5.6	34	34	34		1,2,3
6.0	40	46			1,2
6.4	44				
10.2	40	64	66	50	2,3
10.6	66	70	78		2,3
11.0	56	66			1,2
11.4	76				
16.2	72	74	88	74	2,3
16.6	76	74	80		2,3
17.0	86	94			1,2
17.4	82				
20.7	78	96	110	84	1,2
21.1	98	94	114		2,3
21.5	78	100			1,2
21.9	NG				
25.7	106	80	NG		---
26.1	140	106			---
26.5	134				---
26.9	Stopped by rocks				

Groundwater table after 24 hrs.: 5.75 ft.

Ttest site: H3-2A
Date: 11/9/89
Operators: Hung-yu Wang, Glenn Hunter
Recorder: Hung-yu wang

Ddpth (ft)	Measured Pressure, psi				Cells used
	Cell 1	Cell 2	Cell 3	Cell 4	
6.2	18	20	20	16	1,2
6.6	32	30	26		---
7.0	44	34			---
7.4	46				
10.2	NG	NG	NG	NG	---
10.6	48	48	48		1,2,3
11.0	64	68			1,2
11.4	70				
15.2	80	80	92	74	2,3
15.6	96	96	104		2,3
16.0	92	94			1,2
16.4	90				

Groundwater table after 24 hrs.: 5.6 ft.

 Ttest site: H5
 Date: 4/27/89
 Operators: Hung-yu Wang, Charlie Detrick
 Recorder: Hung-yu wang

Ddpth (ft)	Measured Pressure, psi				Cells used
	Cell 1	Cell 2	Cell 3	Cell 4	
6.1	18	21	18	8	1,2
6.5	30	26	32		2,3
6.9	35	34			---
7.3	27				
11.1	56	55	60	56	2,3
11.5	70	80	92		1,2,3
11.9	92	116			1,2
12.3	98				
16.1	54	56	48	33	1,2
16.5	90	92	90		---
16.9	92	100			1,2
17.3	90				
21.1	83	92	82	86	1,2
21.5	90	90	86		---
21.9	94	100			1,2
22.3	86				
26.1	86	84	78	46	---
26.5	80	96	78		1,2
26.9	112	106			---
27.3	120				
31.1	93	92	88	60	---
31.5	107	109	112		1,2,3
31.9	87	98			1,2
32.3	130				

Groundwater table after 24 hrs.: 10.0 ft.

Ttest site: H5-1
Date: 11/8/89
Operators: Hung-yu Wang, Glenn Hunter
Recorder: Hung-yu wang

Ddpth (ft)	Measured Pressure, psi				Cells used
	Cell 1	Cell 2	Cell 3	Cell 4	
5.0	No data available				
10.2	46	NG	40	28	---
10.6	NG	74	82		2,3
11.0	78	76			---
11.4	NG				
15.2	NG	90	106	80	2,3
15.6	NG	94	104		2,3
16.0	NG	84			---
16.4	NG				
20.2	NG	90	102	78	2,3
20.6	NG	102	100		---
21.0	NG	90			---
21.4	NG				
25.2	NG	90	88	104	3,4
25.6	NG	102	94		---
26.0	NG	82			---
26.4	NG				
30.2	NG	NG	112	94	---
30.6	NG	NG	108		---
31.0	NG	NG			---
31.4	NG				

Groundwater table after 24 hrs.: 24.75 ft.

 Ttest site: H6
 Date: 8/8/89
 Operators: Hung-yu Wang, Shis-hsiung Lee
 Recorder: Hung-yu wang

Dpth (ft)	Measured Pressure, psi				Cells used
	Cell 1	Cell 2	Cell 3	Cell 4	
5.1	NG	28	22	16	---
5.5	NG	28	24		---
5.9	30	32			1,2
6.3	34				
10.9	28	78	60	NG	---
11.3	82	100	112		1,2
11.7	80	110			1,2
12.1	90				
15.9	40	38	44	42	2,3
16.3	86	98	86		1,2
16.7	90	105			1,2
17.1	86				
20.9	64	94	95	40	1,2
21.3	94	94	89		1,2
21.7	104	108			1,2
22.1	106				
25.9	96	98	118	74	2,3
26.3	106	118	130		1,2,3
26.7	112	124			1,2
27.1	108				
30.9	94	100	84	58	1,2
31.3	124	125	116		1,2
31.7	116	142			1,2
32.1	114				

Groundwater table after 24 hrs.: 9.5 ft.

 Ttest site: H7

Date: 7/28/89

Operators: Hung-yu Wang, Shis-hsiung Lee

Recorder: Hung-yu wang

Ddpth (ft)	Measured Pressure, psi				Cells used
	Cell 1	Cell 2	Cell 3	Cell 4	
6.3	30	26	34	34	2,3
6.7	44	58	64		1,2
7.1	NG	54			---
7.5	56				
10.9	61	82	82	52	1,2
11.3	84	104	118		1,2
11.7	88	108			1,2
12.1	70				
17.9	56	80	96	24	1,2
18.3	96	104	104		1,2
18.7	100	92			---
19.1	86				
20.9	54	60	76	60	2,3
21.3	NG	110	118		2,3
21.7	NG	130			---
22.1	NG				

Groundwater table after 24 hrs.: 5.5 ft.

 Ttest site: H7

Date: 7/28/89

Operators: Hung-yu Wang, Shis-hsiung Lee

Recorder: Hung-yu wang

Ddpth (ft)	Measured Pressure, psi				Cells used
	Cell 1	Cell 2	Cell 3	Cell 4	
6.3	30	26	34	34	2,3
6.7	44	58	64		1,2
7.1	NG	54			---
7.5	56				
10.9	61	82	82	52	1,2
11.3	84	104	118		1,2
11.7	88	108			1,2
12.1	70				
17.9	56	80	96	24	1,2
18.3	96	104	104		1,2
18.7	100	92			---
19.1	86				
20.9	54	60	76	60	2,3
21.3	NG	110	118		2,3
21.7	NG	130			---
22.1	NG				

Groundwater table after 24 hrs.: 5.5 ft.

 Ttest site: H8
 Date: 5/11/89
 Operators: Hung-yu Wang, Charlie Detrick
 Recorder: Hung-yu wang

Ddpth (ft)	Measured Pressure, psi				Cells used
	Cell 1	Cell 2	Cell 3	Cell 4	
6.1	28	50	52	28	2,3
6.5	54	56	62		2,3
6.9	56	56			1,2
7.3	56				
11.1	NG	38	82	28	2,3
11.5	58	94	NG		1,2
11.9	42	64			1,2
12.3	58				
16.1	86	96	82	66	1,2
16.5	94	94	98		2,3
16.9	90	98			1,2
17.3	92				
21.1	86	65	90	48	1,2
21.5	100	106	108		1,2
21.9	98	104			1,2
22.3	102				
26.1	60	66	NG	22	1,2
26.5	120	127	80		2,3
26.9	132	124			---
27.3	144				
31.1	102	30	80	68	---
31.5	120	124	136		2,3
31.9	96	110			1,2
32.3	114				
36.1	92	106	104	80	1,2
36.5	130	146	134		1,2
36.9	132	148			1,2
37.1	132				

Groundwater table after 24 hrs.: 8.7 ft.

 Ttest site: H8-1
 Date: 11/4/89
 Operators: Hung-yu Wang, Glenn Hunter
 Recorder: Hung-yu wang

Ddpth (ft)	Measured Pressure, psi				Cells used
	Cell 1	Cell 2	Cell 3	Cell 4	
5.2	42	32	36	36	2,3
5.6	NG	30	24		---
6.0	46	38			---
6.4	48				
10.2	36	36	42	38	2,3
10.6	40	54	50		1,2
11.0	56	58			1,2
11.4	56				
15.5	30	26	34	50	2,3
15.9	58	60	50		1,2
16.3	50	56			1,2
16.7	86				
20.2	92	100	104	102	1,2
20.6	106	104	110		1,2
21.0	94	96			1,2
21.4	104				
25.2	92	96	102	94	1,2,3
25.6	106	102	104		2,3
26.0	100	90			---
26.4	94				
30.2	92	NG	96	60	---
30.6	134	NG	128		---
31.0	126	130			---
31.4	110				

Groundwater table after 24 hrs.: 12 ft.

APPENDIX B

Interpreted Lateral Stresses and K_0 's

Ko at different depths at H1

Depth (ft)	σ_v' (psi)	σ_h (psi)	Pw (psi)	σ_h' (psi)	Ko (σ_h'/σ_v')
8.2	7.3	13.5	0.3	13.2	1.8
8.6	7.4	9.0	0.5	8.5	1.1
9.9	8.4	9.0	0.7	8.3	1.0
13.2	9.7	20.0	2.5	17.5	1.8
13.6	10.0	18.0	2.6	15.4	1.5
18.2	12.2	13.0	4.6	8.4	0.7
18.6	12.4	60.0	4.8	55.2	4.5
28.6	17.3	38.0	9.1	28.9	1.7
29.2	17.7	48.0	9.3	38.7	2.2

Ko at different depths at H1-1

Depth (ft)	σ_v' (psi)	σ_h (psi)	Pw (psi)	σ_h' (psi)	Ko (σ_h'/σ_v')
6.2	5.8	12.5	0.0	12.5	2.2
11.2	10.5	46.5	0.0	46.5	4.4
17.0	15.9	63.5	0.0	63.5	4.0
21.2	19.9	38.0	0.0	38.0	1.9
21.6	20.3	61.0	0.0	61.0	3.0
26.6	23.5	71.0	1.4	69.6	3.0
27.0	23.7	85.0	1.6	83.4	3.5
31.2	25.7	78.0	3.6	74.4	2.9

Ko at different depths at H1-2

Depth (ft)	σ_v' (psi)	σ_h (psi)	Pw (psi)	σ_h' (psi)	Ko (σ_h'/σ_v')
5.2	5.1	29.5	0.0	29.5	5.8
5.6	5.4	29.0	0.0	29.0	5.3
6.0	5.8	39.5	0.0	39.5	6.8
10.2	9.9	50.0	0.0	50.0	5.0
15.2	14.8	64.0	0.0	64.0	4.3
15.6	15.2	75.0	0.0	75.0	4.9
20.2	19.6	74.5	0.0	74.5	3.8
25.2	22.8	66.0	1.7	64.3	2.8
25.6	23.0	53.0	1.9	51.1	2.2
30.2	25.5	53.5	3.9	49.6	1.9
30.6	25.7	46.0	4.1	41.9	1.6
31.0	25.9	62.2	4.2	58.0	2.2

Ko at different depths at H3

Depth (ft)	σ_v' (psi)	σ_h (psi)	Pw (psi)	σ_h' (psi)	Ko (σ_h'/σ_v')
7.2	6.8	6.0	0.2	5.8	0.9
7.2	6.6	10.2	0.4	9.8	1.5
13.2	9.8	17.0	3.0	14.0	1.4
13.6	10.0	28.0	3.2	24.8	2.5
14.0	10.2	46.0	3.4	42.6	4.2
17.7	12.2	26.4	5.0	21.4	1.8
18.1	12.4	37.5	5.2	32.3	2.6
20.2	13.5	55.0	6.1	48.9	3.6
20.6	13.8	65.0	6.2	58.8	4.3
25.2	16.3	56.0	8.2	47.8	2.9
25.6	16.5	94.0	8.4	85.6	5.2

Ko at different depths at H3-1A

Depth (ft)	σ_v' (psi)	σ_h (psi)	Pw (psi)	σ_h' (psi)	Ko (σ_h'/σ_v')
5.6	5.4	34.0	0.0	34.0	6.2
6.0	5.8	30.6	0.0	30.6	5.2
10.2	8.0	58.0	1.9	56.1	7.0
10.6	8.2	50.2	2.1	48.1	5.9
11.0	8.4	40.0	2.3	37.7	4.5
16.2	11.3	44.0	4.5	39.5	3.5
16.6	11.4	58.0	4.7	53.3	4.7
17.0	11.6	72.0	4.9	67.1	5.8
20.7	13.6	52.5	6.5	46.0	3.4
21.1	13.8	52.0	6.7	45.3	3.3
21.5	14.0	48.0	6.9	41.1	2.9

Ko at different depths at H3-2A

Depth (ft)	σ_v' (psi)	σ_h (psi)	Pw (psi)	σ_h' (psi)	Ko (σ_h'/σ_v')
6.2	5.7	14.5	0.3	14.2	2.5
10.2	7.9	48.0	2.0	46.0	5.8
10.6	8.1	57.0	2.2	54.8	6.8
15.2	10.6	52.0	4.2	47.8	4.5
15.6	10.8	75.0	4.4	70.6	6.6
16.0	11.0	88.0	4.6	83.4	7.6

Ko at different depths at H5

Depth (ft)	σ_v' (psi)	σ_h (psi)	Pw (psi)	σ_h' (psi)	Ko (σ_h'/σ_v')
6.1	5.4	13.2	0.0	13.2	2.4
6.5	5.8	14.0	0.0	14.0	2.4
11.1	9.7	43.0	0.5	42.5	4.4
11.5	10.0	53.0	0.6	52.4	5.2
11.9	10.2	57.0	0.8	56.2	5.5
16.1	12.5	50.0	2.6	47.4	3.8
16.9	12.8	74.0	3.0	71.0	5.5
21.1	15.1	67.0	4.8	62.2	4.1
21.9	15.6	82.5	5.1	77.4	5.0
26.5	18.1	55.0	7.1	47.9	2.6
31.5	20.8	101.0	9.3	91.7	4.4
31.9	21.0	78.0	9.5	68.5	3.3

Ko at different depths at H5-1

Depth (ft)	σ_v' (psi)	σ_h (psi)	Pw (psi)	σ_h' (psi)	Ko (σ_h'/σ_v')
10.6	10.3	54.0	0.0	54.0	5.2
15.2	14.8	54.0	0.0	54.0	3.7
15.6	15.2	71.0	0.0	71.0	4.7
20.2	19.6	64.0	0.0	64.0	3.3
25.2	24.4	56.5	0.1	56.4	2.3

Ko at different depths at H6

Depth (ft)	σ_v' (psi)	σ_h (psi)	Pw (psi)	σ_h' (psi)	Ko (σ_h'/σ_v')
5.9	5.7	26.0	0.0	26.0	4.5
11.3	10.2	55.0	0.8	54.2	5.3
11.7	10.4	41.5	1.0	40.5	3.9
15.9	12.7	24.5	2.8	21.7	1.7
16.3	12.9	66.0	2.9	63.1	4.9
16.7	13.1	66.5	3.1	63.4	4.8
20.9	15.4	30.0	4.9	25.1	1.6
21.3	15.6	94.0	5.1	88.9	5.7
21.7	15.8	94.0	5.3	88.7	5.6
25.9	18.1	55.8	7.1	48.7	2.7
26.3	18.3	84.0	7.3	76.7	4.2
26.7	18.5	91.0	7.5	83.5	4.5
30.9	20.7	83.0	9.3	73.7	3.6
31.3	21.0	102.1	9.4	92.7	4.4
31.7	21.2	78.0	9.6	68.4	3.2

Ko at different depths at H7

Depth (ft)	σ_v' (psi)	σ_h (psi)	Pw (psi)	σ_h' (psi)	Ko (σ_h'/σ_v')
6.3	5.7	11.8	0.4	11.4	2.0
6.7	6.0	25.5	0.5	25.0	4.2
10.9	8.3	33.5	2.3	31.2	3.8
11.3	8.5	54.5	2.5	52.0	6.1
11.7	8.7	57.5	2.7	54.8	6.3
17.9	12.0	27.0	5.4	21.6	1.8
18.3	12.2	82.0	5.6	76.4	6.3
20.9	13.6	29.8	6.7	23.1	1.7
21.3	13.9	87.4	6.8	80.6	5.8

Ko at different depths at H8

Depth (ft)	σ_v' (psi)	σ_h (psi)	Pw (psi)	σ_h' (psi)	Ko (σ_h'/σ_v')
6.1	5.6	43.5	0.0	43.5	7.8
6.5	6.1	41.0	0.0	41.0	6.7
11.5	9.7	22.5	1.2	21.3	2.2
11.9	9.9	18.0	1.4	16.6	1.7
16.1	12.0	69.0	3.2	65.8	5.5
16.5	12.2	82.0	3.4	78.6	6.4
16.9	12.5	75.5	3.6	71.9	5.8
21.5	14.9	88.0	5.5	82.5	5.5
21.9	15.1	87.0	5.7	81.3	5.4
26.1	17.2	49.0	7.5	41.5	2.4
26.5	17.4	101.0	7.7	93.3	5.4
31.5	20.0	72.0	9.9	62.1	3.1
31.9	20.3	73.5	10.1	63.4	3.1
36.1	22.4	69.0	11.8	57.2	2.6
36.5	22.6	102.5	12.0	90.5	4.0
36.9	22.8	104.2	12.2	92.0	4.0

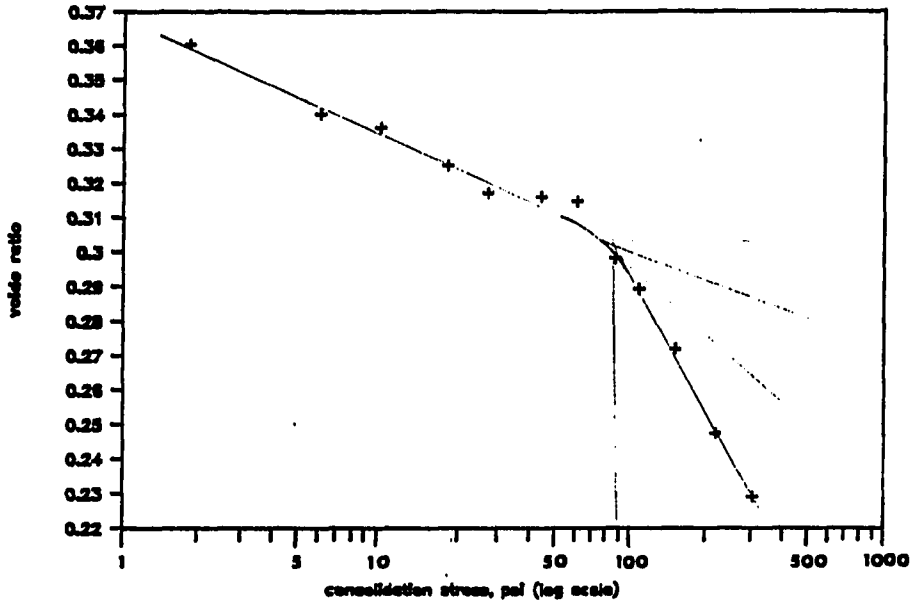
Ko at different depths at H8-1

Depth (ft)	σ_v' (psi)	σ_h (psi)	Pw (psi)	σ_h' (psi)	Ko (σ_h'/σ_v')
5.2	5.1	22.5	0.0	22.5	4.5
10.2	9.9	22.6	0.0	22.6	2.3
10.6	10.3	22.0	0.0	22.0	2.1
11.0	10.7	52.2	0.0	52.2	4.9
15.9	13.8	53.9	1.7	52.2	3.8
16.3	13.9	40.6	1.9	38.7	2.8
20.2	16.0	77.0	3.6	73.4	4.6
20.6	16.2	87.0	3.8	83.2	5.1
21.0	16.4	90.0	4.0	86.0	5.2
25.2	18.8	82.0	5.7	76.3	4.1
25.6	19.0	92.0	5.9	86.1	4.5

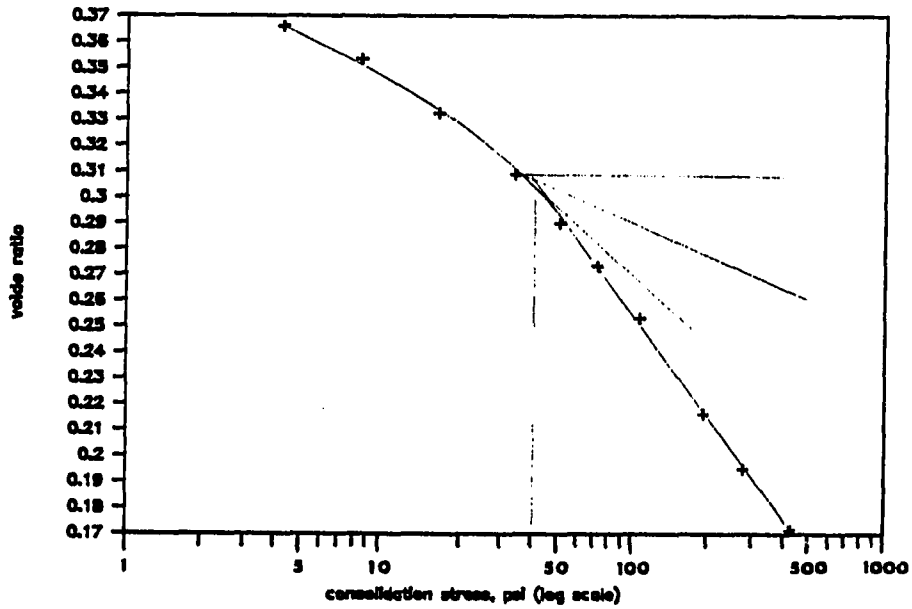
APPENDIX C.

Results of One-dimensional Consolidation Tests

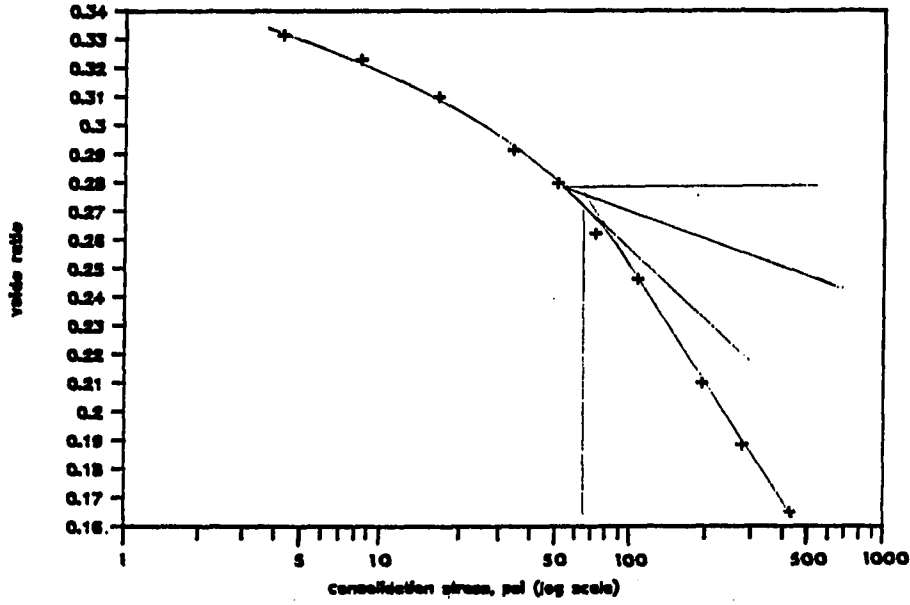
consolidation e-log p, H5-15, v



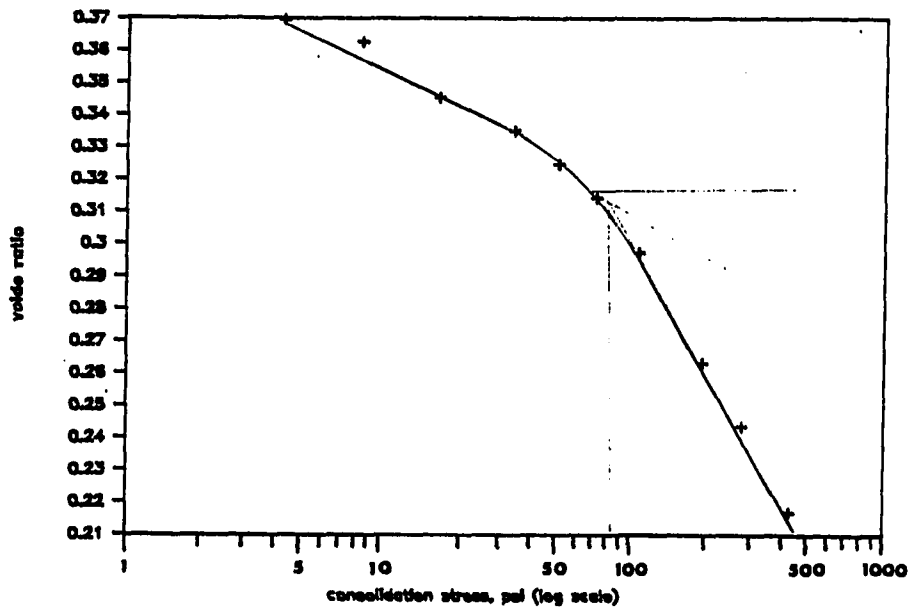
consolidation e-log p, H5-20, v



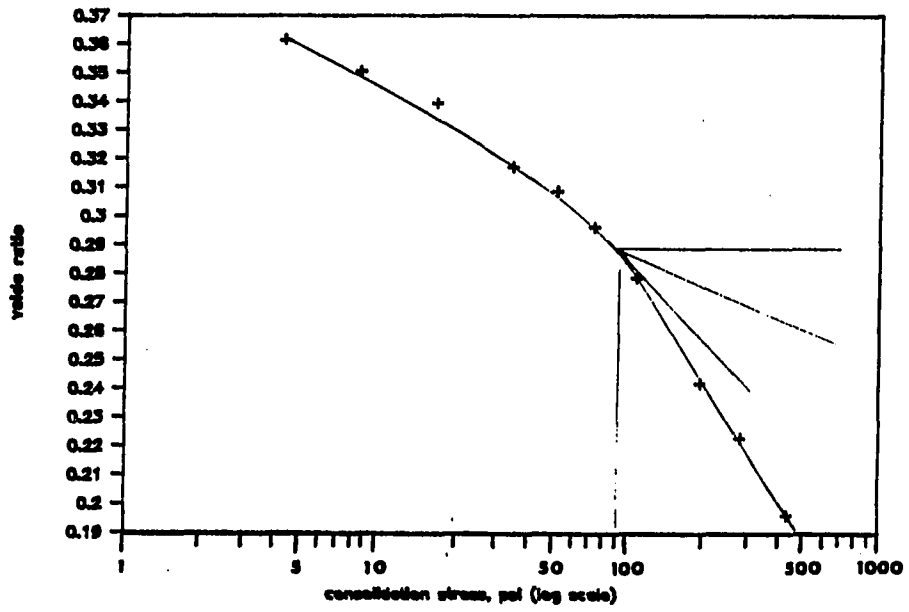
consolidation e-log p, H6-20, h



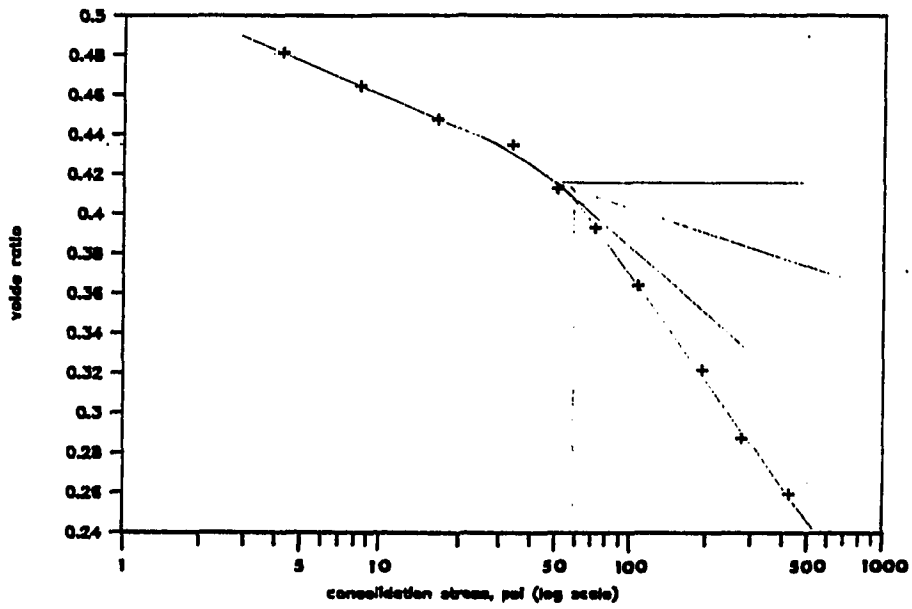
consolidation e-log p, H7-17, h



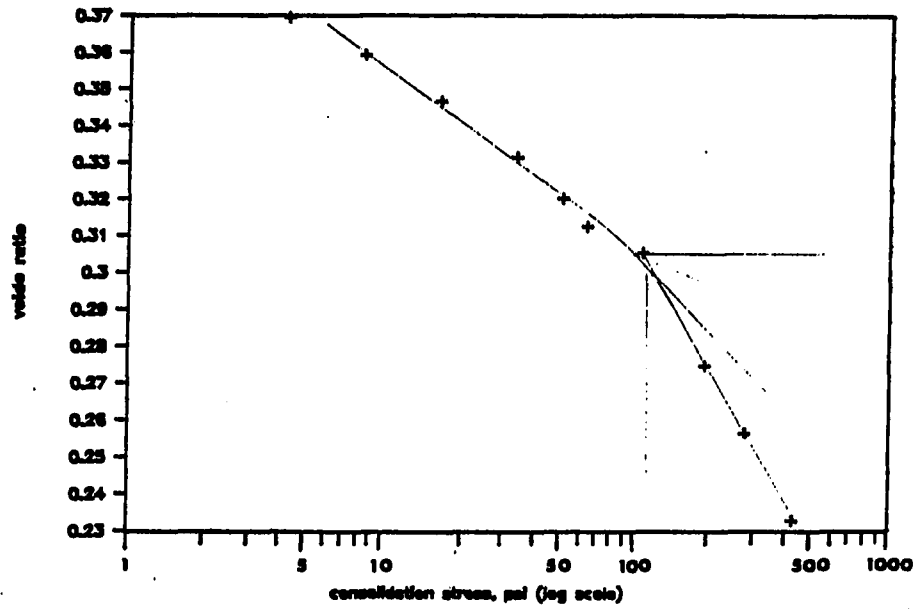
consolidation e-log p, H5-20, h



consolidation e-log p, H6-5, h



consolidation e-log p, H8-25, h



APPENDIX D

Results of Triaxial Confining Permeability Tests

Sample: H5-15 (intact)
 Length: 4.99 in.
 In situ vertical stress: 13 psi

σ_h' (psi)	ho (in)	h1 (in)	t (sec)	K (cm/s)
3	39.94	39.06	44755	1.03E-07
13	38.86	37.69	73920	8.58E-08
20	37.24	37.04	14220	7.68E-08
30	41.02	40.46	52065	5.49E-08
40	40.26	39.69	68190	4.35E-08
50	40.43	39.72	87840	4.19E-08
60	38.97	38.34	81180	4.17E-08

Sample: H5-15 (split)
 Length: 4.99 in.
 In situ vertical stress: 13 psi

σ_h' (psi)	ho (in)	h1 (in)	t (sec)	K (cm/s)
3	41.62	39.63	65370	1.56E-07
13	40.98	39.60	81990	8.69E-08
20	40.81	40.04	68700	5.76E-08
25	41.08	40.35	69075	5.40E-08
18	41.35	40.40	87840	5.50E-08
13	41.62	40.65	85170	5.76E-08
25	41.08	40.17	86760	5.37E-08
35	40.64	39.75	83040	5.54E-08
45	40.27	39.35	85230	5.64E-08

Sample: H6-10 (intact)
 Length: 4.75 in.
 Triaxial confined test ($K_0 = 1$)

σ_h' (psi)	ho (in)	h1 (in)	t (sec)	K (cm/s)
4	41.46	31.72	84060	6.30E-07
7	40.70	32.48	85140	5.24E-07
10	41.73	34.53	71712	5.23E-07
15	39.40	33.77	66528	4.59E-07
20	39.67	35.51	56268	3.90E-07
25	35.23	30.37	88128	3.33E-07
30	34.53	31.29	69288	2.81E-07
35	40.29	36.48	71820	2.74E-07
40	40.54	37.45	64872	2.42E-07
45	33.29	31.12	61380	2.17E-07
50	39.83	35.54	76680	2.94E-07
55	39.35	36.10	52308	3.26E-07

Sample: H6-10 (split)
 Length: 4.75 in.
 In situ vertical stress: 10 psi.

σ_h' (psi)	ho (in)	h1 (in)	t (sec)	K (cm/s)
4	41.59	27.99	37640	2.08E-06
7	41.56	29.69	29040	2.29E-06
10	41.92	39.27	10440	1.24E-06
15	34.75	28.15	70020	5.95E-07
20	41.67	35.29	63960	5.14E-07
25	41.73	36.32	52920	5.19E-07
40	41.73	35.88	85980	3.48E-07
3	41.19	35.23	67500	4.58E-07

Sample: H8-15 (intact)
 Length: 4.375 in.
 In situ vertical stress: 15 psi

σ_h' (psi)	ho (in)	h1 (in)	t (sec)	K (cm/s)
5	41.02	38.64	79500	1.37E-07
10	42.11	39.43	79020	1.52E-07
15	42.16	39.64	75600	1.49E-07
20	41.67	40.05	80640	8.96E-08
25	41.94	40.64	76500	7.50E-08
30	40.81	39.73	84180	5.81E-08
40	42.21	41.21	87420	5.00E-08
50	41.56	40.05	166140	4.06E-08
60	39.51	39.08	79980	2.49E-08
70	41.83	41.44	86400	1.98E-08
50	40.54	40.05	86400	2.56E-08
20	40.70	40.10	91440	2.96E-08

Sample: H8-15 (split)
 Length: 4.375 in.
 In situ vertical stress: 15 psi

σ_h' (psi)	ho (in)	h1 (in)	t (sec)	K (cm/s)
3	41.02	38.59	11520	9.66E-07
6	42.00	38.48	64320	2.48E-07
10	41.62	40.16	64500	1.01E-07
15	41.46	40.75	45480	6.92E-08
20	41.19	40.78	42060	4.33E-08
25	41.35	40.54	80400	4.48E-08
15	39.62	38.70	95940	4.46E-08
5	40.75	39.89	90360	4.30E-08

Sample: H5-20 (intact)
Length: 4.5 in.
In situ vertical stress: 15 psi

σ_h' (psi)	h0 (in)	h1 (in)	t (sec)	K (cm/s)
5	41.81	38.97	79620	1.66E-07
10	40.54	39.13	68340	9.71E-08
15	41.70	40.29	79920	8.07E-08
20	39.13	37.83	80640	7.85E-08
30	40.86	39.45	90960	7.24E-08
40	39.18	38.37	61440	6.37E-08
50	41.02	40.45	77640	3.40E-08
60	39.32	38.89	66900	3.08E-08
70 test was terminated by leak of triaxial cell				
